Smithsonian Institution
Scholarly Press

SMITHSONIAN CONTRIBUTIONS TO PALEOBIOLOGY • NUMBER 95

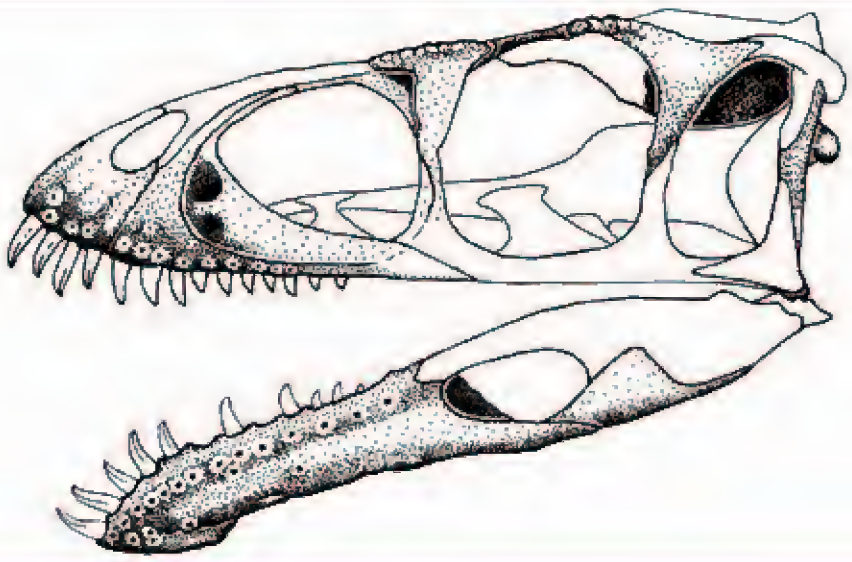

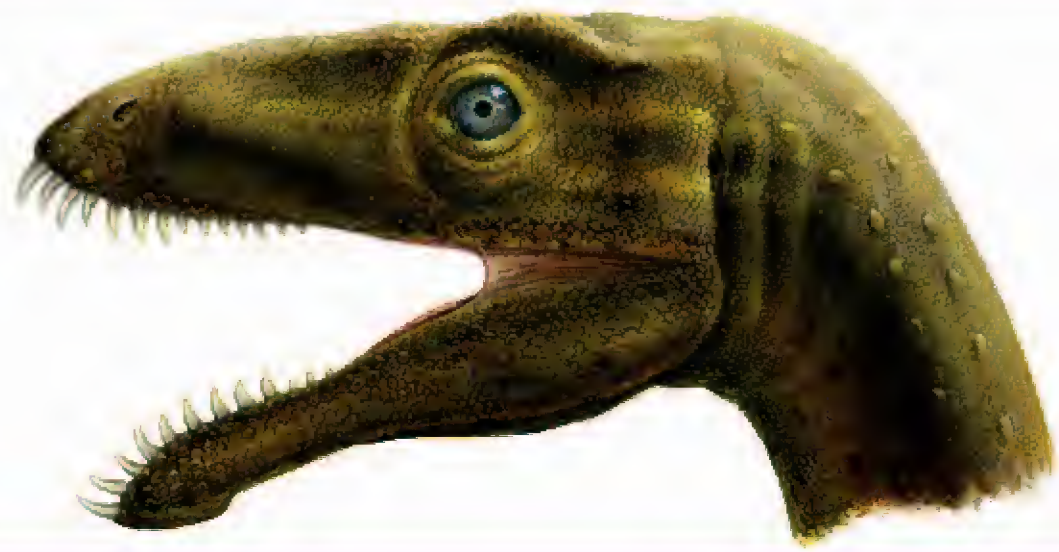

New Materials of *Masiakasaurus knopfleri* Sampson, Carrano, and Forster, 2001, and Implications for the Morphology of the Noasauridae (Theropoda: Ceratosauria)

Matthew T. Carrano, Mark A. Loewen, and Joseph J. W. Sertich

SERIES PUBLICATIONS OF THE SMITHSONIAN INSTITUTION

Emphasis upon publication as a means of "diffusing knowledge" was expressed by the first Secretary of the Smithsonian. In his formal plan for the Institution, Joseph Henry outlined a program that included the following statement: "It is proposed to publish a series of reports, giving an account of the new discoveries in science, and of the changes made from year to year in all branches of knowledge." This theme of basic research has been adhered to through the years by thousands of titles issued in series publications under the Smithsonian imprint, commencing with Smithsonian Contributions to Knowledge in 1848 and continuing with the following active series:

Smithsonian Contributions to Anthropology
Smithsonian Contributions to Botany
Smithsonian Contributions to History and Technology
Smithsonian Contributions to the Marine Sciences
Smithsonian Contributions to Museum Conservation
Smithsonian Contributions to Paleobiology
Smithsonian Contributions to Zoology

In these series, the Institution publishes small papers and full-scale monographs that report on the research and collections of its various museums and bureaus. The Smithsonian Contributions Series are distributed via mailing lists to libraries, universities, and similar institutions throughout the world.

Manuscripts submitted for series publication are received by the Smithsonian Institution Scholarly Press from authors with direct affiliation with the various Smithsonian museums or bureaus and are subject to peer review and review for compliance with manuscript preparation guidelines. General requirements for manuscript preparation are on the inside back cover of printed volumes. For detailed submissions requirements and to review the "Manuscript Preparation and Style Guide for Authors," visit the Submissions page at www.scholarlypress.si.edu.

SMITHSONIAN CONTRIBUTIONS TO PALEOBIOLOGY • NUMBER 95

New Materials of *Masiakasaurus knopfleri* Sampson, Carrano, and Forster, 2001, and Implications for the Morphology of the Noasauridae (Theropoda: Ceratosauria)

Matthew T. Carrano, Mark A. Loewen, and Joseph J. W. Sertich

Smithsonian Institution
Scholarly Press
WASHINGTON D.C.
2011

ABSTRACT

Carrano, Matthew T., Mark A. Loewen, and Joseph J. W. Sertich. New Materials of *Masiakasaurus knopfleri* Sampson, Carrano, and Forster, 2001, and Implications for the Morphology of the Noasauridae (Theropoda: Ceratosauria). *Smithsonian Contributions to Paleobiology*, number 95, viii + 53 pages, 26 figures, 3 tables, 2011. — Osteology of the noasaurid theropod *Masiakasaurus knopfleri* Sampson et al., 2001, is now two-thirds complete. We describe *Masiakasaurus knopfleri* in detail on the basis of examination of new specimens and emphasis on previously unknown elements. The skull is anteroposteriorly long but low in height, unlike the foreshortened abelisaurid condition. Premaxillary teeth are procumbent, like those of the dentary. Frontal bones are flat and unornamented, but the lacrimal and postorbital exhibit surface texturing. The braincase resembles that of abelisaurids but is more highly pneumatized. The neck is curved anteriorly but horizontal posteriorly, and it transitions to the trunk without significant proportional changes. Centrum pneumaticity appears confined to the neck and anterior trunk. The sacrum includes six vertebrae, and the expanded transverse processes of caudal vertebrae may articulate with caudal ribs. The scapulocoracoid is large and broad. The ilium is both anteroposteriorly long and dorsoventrally deep, and it bears pegs for articulation with sockets on the pubis and ischium, as in other ceratosaurs. The nearly complete pes shows no particular locomotor specializations and allows reinterpretation of the "raptorial" pedal ungual of *Noasaurus* as a manual element. These new specimens also illuminate the morphology of other noasaurids, especially those from the Lameta Formation.

In addition to Madagascar, noasaurids are known from Europe, India, South America, and Africa, spanning at least Aptian–Albian through Maastrichtian time. The new materials of *Masiakasaurus* increase character resolution within Abelisauroidea, identifying many formerly equivocal features as synapomorphies of the nodes Noasauridae, Abelisauridae, or Abelisauroidea. Unfortunately, the fragmentary nature of nearly all other noasaurids obviates any meaningful ingroup resolution, and as a result no particular evolutionary or biogeographic scenarios for the clade can presently be supported (or rejected) with confidence.

Cover images: Skeletal reconstruction of skull (left) and life restoration of head (right) of the theropod *Masiakasaurus knopfleri*. Skull image by Mark Loewen; head restoration by Lukas Panzarin.

Published by SMITHSONIAN INSTITUTION SCHOLARLY PRESS
P.O. Box 37012, MRC 957
Washington, D.C. 20013-7012
www.scholarlypress.si.edu

Library of Congress Cataloging-in-Publication Data
Carrano, Matthew T.
New materials of *Masiakasaurus knopfleri* Sampson, Carrano, and Forster, 2001, and implications for the morphology of the Noasauridae (Theropoda: Ceratosauria) / Matthew T. Carrano, Mark A. Loewen, and Joseph J. W. Sertich.
p. cm. — (Smithsonian contributions to paleobiology, ISSN 0081-0266 ; no. 95)
Includes bibliographical references.
1. Masiakasaurus. 2. Noasauridae—Morphology. 3. Paleontology—Cretaceous. I. Loewen, Mark A. II. Sertich, Joseph J. W. III. Title.
QE862.S3C276 2011
567.912—dc22 2010042359

ISSN: 0081-0266 (print) / 1943-6688 (online)

♾ The paper used in this publication meets the minimum requirements of the American National Standard for Permanence of Paper for Printed Library Materials Z39.48–1992.

Contents

Figures

Tables

New Materials of *Masiakasaurus knopfleri* Sampson, Carrano, and Forster, 2001, and Implications for the Morphology of the Noasauridae (Theropoda: Ceratosauria)

***Matthew T. Carrano**, Curator of Dinosauria, Department of Paleobiology, National Museum of Natural History, Smithsonian Institution, P.O. Box 37012, MRC 121, Washington, D.C. 20013-7012, USA; **Mark A. Loewen**, Department of Geology and Geophysics, University of Utah, 1390 East Presidents Circle, Salt Lake City, Utah 84112-0050, USA; and **Joseph J. W. Sertich**, Department of Anatomical Sciences, Stony Brook University, Stony Brook, New York 11794-8081, USA. **Correspondence:** M. T. Carrano, carranom@si.edu.*

Manuscript received 2 February 2009; accepted 9 June 2010.

INTRODUCTION

Masiakasaurus knopfleri was first described from disassociated elements discovered in the Upper Cretaceous Maevarano Formation of northwestern Madagascar (Sampson et al., 2001). Representing nearly 40% of the skeleton, these remains were identified as pertaining to a small-bodied abelisauroid, which implied a greater morphological diversity within Ceratosauria than had been depicted by the better-known *Ceratosaurus*, *Elaphrosaurus*, and Abelisauridae. *Masiakasaurus* bore specific resemblances to otherwise poorly understood forms such as *Noasaurus* and *Laevisuchus*, but little more could be said about its relationships at that time.

A more detailed study of *Masiakasaurus* by Carrano et al. (2002) elaborated on these similarities and proposed that the three latter taxa—*Masiakasaurus*, *Noasaurus*, and *Laevisuchus*—might pertain to a single clade, Noasauridae, albeit with equivocal phylogenetic support. A secondary result was an increase in the evidence supporting the dissolution of Ceratosauria *sensu* Gauthier (1986), in favor of a more basal placement for Coelophysoidea within Theropoda. This hypothesis has since received further support (Rauhut, 2002; Wilson et al., 2003; Sereno et al., 2004), although it is not universally accepted (e.g., Tykoski and Rowe, 2004; Allain et al., 2007).

A recent phylogeny of Ceratosauria (Carrano and Sampson, 2008) provided further evidence for a monophyletic Noasauridae, which also included *Velocisaurus* and *Genusaurus* but not *Deltadromeus* or *Elaphrosaurus*, as has been suggested (Sereno et al., 2004; Canale et al., 2009). Noasaurids have now been recognized in South America, Africa, Madagascar, India, and Europe, and in deposits as ancient as Aptian, implying a history reaching back at least into the earliest Cretaceous (Carrano and Sampson, 2008). Jurassic ceratosaurs appear to be more primitive, for example *Ceratosaurus*, *Elaphrosaurus*, and

Limusaurus (Xu et al., 2009), but also include indeterminate abelisauroids (Rauhut, 2005).

Unfortunately, most noasaurid species are represented by extremely fragmentary remains (e.g., Novas et al., 2004), and as a result several important aspects of the noasaurid skeleton remain poorly known, particularly the skull and forearm. This makes it difficult to resolve many important character states within Ceratosauria. In particular, it remains equivocal whether numerous distinctive "ceratosaur" features are primitive for Ceratosauria or Abelisauroidea, or instead characterize only more highly nested clades.

Here we describe abundant new materials of *Masiakasaurus* that help resolve several of these problems (a complete list is given in the Appendix). Most of the skull is now known, along with nearly the entire vertebral series and hind limb, and additional bones from the forelimb. Overall, approximately 65% of the skeletal elements of *Masiakasaurus* have been found (Figure 1). These new specimens, some of which derive from associated individuals, permit a much more accurate reconstruction of *Masiakasaurus* and allow greater insight into the anatomical specializations of noasaurids more generally.

Institutional Abbreviations

The following institution names are abbreviated for subsequent mention in the text.

FMNH	Field Museum of Natural History, Chicago
GSI	Geological Survey of India, Kolkata
UA	Université d'Antananarivo, Madagascar

Acknowledgments

We are very thankful for the efforts of participants in the 2001, 2003, 2005, and 2007 Mahajanga Basin Project expeditions (funded by the National Science Foundation and the National Geographic Society), which yielded these new discoveries of *Masiakasaurus*, as well as participants in previous expeditions for the original finds. D. Krause (Stony Brook University) and S. Sampson (University of Utah) have been particularly supportive of our research and encouraged us to continue as new materials were unearthed, and C. Forster (George Washington University) was especially helpful with access to specimens. We thank J. Groenke and V. Heisey (Stony Brook University) for their expert preparation of the fossils, often on short notice, and W. Simpson (Field Museum) for curatorial work. The manuscript was significantly improved thanks to thorough reviews by M. Lamanna and C. Forster. Figure 6 was skillfully rendered by M. Parrish (Department of Paleobiology, National Museum of Natural History). Translations of Accarie et al. (1995), Bonaparte and Novas (1985), and Janensch (1925) are available from the Polyglot Paleontologist web site (http://www.paleoglot.org).

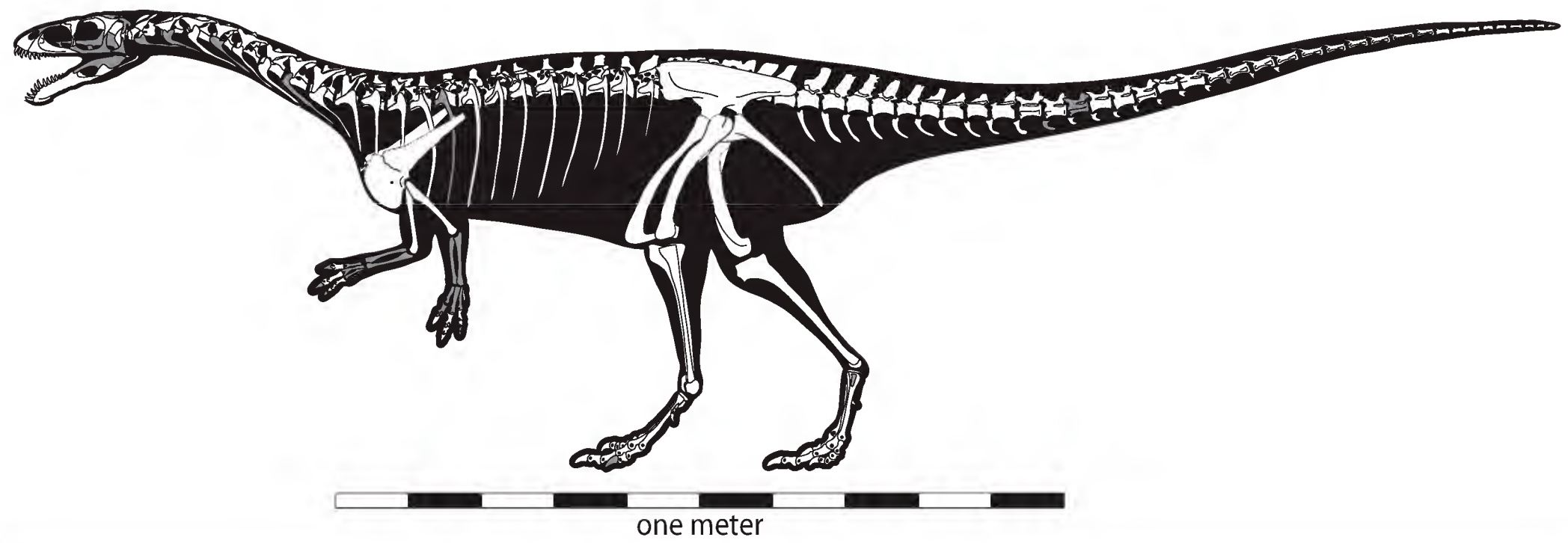

FIGURE 1. Composite skeletal reconstruction of *Masiakasaurus knopfleri* in left lateral view, showing recovered (white) and missing (gray) elements. Scale bar = 1 m.

SYSTEMATIC PALEONTOLOGY

DINOSAURIA Owen, 1842

SAURISCHIA Seeley, 1888

THEROPODA Marsh, 1881

CERATOSAURIA Marsh, 1884

ABELISAUROIDEA (Bonaparte and Novas, 1985) Bonaparte, 1991

NOASAURIDAE Bonaparte and Powell, 1980

TYPE TAXON. *Noasaurus leali* Bonaparte and Powell, 1980.

INCLUDED TAXA. *Compsosuchus solus* Huene and Matley, 1933; *Genusaurus sisteronis* Accarie et al., 1995; *Jubbulpuria tenuis* Huene and Matley, 1933; *Laevisuchus indicus* Huene and Matley, 1933; *Masiakasaurus knopfleri* Sampson et al., 2001; *Ornithomimoides? barasimlensis* Huene and Matley, 1933; *Velocisaurus unicus* Bonaparte, 1991. Note that not all of these are valid, although they do represent noasaurids, and that the clade Noasauridae also includes unnamed taxa from Niger (Sereno et al., 2004; Sereno and Brusatte, 2008) and Argentina (Brissón Egli and Apesteguía, 2008).

GEOGRAPHIC RANGE. Europe (France), South America (Argentina), India, Madagascar, and Africa (Niger).

TEMPORAL RANGE. Cretaceous, Aptian–Albian through Maastrichtian (minimum).

Masiakasaurus knopfleri Sampson, Carrano, and Forster, 2001

FIGURES 1–20

HOLOTYPE. UA 8680, a right dentary with several teeth (Sampson et al., 2001).

REFERRED SPECIMENS. See Appendix for complete list.

LOCALITIES. Thirty distinct localities near the village of Berivotra, along Route National 4 in Mahajanga Province (Boeny Region), northwestern Madagascar (see Appendix for complete list).

AGE. Maastrichtian, Late Cretaceous (Rogers and Hartman, 1998; Rogers et al., 2000, 2007).

STRATA. Anembalemba and Masorobe members, Maevarano Formation.

DESCRIPTION.

Skull and Lower Jaw

Important new materials from the skull of *Masiakasaurus* provide a far better understanding of the general morphology of the skull. Only the nasal, squamosal, parietal, jugal, quadratojugal, and palate remain unknown, and whereas only three elements from the lower jaw were previously known, only the surangular is now lacking.

Premaxilla: A partial left premaxilla (FMNH PR 2453, Figure 2) reveals that this element mirrors some of the unusual morphologies of the dentary (Sampson et al., 2001; Carrano et al., 2002). This fragment preserves two anterior alveoli along with the adjacent body of the bone; the narial margin and maxillary contact are absent. However, if the ventral margin of the preserved premaxilla is held horizontally, these two alveoli are anteroventrally oriented (Figure 2A). Thus, the first and second premaxillary teeth (missing in this specimen) complemented the anterodorsal orientation of the anterior dentary teeth. This had been suggested previously on the basis of the anteroventral orientation of the first maxillary alveolus (FMNH PR 2183; Carrano et al., 2002) and is confirmed here, but the premaxillary teeth appear to be more strongly angled than the first maxillary tooth.

In ventral view, the alveoli are large, oval, and separated by a thin interdental plate (Figure 2B). The medial surface is flat and largely featureless, and presumably articulated against the contralateral element. The lateral surface is broadly convex and exhibits a number of small foramina that open into neurovascular channels directed toward the ventral margin of the bone (Figure 2A).

Lacrimal: One nearly complete lacrimal is known (FMNH PR 2473; Figure 3A–D), preserving most of the ventral ramus. The lateral surface shows a high degree of texturing and numerous vessel traces, as in abelisaurids (Figure 3B), but is otherwise flat, with sinuous anterior and posterior margins. The presence of an orbital flange cannot be definitively ascertained, but the preserved orbital curvature is consistent with an eye that filled most of the orbital fenestra, as is typical for small theropods. As in most theropods, the dorsal and ventral moieties of the lacrimal antorbital fossa are separated on the external bone surface; however, unlike nearly all other theropods except *Torvosaurus*, this separation is incomplete.

Anteriorly, the ventral portion of the antorbital fossa is well developed but shallow, whereas the dorsal portion houses a large opening into the nasolacrimal canal, as in

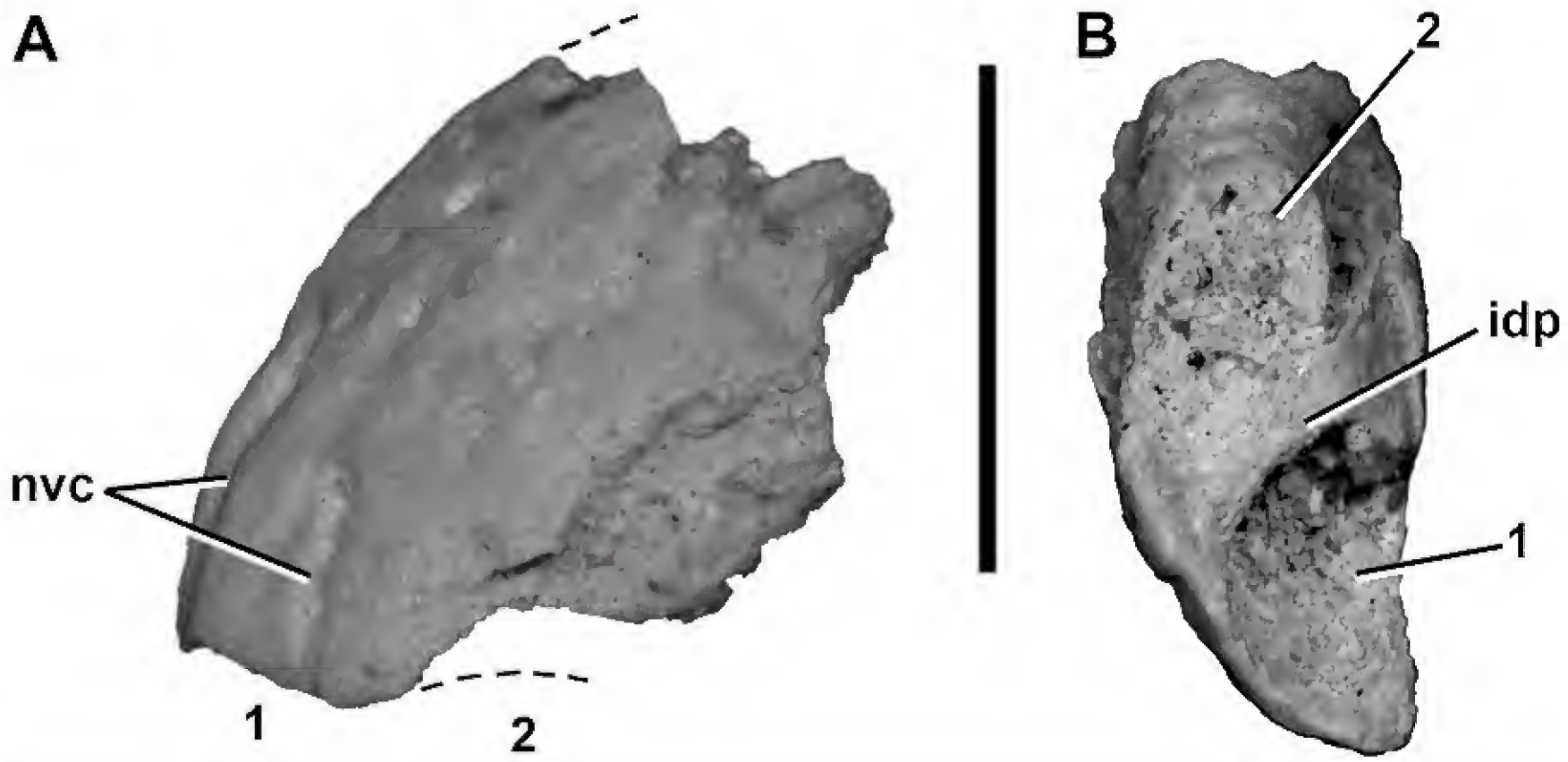

FIGURE 2. Left premaxilla (FMNH PR 2453) of *Masiakasaurus knopfleri* in lateral (A) and ventral (B) views. Abbreviations: idp = interdental plate; nvc = neurovascular channel; 1, 2 = alveoli. Scale bar = 1 cm. (Anterior is down in B.)

Ceratosaurus and abelisaurids (Figure 3A; e.g., Sampson et al., 1998; Sampson and Witmer, 2007). Only the ventral margin of this foramen can be seen; it connected to a large internal chamber, the lacrimal pneumatic recess, which is visible through the broken dorsal surface of the bone. Also in anterior view, a vertical ridge separates the lateral components of the antorbital fossa from the shallow medial vacuity.

Posteriorly, a large, teardrop-shaped medial nasal pneumatic fossa (Sampson and Witmer, 2007) is visible at the level of the mediolateral widening of the lacrimal (Figure 3C). It sits nearly centered within the concave anterior orbital wall and leads to a foramen that enters the body of the bone. The medial surface of the lacrimal is marked by a thin ridge that connects dorsally with a triangular concave area (Figure 3D). It is not clear whether this represents the contact surface for the ventral process of the prefrontal or the medial surface of a fused prefrontal.

Postorbital: Like the lacrimal, the postorbital (Figure 3E–G) exhibits some of the characteristic texturing seen in abelisaurids. The lateral surface of the ventral ramus bears numerous vessel traces and small tubercles, which continue onto the anterior ramus (Figure 3E). A thickened and roughened brow ridge, also bearing vessel traces, emerges where these two rami join. The ventral ramus curves slightly anteriorly as it descends to its distal point, but lacks a flange that enters the orbital fenestra, as in many abelisaurids. The posterior, or squamosal, ramus is a shorter, flat, blunt triangle of bone that would have lodged within a slotted facet on the squamosal.

The medial surface of the ventral ramus (Figure 3F) is marked by a distinct curving ridge that separates the orbital and lateral temporal fossae, as in many theropods including abelisaurids such as *Carnotaurus* and *Majungasaurus* (Sampson and Witmer, 2007). Dorsally, this ridge terminates at an elongate fossa for the laterosphenoid head. The dorsal margin of this fossa is adjacent to a very dorsoventrally thin, medially facing articular surface, probably for the parietal. The more expansive frontal articulation would have been present along the thin anterolateral and anterior margins, and is only partly preserved in the present specimens. Finally, the posterodorsal corner of the orbital fenestra houses a shallow, elliptical fossa containing a small foramen. In *Majungasaurus*, a similar foramen is present but without a corresponding fossa (Sampson and Witmer, 2007).

The dorsal surface of the postorbital is triangular, broad anteriorly along the frontal but tapering to a point posteriorly where it articulates with the squamosal (Figure 3G). This surface is most markedly textured along the lateral edge. The medial margin is smooth along much of its length, where it forms the anterolateral corner and lateral margin of the upper temporal fenestra. The parietal contact is straight and may have been a lappet joint.

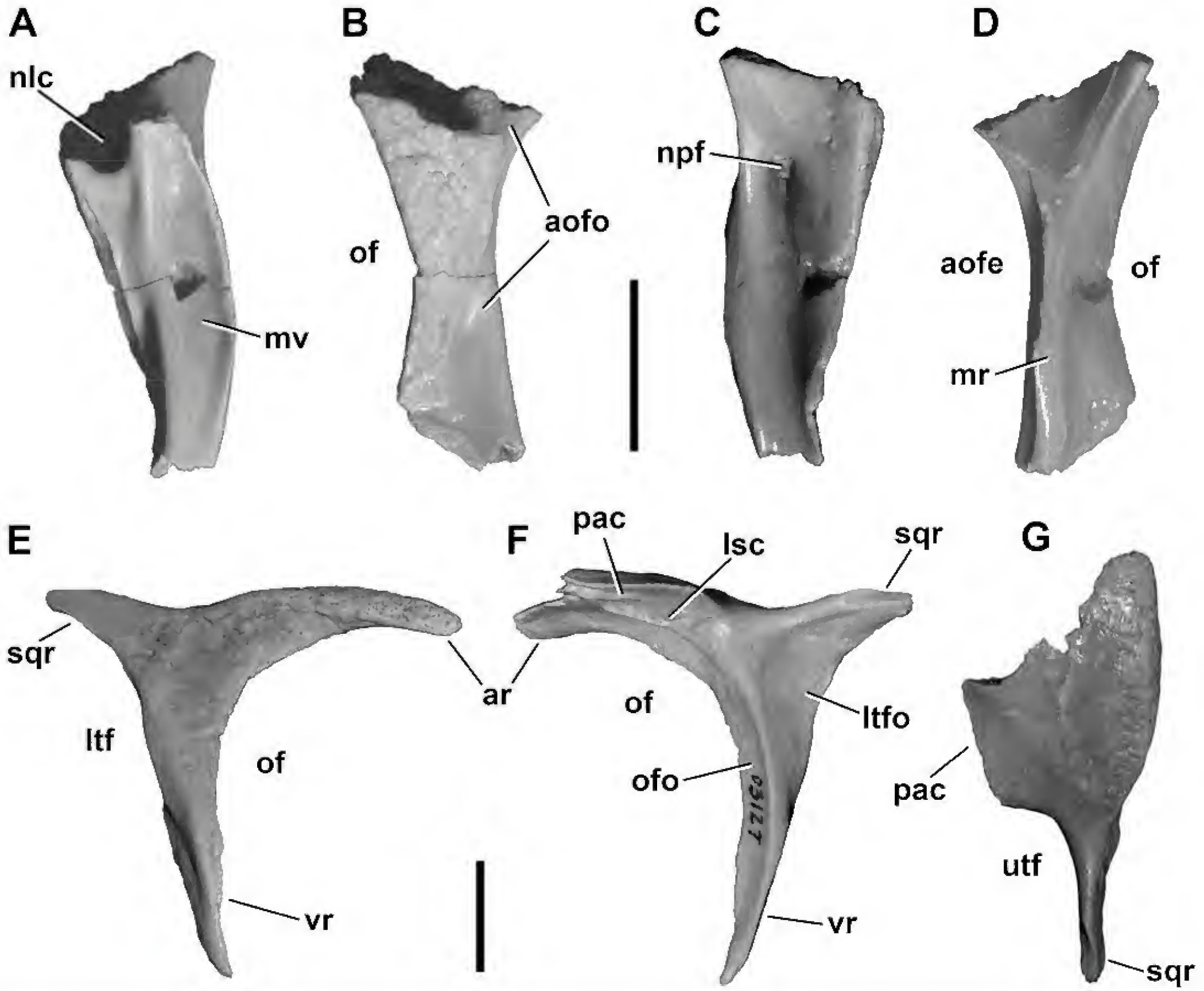

FIGURE 3. Lacrimal (A–D) and postorbital (E–G) of *Masiakasaurus knopfleri*. Partial right lacrimal (FMNH PR 2473) in anterior (A), lateral (B), posterior (C), and medial (D) views. Right postorbital (FMNH PR 2456) in lateral (E), medial (F), and dorsal (G) views. Abbreviations: aofe = antorbital fenestra; aofo = antorbital fossa; ar = anterior ramus; lsc = laterosphenoid contact; ltf = lateral temporal fenestra; ltfo = lateral temporal fossa; mr = medial ridge; mv = medial vacuity; nlc = opening into nasolacrimal canal; npf = nasal pneumatic fossa; of = orbital fenestra; ofo = orbital fossa; pac = parietal contact; sqr = squamosal ramus; utf = upper temporal fenestra; vr = ventral ramus. Scale bar = 1 cm. (Anterior is up in G.)

Frontal: The frontal (Figure 4) is a very dorsoventrally thin, gently curved bone that entirely lacks the texturing or thickening seen in many abelisaurids (e.g., *Majungasaurus*; Sampson and Witmer, 2007). Instead, it more closely resembles the frontals of other small-bodied, primitive theropods such as *Coelophysis* in its proportions (quadrangular in dorsal view) and in the large orbital component along its lateral edge. It is also quite long relative to its width; it exhibits none of the anterior shortening seen in many larger or more derived theropods.

The anterior fifth of the lateral edge is occupied by a triangular articulation that leads into a conical socket for

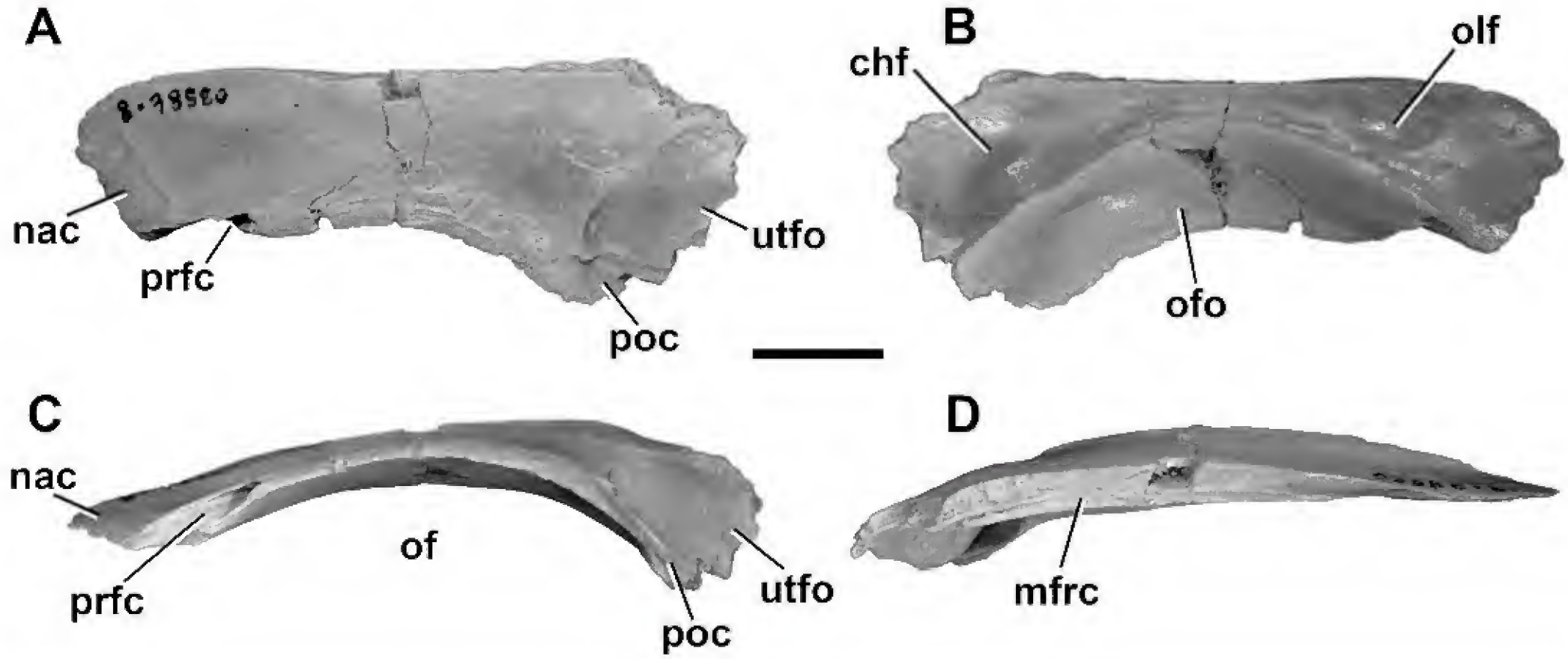

FIGURE 4. Left frontal (FMNH PR 2475) of *Masiakasaurus knopfleri* in dorsal (A), ventral (B), lateral (C), and medial (D) views. Abbreviations: chf = cerebral hemisphere fossa; mfrc = midline frontal contact; nac = nasal contact; of = orbital fenestra; ofo = orbital fossa; olf = olfactory lobe fossa; poc = postorbital contact; prfc = prefrontal contact; utfo = upper temporal fossa. Scale bar = 1 cm.

the prefrontal (Figure 4C). The depth of this socket suggests that it may have allowed for limited invasion of the frontal by pneumatic structures from the lacrimal, as in *Majungasaurus* (Sampson and Witmer, 2007). The posterior fifth bears a small, flat, triangular facet for the anterior ramus of the postorbital. Between these two articulations, the lateral edge of the frontal is sharp, subtends an arc of approximately 70°, and forms the dorsal rim of the orbit.

The anterior edge is also sharp, forming the underside of a broad lappet joint for the nasal that covers approximately 10% of the dorsal surface (Figure 4A). This edge is relatively straight and meets the midline at an angle of about 20°. The medial surface is a nearly flat and weakly striated facet for the opposing frontal (Figure 4D). It exhibits almost no curvature, and tapers in thickness both anteriorly and posteriorly from its thickest point, dorsal to the posterior half of the orbit. Although broken in both specimens, the posterior frontal appears to have been thicker and more rounded than the anterior. It arcs ventrally to form the anteromedial wall of the upper temporal fossa, the border of which is marked by a distinct rim. This fossa occupies about one-fifth of the surface of the frontal.

Ventrally, the lateral portion of the frontal is markedly concave and forms the roof of the orbital fossa (Figure 4B). It is demarcated from the medial portion by a strongly curving ridge that thins mediolaterally from anterior to posterior. This medial moiety is flat and narrows between its expanded anterior and posterior portions. The anterior expansion contains a small, elliptical fossa for the olfactory lobe of the brain. Posteriorly, the expansion marks the location of the cerebral hemisphere, which is followed by a deeper concavity. A groove runs along the medial edge of the curved ridge anteriorly from the cerebral fossa.

Quadrate: A partial right quadrate (Figure 5; FMNH PR 2496) is one of few elements that can be directly compared with material in other noasaurids (i.e., *Noasaurus*). It has a fairly straight shaft, as in most abelisaurids, but unlike the strongly posteriorly concave condition seen in *Noasaurus*.

There is no evidence of a foramen on the posterior surface, either in the body of the bone or along the quadratojugal contact (Figure 5B). However, the body is sufficiently damaged that the presence of a small foramen or fossa (as in *Majungasaurus*; Sampson and Witmer, 2007) cannot be ruled out. The quadratojugal contact is very thin, and wraps around onto the posterior surface along the ventralmost portion of the bone (Figure 5A), as in *Carnotaurus*, *Abelisaurus*, and other abelisaurids.

The quadrate condyles are similar in width but markedly asymmetrical in anteroposterior length, with the medial condyle length nearly twice that of the lateral. The two condyles are oriented at an acute angle to one another

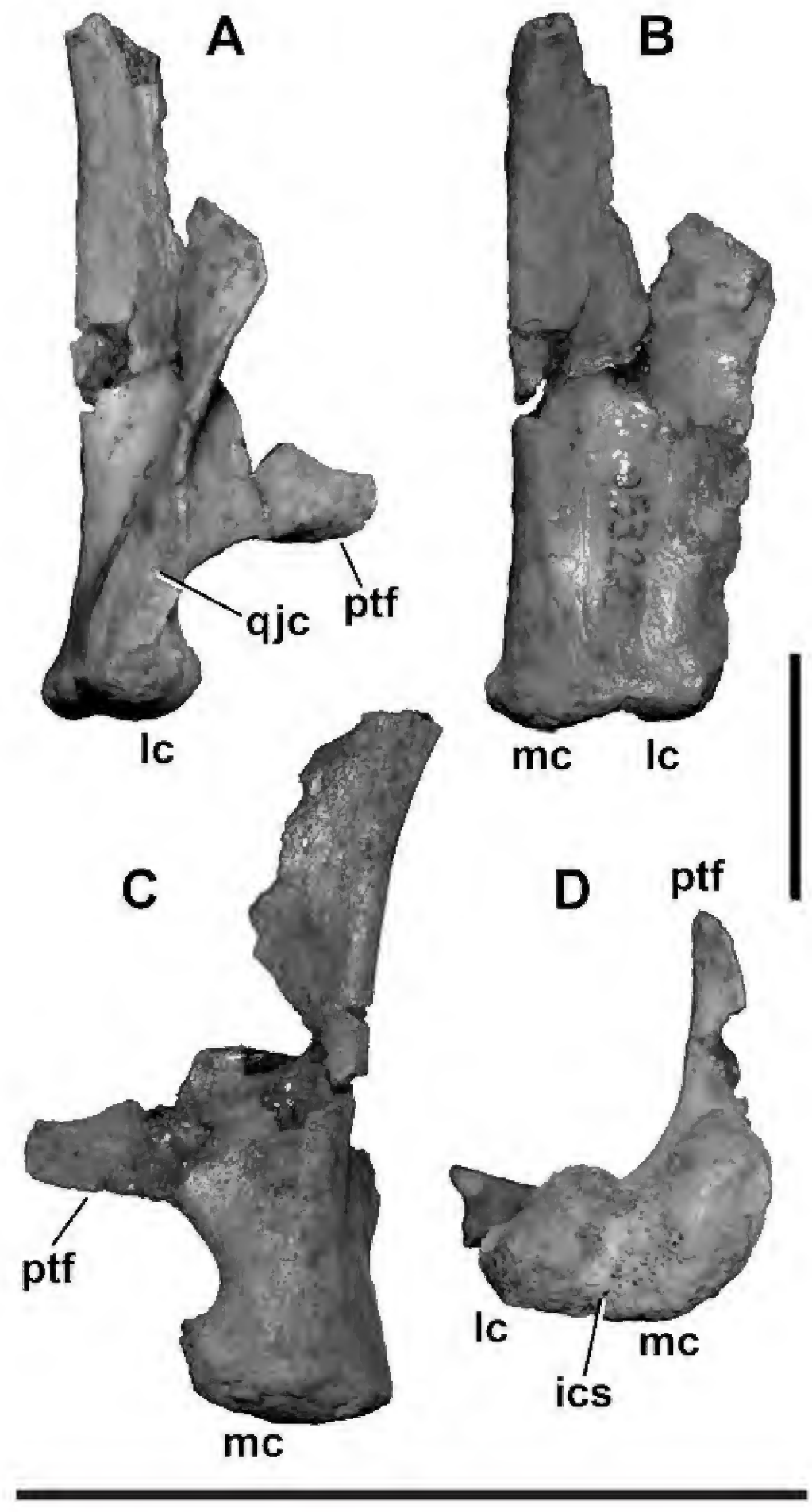

FIGURE 5. Right quadrate (FMNH PR 2496) of *Masiakasaurus knopfleri* in posterolateral (A), posterior (B), medial (C), and ventral (D) views. Abbreviations: ics = intercondylar sulcus; lc = lateral condyle; mc = medial condyle; ptf = pterygoid flange; qjc = quadratojugal contact. Scale bar = 1 cm.

(Figure 5D). This is comparable to the condition in *Noasaurus*, *Ilokelesia*, and *Majungasaurus*. The intercondylar sulcus is only about two-thirds of the width of either condyle, and is oriented approximately 45° anteromedially.

On the medial side of the quadrate, the pterygoid articular flange is only partly preserved (Figure 5C). Its ventral extent reaches nearly to the base of the quadrate, unlike the condition in some theropods (e.g., *Afrovenator*, *Baryonyx*) where up to one-third of the quadrate shaft extends ventral to the flange. There does not appear to be a ventral shelf on the pterygoid ramus, as seen in *Majungasaurus* (Sampson and Witmer, 2007).

Braincase: FMNH PR 2457 (Figures 6, 7) is a partial braincase that comprises the basioccipital, basisphenoid, and left exoccipital-opisthotic. It is evidently from a subadult individual because the right exoccipital–opisthotic has separated from the remaining braincase elements part way along their natural sutural planes. The braincase is broken just anterior to the prootic pendant, transecting the hypophyseal fossa. This affords an anterior view of the fossa along with the foramina for the entrance of cranial nerve VI.

As seen in posterior view, the foramen magnum is large (Figure 6A). A wide, shallow furrow in the dorsal surface of the occipital condyle indicates the path of the spinal cord. The condyle itself is semilunate; its dorsolateral edges are formed by the exoccipitals but the remainder is composed of the basioccipital. The exoccipital gives rise to a narrow ridge along the edge of the foramen magnum, ventrolateral to which are found the exits for cranial nerves XI and XII. A median vertical ridge descends from the base of the condyle and is flanked laterally by gently concave areas that probably represent a ventral extension of the paracondylar recesses. The basioccipital–basisphenoid contact is incomplete, but appears to have been horizontal (transverse) as in abelisaurids, rather than oblique as in most other theropods.

When observed in lateral view (Figures 6B, 7A), the braincase is extensively pneumatized by numerous fossae, many of which are also present in the braincases of the basal tetanurans *Eustreptospondylus* and *Piatnitzkysaurus* (Rauhut, 2004; Sadleir et al., 2008), as well as the abelisaurid *Majungasaurus* (Sampson and Witmer, 2007). These include a large triangular fossa that comprises the columellar recess and the foramen ovale. The anterior tympanic recess is oval and located posteroventral to the prootic pendant. Smaller fossae are present both dorsal and posterodorsal to this recess, separated from it by an oblique ridge.

The prootic pendant has a short, ventrally directed ala. Its anteroventral edges are much less distinct than its posterior ones, similar to *Majungasaurus* (Sampson and Witmer, 2007) and *Carnotaurus*, but unlike *Sinraptor* (Currie and Zhao, 1993 [1994]) in which the ala is strongly demarcated around its entire margin. The ala itself floored a fossa, bounded by a dorsally situated ridge. Ventral to the ala, the canal for the cerebral carotid artery

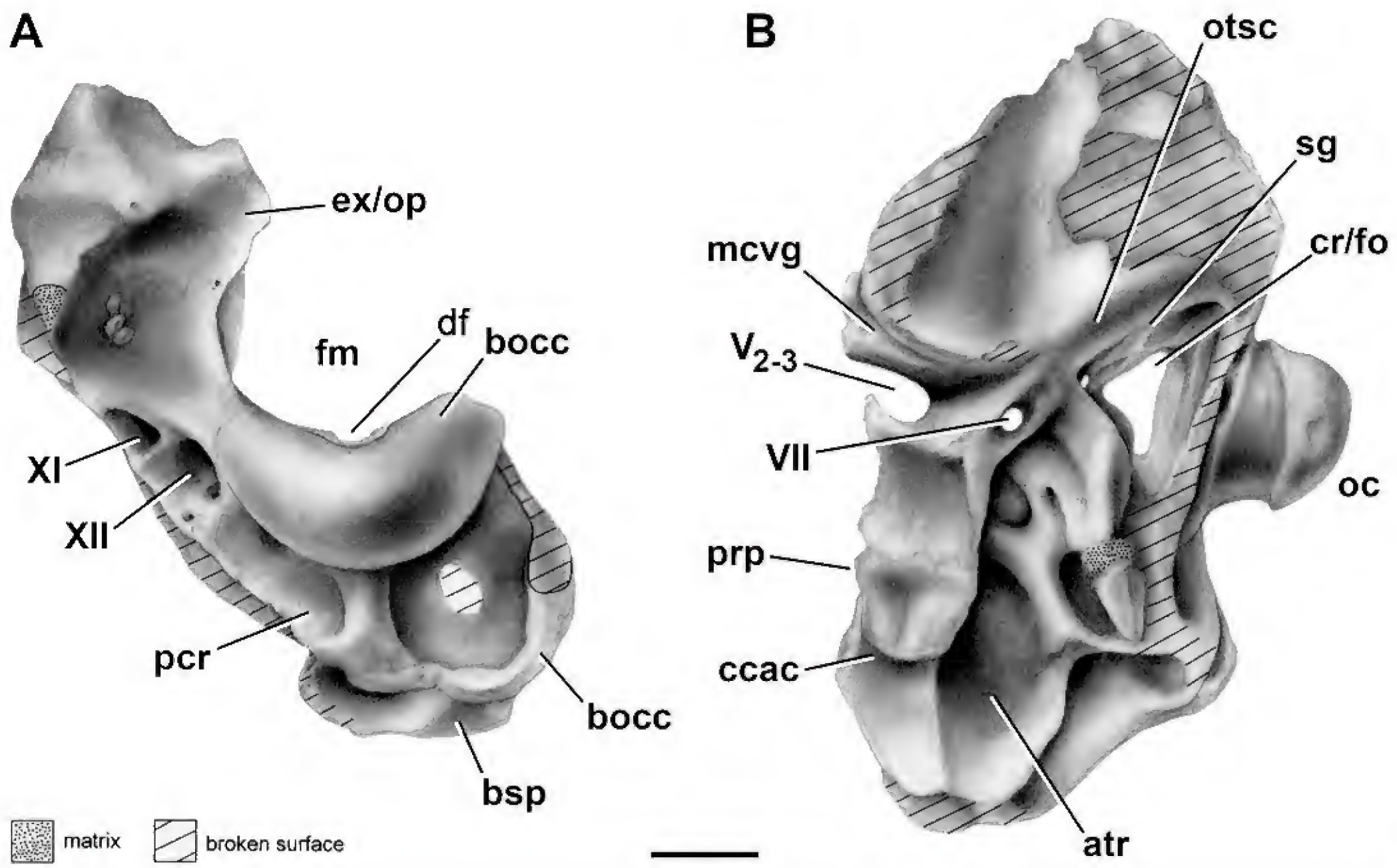

FIGURE 6. Braincase (FMNH PR 2457) of *Masiakasaurus knopfleri* in posterior (A) and left lateral (B) views. Abbreviations: atr = anterior tympanic recess; bocc = basioccipital; bsp = basisphenoid; ccac = cerebral carotid artery canal; cr/fo = columellar recess/foramen ovale; ex/op = exoccipital/opisthotic; df = dorsal furrow; fm = foramen magnum; mcvg = middle cerebral vein groove; oc = occipital condyle; otsc = otosphenoidal crest; pcr = paracondylar recess; prp = prootic pendant; sg = stapedial groove; V_{2-3}, VII, XI, XII = exits for respective cranial nerves. Scale bar = 1 cm.

passes horizontally into the anterior tympanic recess and toward the exit for the internal carotid artery. The large, oval trigeminal foramen lies dorsal to the prootic pendant, along the broken anterior margin of the braincase. Although the margins of the foramen are incomplete as a result of breakage, the dorsal edge appears to be complete and the ventral edge exhibits a partial partition; thus we interpret that the exit for cranial nerve V was incompletely segregated into distinct openings for the ophthalmic (V_1) and maxillary (V_2) plus mandibular (V_3) nerves, as in abelisaurids (Sampson and Witmer, 2007; Carrano and Sampson, 2008). The groove for the middle cerebral vein is visible along the dorsal margin of the trigeminal foramen. The exit for cranial nerve VII is posteroventral to this, separated from it by a low ridge. Further posterodorsally, the otosphenoidal crest (crista prootica) bounds the stapedial groove and forms the anterodorsal margin of the columellar recess/foramen ovale. This large fossa would have housed the exits for cranial nerves IX and X; the margins of these exits are broken, but are more intact on the endocranial surface.

Much of the ventral surface has been damaged, but a deep basisphenoidal recess is present, including the remnant of a laminar median partition. The recess appears to have been teardrop-shaped, as in abelisaurids, rather than oval, as is typical of other theropods. Anterior to it lies the base of the cultriform recess, which is transversely narrow and would have invaginated into the (now lost) ventral portion of the basisphenoid.

Some of the internal structures of the braincase can be seen, including foramina for the passage of cranial nerves and cerebral vasculature, as well as portions of the inner

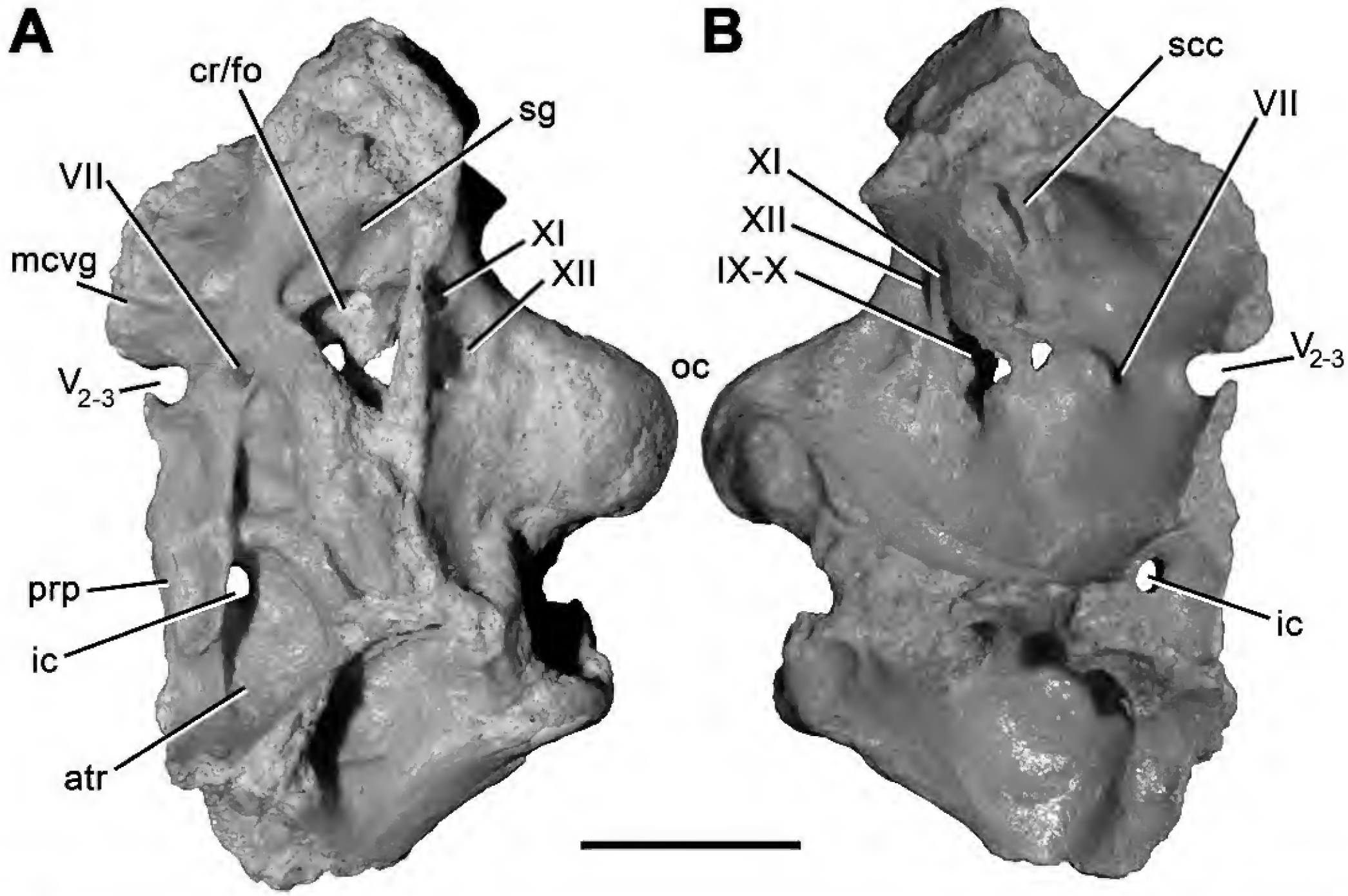

FIGURE 7. Braincase (FMNH PR 2457) of *Masiakasaurus knopfleri* in left lateral (A) and left medial (B) views. Abbreviations: atr = anterior tympanic recess; cr/fo = columellar recess/foramen ovale; ic = foramen for internal carotid artery; mcvg = middle cerebral vein groove; oc = occipital condyle; prp = prootic pendant; scc = region housing semicircular canals; sg = stapedial groove; V_{2-3}, VII, IX, X, XI, XII = foramina for respective cranial nerves. Scale bar = 1 cm.

ear and semicircular canals (Figure 7B). Details on these will be reported elsewhere (e.g., Sipla, 2007).

Dentary: A complete left dentary (Figure 8A; FMNH PR 2471) shows—for the first time—the true proportions of this bone, which are somewhat more elongate than had been reconstructed originally (Sampson et al., 2001; Carrano et al., 2002). Specifically, the ventral process of the dentary is not shortened as in abelisaurids, but extends posteriorly far past the surangular contacts.

The articulations with the postdentary bones are also better preserved than in previously described specimens and reveal more detail about the unusual morphology of the intramandibular articulations. The posterior region of the dentary is very similar to that of both *Carnotaurus* and *Majungasaurus* in exhibiting four distinct processes, three of which form a dorsally placed "socket" for reception of a prong from the surangular (Figure 8B). These three dorsal processes are arrayed in close proximity to one another: the short dorsal and ventral surangular processes mark the lateral margins of this socket; the moderate-sized intermediate surangular process forms the medial wall (Sampson and Witmer, 2007). The proportions of these three processes are more heterogeneous in *Masiakasaurus* than in *Majungasaurus*, and the fossa is narrower and deeper.

In medial view, the intermediate surangular process lies at the terminus of a longitudinal buttress that is ventral to the paradental plates and forms the dorsal limit of the splenial articulation (Figure 8C). This articulation is particularly pronounced toward its anterior end, at about midlength along the dentary. Along the ventral dentary,

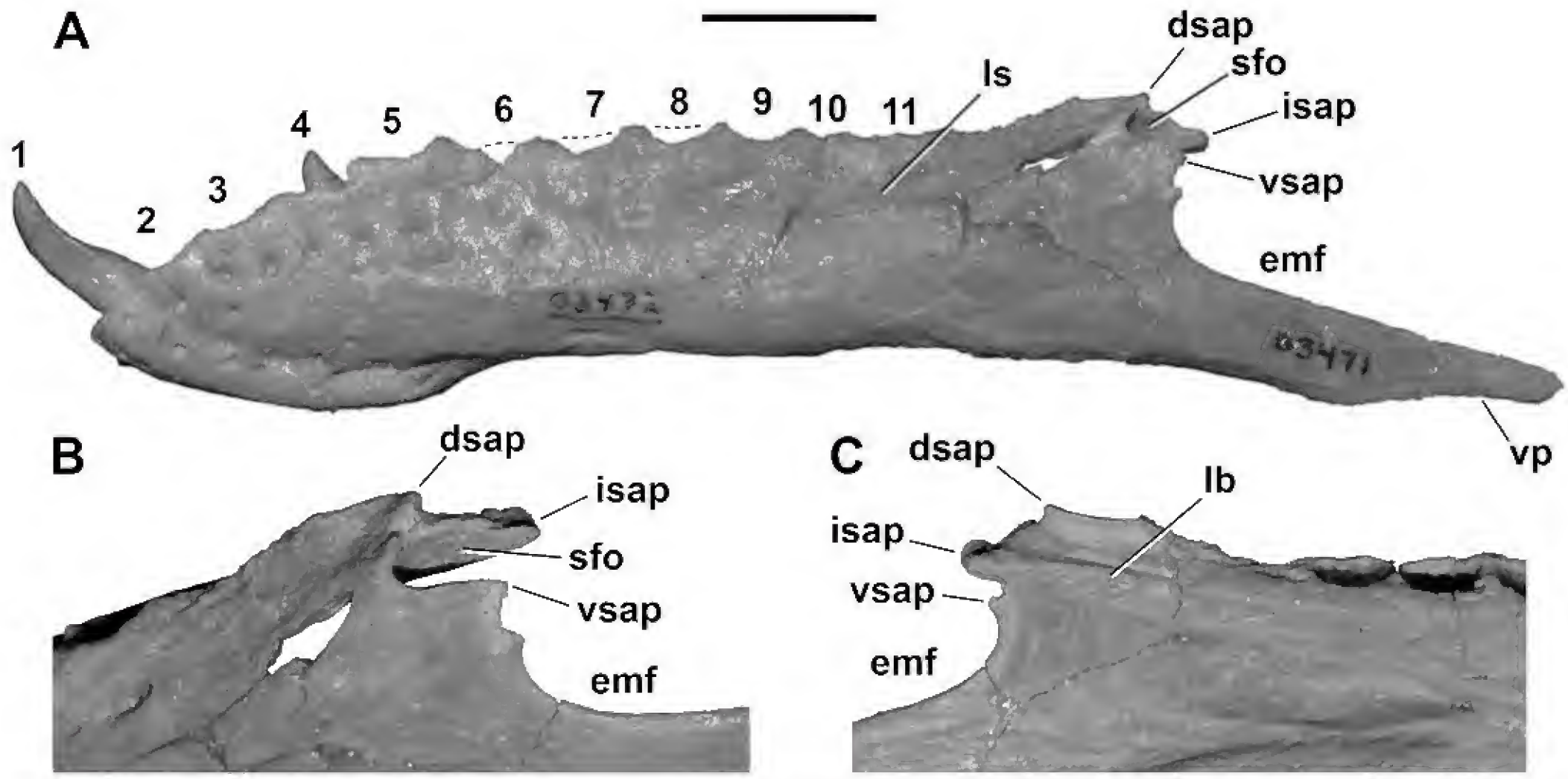

FIGURE 8. Left dentary (FMNH PR 2471) of *Masiakasaurus knopfleri* in lateral view (A). Enlargement of intramandibular joint in posterolateral (B) and medial (C) views. Abbreviations: dsap = dorsal surangular process; emf = external mandibular fenestra; isap = internal surangular process; lb = longitudinal buttress; ls = longitudinal sulcus; sfo = surangular fossa ["socket"]; vp = ventral process of dentary; vsap = ventral surangular process; 1–11 = tooth positions/alveoli. Scale bar in A = 1 cm.

the splenial ridge is more elongate and farther from the ventral margin of the bone than in *Majungasaurus* (Sampson and Witmer, 2007). As in *Majungasaurus*, a single neurovascular foramen is visible at the base of the first alveolus on the medial side, although this is correspondingly more posteriorly placed in *Masiakasaurus*.

The neurovascular foramina on the lateral surface of the dentary are relatively large and arrayed serially within the longitudinal sulcus (Figure 8A). They become more elliptical posteriorly. Unusually, these foramina also extend down along the dorsoventral depth of the first alveolus.

Angular: Two nearly complete left angulars (FMNH PR 2455, UA 9147) throw suspicion on the identification of FMNH PR 2166, previously described as a right angular (Carrano et al., 2002). The identities of FMNH PR 2166 and its parent taxon remain unclear.

The angular of *Masiakasaurus* is triangular in mediolateral view and broadly curved along its dorsal and ventral edges (Figure 9). In this view, the dorsal curve suggests an anteroposteriorly elongate external mandibular fenestra, the posterior terminus of which is indicated by a subtle change in curvature (Figure 9A). The posterior edge of the element is blunt but incomplete at the

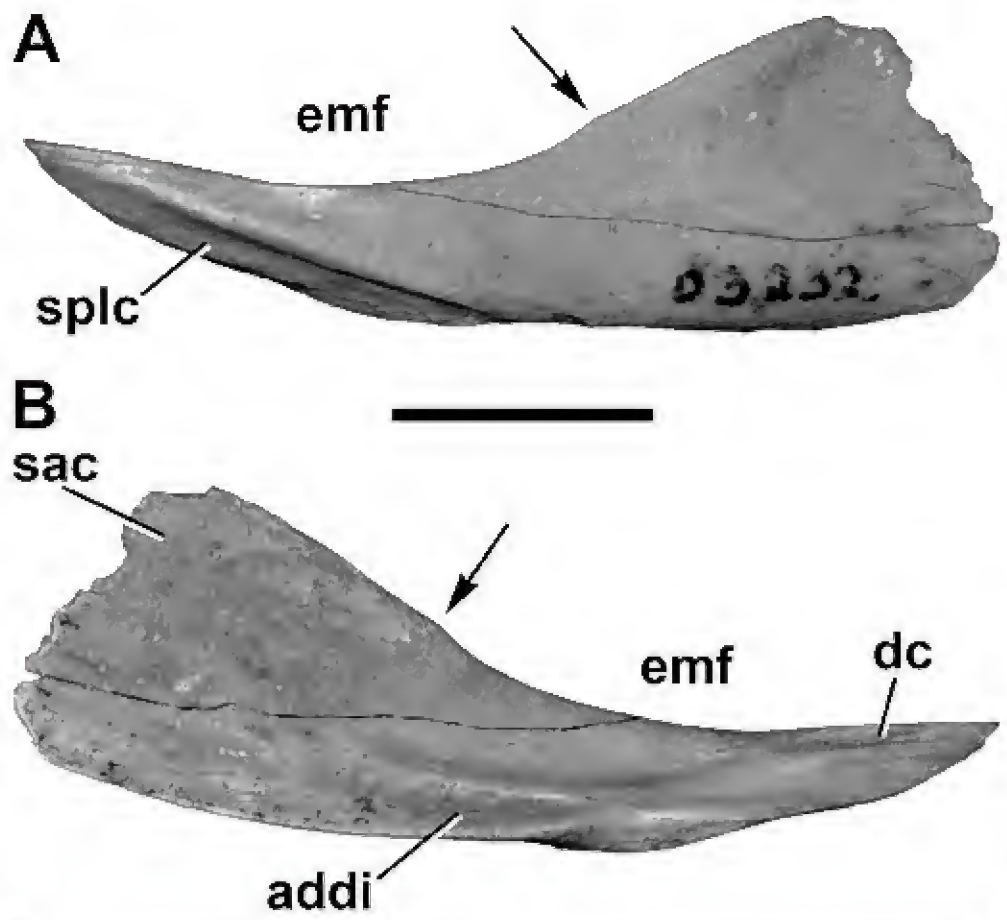

FIGURE 9. Left angular (UA 9147) of *Masiakasaurus knopfleri* in lateral (A) and medial (B) views. Abbreviations: addi = insertion for adductor musculature; dc = dentary contact; emf = external mandibular fenestra; sac = surangular contact; splc = splenial contact; arrow marks posterior extent of emf. Scale bar = 1 cm.

posteroventral corner, where it presumably had a long, thin extension along the ventral mandible as in other theropods. The anterior end tapers to a slender point. A long, convexo-concave facet along the anteroventral edge represents the splenial articulation, above which the angular is slightly textured and thickened. This facet is longer and more laterally exposed than in *Majungasaurus* (FMNH PR 2100). A shallow fossa is also present near the posterodorsal corner, presumably for the anterior portion of the M. pterygoideus ventralis (Holliday, 2009).

Medially, the posterior part of the angular bears a long, dorsally facing, oval fossa that marks the insertion site of the adductor musculature (Figure 9B). This fossa lies adjacent to a faint contact surface along the vertical face of the posterior angular for the surangular. A flat, dorsally facing facet sits on the dorsomedial surface of the anterior prong, marking the dentary contact. This is unlike the condition in *Majungasaurus*, where these two bones were not in direct articulation (Sampson and Witmer, 2007). The prearticular would have articulated along the convex ventral margin of the bone.

Prearticular: The prearticular resembles that of most basal theropods in overall shape (Figure 10). In mediolateral view, it is much longer than tall, gently curved along its ventral edge, and more strongly curved dorsally, where it forms the ventral border of the internal mandibular fenestra (Figure 10A,B). This curvature is shallow, contrasting the stronger arc seen in the foreshortened jaws of the abelisaurids *Majungasaurus* and *Carnotaurus*.

Anteriorly and posteriorly, the prearticular expands to approximately equal dorsoventral depths. The anterior flange is incompletely known, but a short portion of convex curvature along its ventral edge suggests that it may have had a shape similar to *Majungasaurus* (Sampson and Witmer, 2007). The posterior flange articulates against and is partly ventral to the lateral portion of the articular. This flange is complete in UA 9149, where it tapers posteroventrally to a long, finger-like projection with a concave dorsal surface for the articular.

The prearticular curves ventrolaterally to create a concavity (Figure 10A). Below this, the ventral edge forms a flat, posteromedially twisted facet for the angular. The lateral surface is marked by thickenings along the ventral and dorsal edges, which bound a narrow furrow that runs from the articular contact to the anterior flange. A roughened patch at the posterodorsal edge of the internal

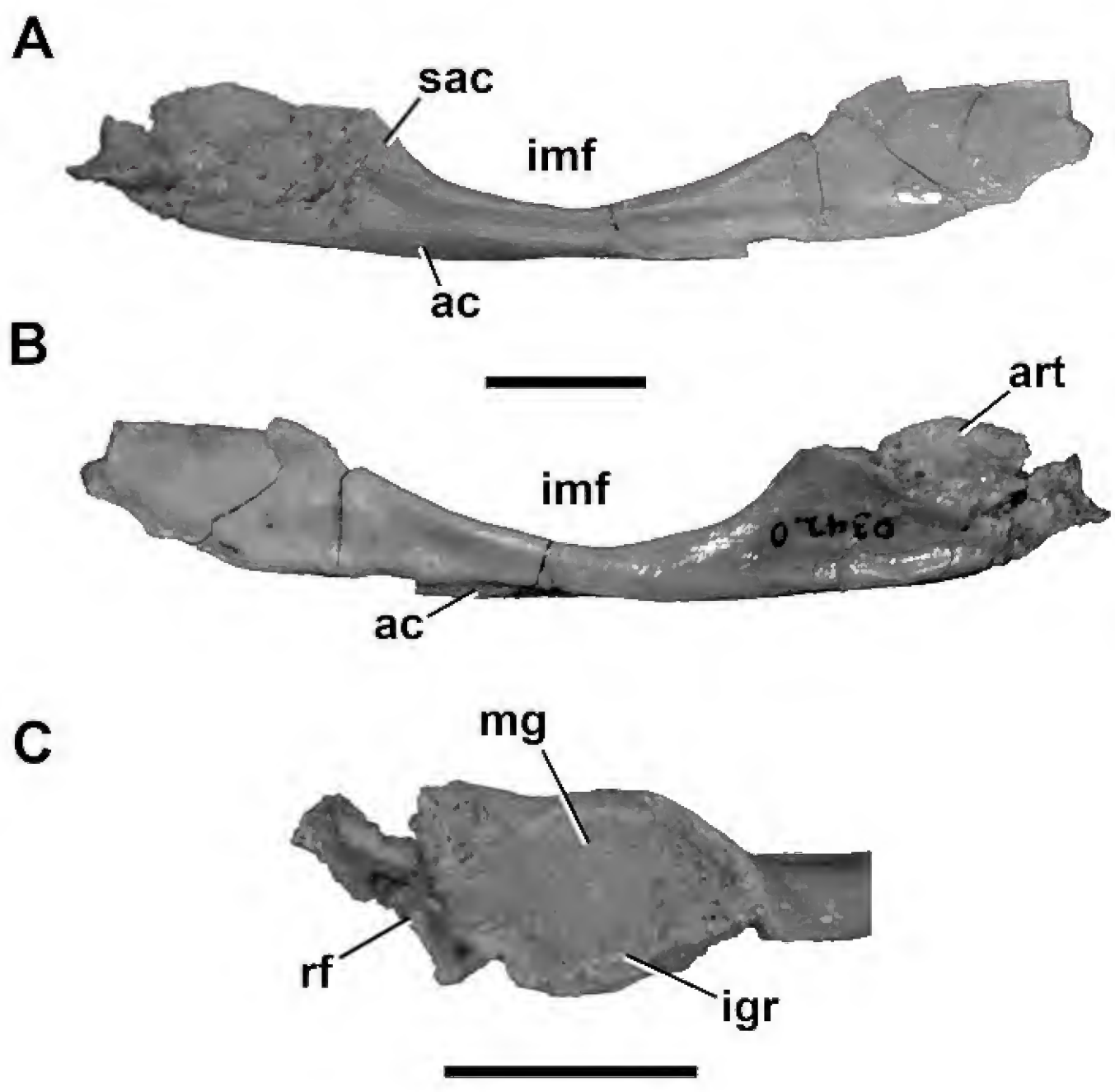

FIGURE 10. Right prearticular and articular (UA 9166) of *Masiakasaurus knopfleri* in lateral (A) and medial (B) views. Dorsal view (C) of mandibular glenoid. Abbreviations: ac = angular contact; art = articular; igr = inerglenoid ridge; imf = internal mandibular fenestra; mg = medial glenoid fossa; rf = retroarticular fossa; sac = surangular contact. Scale bars = 1 cm.

mandibular fenestra represents the contact surface for the surangular.

Articular: The single right articular (UA 9166) is articulated with the corresponding prearticular but is somewhat damaged, obscuring several of its surfaces. However, most of the medial glenoid fossa is intact, and presents a deeply concave trough for the medial quadrate condyle that is oriented approximately 30° anteromedial to the midline axis (Figure 10C). The medial edge of the fossa is tall, and the lateral edge is marked by a low interglenoid ridge. The surangular would have contacted the angular lateral to this point, forming most of the lateral glenoid fossa for articulation with the lateral quadrate condyle. A concave fragment lying posterior to the medial glenoid fossa represents the anteriormost portion of the dorsally facing retroarticular fossa, the lateral side of which would have been formed by the surangular.

In medial view, a small, convex portion of the articular is exposed dorsal to the prearticular, but the remainder is covered (Figure 10B). The lateral side is damaged and much is missing, including the lateral glenoid fossa and the area of the chorda tympani foramen.

Hyoid: A long, slender, curved element associated with FMNH PR 2481 is identified as a ceratobranchial. The articulation with the basihyal has two facets that meet at a 120° angle. The shaft tapers adjacent to the articulation, but remains uniformly narrow throughout most of the rest of its length. The distal end is not preserved. The lateral surface is convex, but a thin concavity runs along the medial side. Overall it is similar to the same element in *Carnotaurus* (Bonaparte et al., 1990) and *Majungasaurus*.

General skull morphology: With these new elements we have attempted to reconstruct the entire skull and lower jaw (Figure 11). We have restored the skull to be relatively long and low based on the primitively proportioned maxilla and frontal. Nonetheless, an accurate length:height ratio cannot yet be provided. In profile the skull of *Masiakasaurus* superficially resembles those of other small theropods, including *Coelophysis*, *Compsognathus*, and *Ornitholestes*; these similarities are a result of the relatively large orbit and long snout rather than any particular phylogenetic affinity. The most unusual features of the skull are confined to the anterior portions of the jaws. In dorsal view, the skull likely had a similarly plesiomorphic shape, tapering to a narrow snout from its widest point near the anterior edge of the frontal; posteriorly, the sides of the skull were approximately parallel. The lower jaw is closer to the abelisaurid condition than to that of other theropods, particularly in the morphology of the intramandibular joint.

Axial Column

Numerous vertebrae from all parts of the column greatly extend our knowledge of axial column morphology

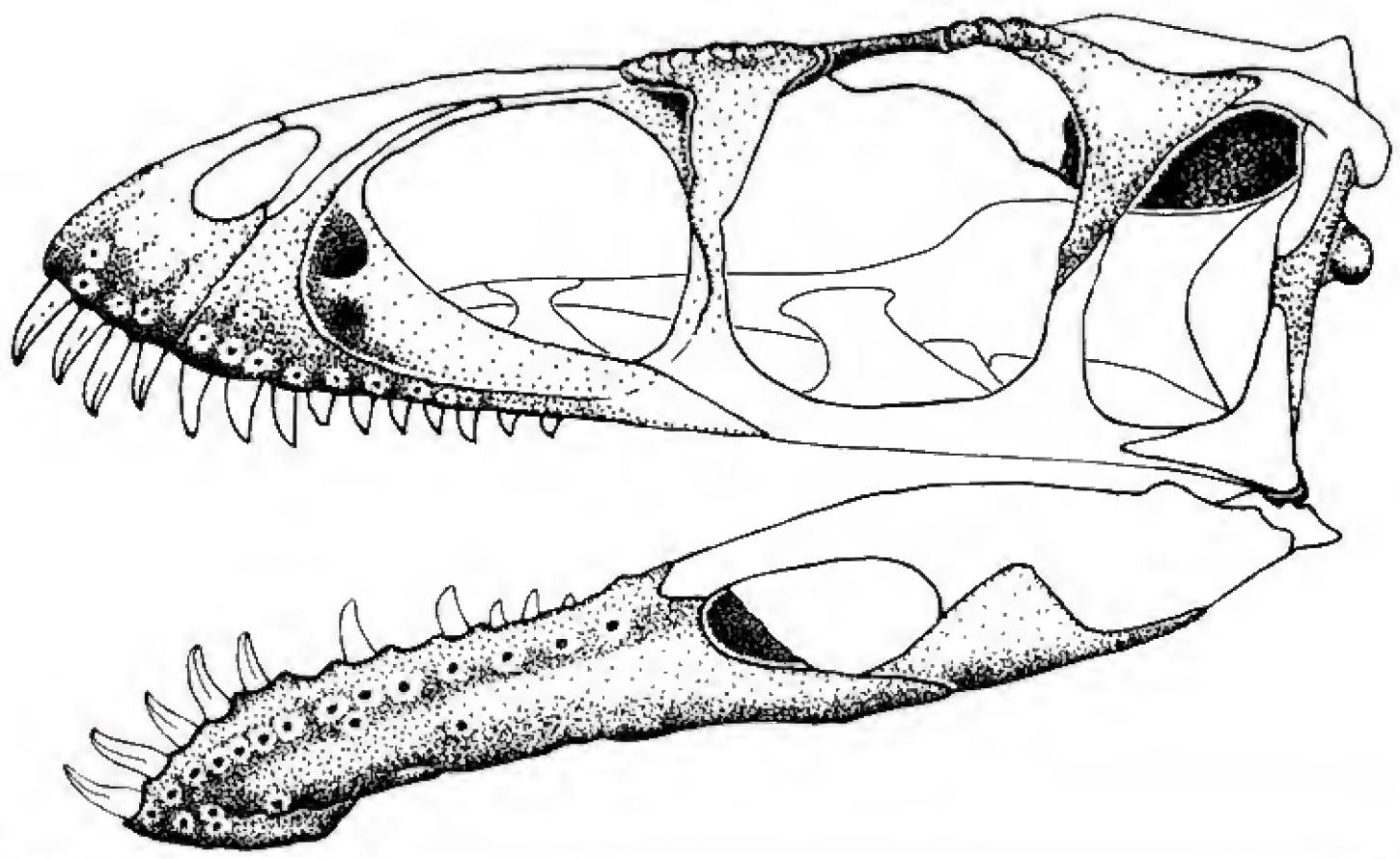

FIGURE 11. Reconstructed skull of *Masiakasaurus knopfleri* in left lateral view. Known elements (or parts thereof) are stippled; unknown elements are outlined.

in *Masiakasaurus* and clarify comparisons with *Noasaurus* and *Laevisuchus* (Huene and Matley, 1933; Bonaparte and Powell, 1980; Carrano et al., 2002). Most of the cervical series is represented; only the atlas is missing. Among the dorsals, only portions of the midtrunk remain unknown or unidentified. All sacrals and portions of all of the major caudal regions are also represented.

Although individual variations make precise identification of position uncertain for some specimens, the relatively complete cervical and dorsal series of *Carnotaurus* (Bonaparte, 1991), *Elaphrosaurus* (Janensch, 1925), *Majungasaurus* (O'Connor, 2007), and *Spinostropheus* (Sereno et al., 2004) provide instructive comparative materials. We can also clarify the positions of some previously identified cervicals (Carrano et al., 2002). The pre-caudal vertebral formula of *Masiakasaurus* matches well with that of *Carnotaurus*, which possesses 10 cervicals, 12 free dorsals, and 6 sacrals (including 2 dorsosacrals and 2 caudosacrals). The terminology of Wilson (1999) regarding most laminae and fossae is followed here.

Cervical vertebrae: The axis (Figure 12A–D) is known from two specimens (FMNH PR 2462, 2466), and in both cases the axial centrum and atlantal intercentrum are coossified. Two isolated atlantal intercentra (FMNH PR 2477, 2630) show a morphology consistent with these fused examples.

In lateral view, the axis bears a small but distinct oval parapophysis; the long axis is oriented slightly posteroventrally (Figure 12A). A large, horizontally oval pneumatic foramen lies posterior to the parapophysis and leads into a sizable internal chamber. A second, smaller foramen is present more posteriorly in FMNH PR 2462. Unlike in *Majungasaurus*, this foramen is not located exclusively posterior to the diapophysis but also partly ventromedial to it (O'Connor, 2007). The outer edges of the foramen are smooth, showing no evidence of a surrounding pneumatic fossa. The chamber is separated from its opposite by a median septum; it is further subdivided in FMNH PR 2466. The neurocentral suture can still be seen although it is clearly tightly closed in both specimens. The intercentrum projects horizontally anterior to the parapophysis; it is not upturned as in *Sinraptor* (Currie and Zhao, 1993 [1994]). The odontoid projects farther anteriorly than the intercentrum and bears a shallow lateral fossa.

On the neural arch, a distinct oval facet marks the articular surface of the prezygapophysis. The pendant diapophysis is located directly posteroventrally and is angled slightly posteriorly. On its posteroventral surface, a small infradiapophyseal fossa is demarcated by anterior and posterior laminae. The diapophysis is connected to the epipophysis and postzygapophysis by a pronounced postzygodiapophyseal lamina. This lamina forms the anterodorsal edge of the infrapostzygapophyseal fossa, which houses either a distinct foramen or a deep fossa. The postzygapophysis is quadrangular, and is considerably surpassed by the dorsoventrally flat epipophysis. In lateral view, the neural spine is broadly arched, closer in shape to that of *Carnotaurus* than *Majungasaurus*, and hangs slightly posteriorly over the centrum.

Ventrally, the axis is nearly flat, with a very faint midline ridge but no keel. A similar transverse ridge connects the parapophyses. The centrum is somewhat spool-shaped, and its width is subequal to that of the atlantal intercentrum.

Anteriorly, the intercentrum presents a wide, reniform, concave articular facet for the atlantal centrum (Figure 12B). It sits ventral to the prominent, D-shaped odontoid, which has a nearly flat dorsal surface, flanked laterally by slight ridges that would have floored the neural canal. The odontoid is rounded anteriorly. In this view the diapophyses curve ventrolaterally, whereas the prezygapophyses face dorsolaterally. In posterior view the epipophyses are nearly as wide as the postzygapophyses (Figure 12C), although they do not project laterally as in *Majungasaurus* (O'Connor, 2007).

The third cervical vertebra (C3) is characterized by anterior and posterior centrum faces that are dorsoventrally offset and not parallel in lateral view. A small, round pneumatic foramen pierces the centrum posterodorsal to the parapophysis, which is broken in the only known specimen (UA 9121). On the arch, a strong posterior centrodiapophyseal lamina runs from the diapophysis to the posterior end of the neurocentral suture, separating the elongate infradiapophyseal fossa ventrally from the expansive infrapostzygapophyseal fossa dorsally. A longer postzygodiapophyseal lamina is discriminated from the diapophysis by a kink in its trajectory. The infraprezygapophyseal fossa is shallow and faces anteriorly. The prezygapophyseal–epipophyseal lamina is pronounced, and exhibits a small rise and thickening at its midlength. The short diapophysis hangs nearly vertically.

Anteriorly, the centrum face is flat and approximately rectangular. More dorsally, the neural canal is circular and approximately 80% as large as the centrum face. The small, triangular infraprezygapophyseal fossa is separated from the more medially placed anterior peduncular fossa by an additional lamina. The prezygapophyses are widely separated from the midline, where they flank a deep prespinal fossa. The posterior centrum face is concave and D-shaped. The postzygapophyses are angled laterally approximately

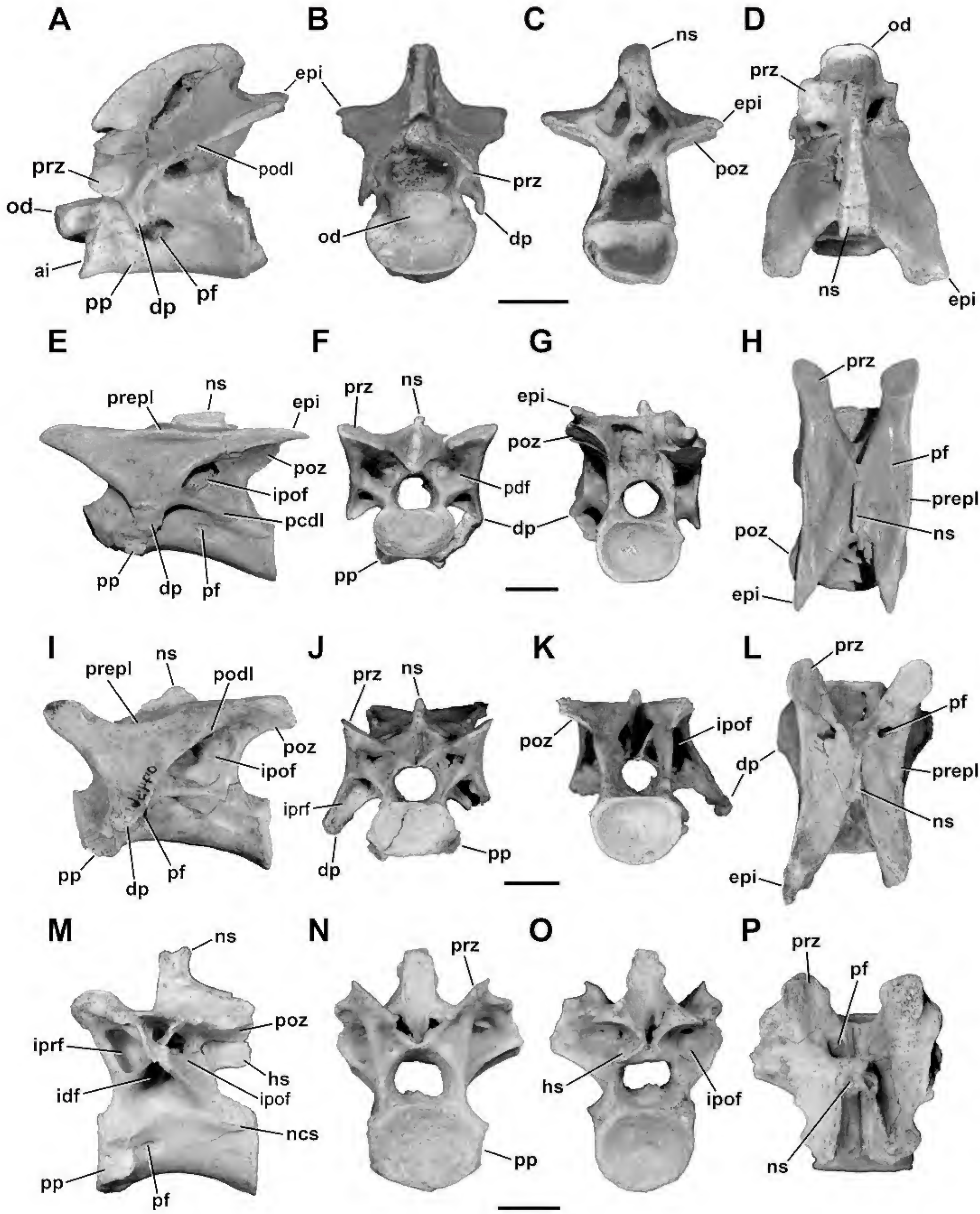
A
prz
od
podl
ai
pp
dp
pf
B
epi
od
prz
dp
C
ns
epi
poz
D
od
prz
epi
ns
E
prepl
ns
epi
poz
ipof
pcdl
pp
dp
pf
F
prz
ns
pdf
pp
G
epi
poz
dp
H
prz
pf
prepl
ns
poz
epi
I
prepl
ns
podl
poz
ipof
pp
dp
pf
J
prz
ns
iprf
dp
pp
K
poz
ipof
L
prz
pf
dp
prepl
ns
epi
M
ns
poz
iprf
hs
idf
ipof
ncs
pp
pf
N
prz
pp
O
hs
ipof
P
prz
pf
ns

FIGURE 12. Cervical (A–O) and anterior dorsal (M–P) vertebrae of *Masiakasaurus knopfleri* in left lateral (A, E, I, M), anterior (B, F, J, N), posterior (C, G, K, O), and dorsal (D, H, L, P) views. A–D, axis (FMNH PR 2466); E–H, fourth cervical vertebra (UA 9106); I–L, sixth cervical vertebra (FMNH PR 2481); M–P, first dorsal vertebra (FMNH PR 2837). Abbreviations: ai = atlantal intercentrum; dp = diapophysis; epi = epipophysis; hs = hyposphene; idf = infradiapophyseal fossa; ipof = infrapostzygapophyseal fossa; iprf = infraprezygapophyseal fossa; ncs = neurocentral suture; ns = neural spine; od = odontoid; pcdl = posterior centrodiapophyseal lamina; pdf = peduncular fossa; pf = pneumatic foramen or fossa; podl = postzygodiapophyseal lamina; poz = postzygapophysis; pp = parapophysis; prepl = prezygapophyseal-epipophyseal lamina; prz = prezygapophysis. Scale bars = 1 cm. (Anterior is up in D, H, L, and P.)

30°. The deep postspinal fossa houses a pair of large subsidiary foramina, and is separated from the triangular peduncular fossae ventral to it by thin laminae.

In dorsal view, the arch is rectangular, with two V-shaped incisions marking the prespinal and postspinal fossae between their respective zygapophyses. A distinct dorsal fossa is visible adjacent to the prezygapophyseal–epipophyseal lamina, near the base of the prezygapophysis. The neural spine is very thin transversely, located above the midlength of the centrum, and extends only a few millimeters above the flat dorsal surface. The ventral surface of the centrum is nearly flat.

The fourth cervical vertebra (C4; Figure 12E–H) more strongly resembles the only known cervical of *Noasaurus* than any of those previously described, especially in its elongate proportions (Carrano et al., 2002). It is generally similar to C3, although the centrum faces are more strongly offset, and a second pneumatic foramen is present on the centrum (Figure 12E). This smaller foramen is located posterior to the diapophysis, and on one specimen (UA 9106) has a scalloped posteroventral margin marking the path of associated soft-tissues. In this specimen, a portion of the cervical rib is still articulated, but not fused, with the left diapophysis.

The proportions of the laminae and fossae are similar to those of C3. Here, the infrapostzygapophyseal fossa is partitioned into a large dorsal chamber, which communicates with the interior of the arch, and a smaller, blind posteroventral fossa. The infradiapophyseal fossa has an uneven surface, and may connect to the infrapostzygapophyseal fossa on the right side. The neural spine is thicker and more rectangular than in C3. In C4 the prezygapophyseal–epipophyseal lamina undulates such that the zygapophyses are more dorsally positioned than is the midpoint of this lamina. The epipophysis is long and acuminate, extending posteriorly well past the postzygapophysis and the posterior centrum face. The neural spine is half as long anteroposteriorly as the centrum, and bears a sloping anterior edge but a more vertical posterior one (Figure 12E, H).

Anteriorly, the centrum face is reniform, and the peduncular fossae are more conical and larger than in C3 (Figure 12F). The prezygapophyses extend laterally only as far as the diapophysis, which has a shallower infraprezygapophyseal fossa. The prespinal fossa is narrower and deeper than in the preceding vertebra. The posterior centrum face is rounder than the anterior face. In dorsal view, the prezygapophyses are oblate, and the postzygapophyses are visible laterally, ventral to the acuminate epipophyses (Figure 12H). The prezygapophyseal–epipophyseal lamina is straight. Ventrally, the centrum is more elongate than in C3; the anterior and posterior edges are twice as wide as the midcentrum.

The fifth cervical vertebra (C5) is generally similar to the preceding elements, but the prezygapophyseal–epipophyseal lamina is less distinct at its midlength, represented by an undulating curve rather than a marked ridge. This change is related to the emergent elevation of the prezygapophysis relative to the dorsal arch surface. The neural spine is shorter anteroposteriorly and more posteriorly positioned over the neural arch; the epipophysis is more downturned.

The anterior centrum face is more rounded than in C3 and C4, and the prezygapophyses are more horizontally oriented and spaced farther apart laterally. The infraprezygapophyseal fossa is very small and shallow, and is contiguous with a fossa on the medial portion of the cervical rib in FMNH PR 2465. The shallow prespinal fossa is wide and more open dorsally. Posteriorly, the peduncular fossae are very shallow.

In the only known sixth cervical vertebra (C6; Figure 12I–L; FMNH PR 2628), the centrum faces remain offset from one another and are vertically inclined (Figure 12I). A single pneumatic foramen is present, adjacent to the left parapophysis, but faint traces of a pair of pneumatic fossae are evident on both sides of the centrum. The prezygapophysis is now elevated to the same height as the neural spine, and the infrapostzygapophyseal fossa is large but less pronounced than in preceding vertebrae. The prezygapophyseal–epipophyseal lamina dips ventrally

before rising to meet the very small epipophysis, and lacks any thickening at midlength. The neural spine is shorter anteroposteriorly than in C3–C5.

Anteriorly, the infraprezygapophyseal fossa is deeper and extends along the length of the extended diapophysis, whereas the peduncular fossa is very shallow (Figure 12J). The prezygapophyses are angled at 45°. As seen in posterior view, the postspinal fossa is very deep but narrow, and the peduncular fossa is small but also deep (Figure 12K). The posterior centrum face is more transversely oval than in preceding vertebrae.

The prezygapophyseal–epipophyseal lamina is more distinct in dorsal view than in more anterior cervicals, and is slightly concave along its course (Figure 12L). A U-shaped margin leads to the prespinal fossa; the postspinal fossa sits at the base of a V-shaped embayment. A pair of large foramina is evident on the dorsal surface, just posteromedial to the prezygapophyses. In ventral view, the parapophyses are connected by a thin transverse ridge, and the infradiapophyseal fossa appears deep and multi-chambered.

The previously illustrated *Laevisuchus* vertebra (GSI K27/696; Carrano et al., 2002: fig. 7B) is very similar to this specimen in proportions, and we intepret it as C6 based on the offset of the centrum faces and the relative positions of the neural spine and neural arch processes.

The seventh and eighth cervical vertebrae (C7, C8) lack any offset between the centrum faces but are otherwise similar to C6. In these elements the epipophysis is slender and does not extend posteriorly past the postzygapophysis; the neural spine is small and blocky. Note that three specimens (FMNH PR 2140, 2139, and 2141) were originally assigned to three successive positions within the neck (Carrano et al., 2002). Based on comparison with newly discovered material, we now identify FMNH PR 2139 as C7, FMNH PR 2141 as C8, and FMNH PR 2140 as C10 (see Appendix). C7 and C8 have, therefore, been previously described in detail (Carrano et al., 2002).

In lateral view, the ninth cervical vertebra (C9) differs from the two preceding elements in that it exhibits a slightly backswept neural arch. The distance between the prezygapophysis and postzygapophysis is reduced such that the prezygapophyseal–epipophyseal lamina is folded. The epipophysis is very small. The postzygodiapophyseal lamina exhibits a distinct kink along its trajectory.

Relative to more anterior elements, in C9 the diapophysis extends more directly laterally and bears a well-defined infraprezygapophyseal fossa that is very deep medially. Anteriorly, the peduncular fossa is absent, and the neural canal is smaller relative to the centrum face. The prespinal fossa is very shallow and fully opened anteriorly. Posteriorly, the peduncular fossa is much smaller than the postspinal fossa, and the infrapostzygapophyseal fossa exhibits deep foramina.

The tenth cervical vertebra (C10) lies at or near the cervicodorsal transition, although this can be difficult to define in theropods. Its unusually long proportions indicate that *Masiakasaurus* was characterized by anteroposteriorly lengthened centra throughout the presacral vertebral column. This is unlike the condition in most theropods, where the cervicodorsal transition is marked by one or two anteroposteriorly short vertebrae.

Vertebra C10 retains a small, anteriorly placed pneumatic foramen, but lacks any evidence of a more posterior foramen or fossa. The parapophysis is elevated just dorsal to the ventral margin of the centrum. Unlike all other cervicals (and dorsals), the prezygapophysis is oriented nearly vertically, such that its posterior margin is approximately even with the anterior edge of the neural spine. In addition, the postzygodiapophyseal lamina is not concave but bears an outward kink close to its dorsal terminus.

In anterior view, the diapophysis is more elevated than in C9, with a more expansive anterior face and associated infraprezygapophyseal fossa. As seen in posterior view, the postzygapophysis is elevated to the level of the neural spine. As in C8 and C9, the dorsal surface of the arch bears a pneumatic foramen that faces the area of the prezygapophysis. The arch is visibly set back from the anterior border of the centrum in dorsal view.

Trends within the cervical series: The entire cervical series of *Masiakasaurus* is highly pneumatized. This pneumaticity includes: (1) two fossae on the centrum, the anterior of which consistently forms a foramen; (2) communications between the centrum and arch pneumaticity via the neurocentral suture; (3) three deeply invaginated fossae ventral to the transverse process on the neural arch, each with one or more foramina; and (4) peduncular fossae and foramina. Within the series, pneumaticity increases posteriorly; examples include the appearance of peduncular fossae subsequent to C4 and the presence of foramina on the dorsal surface of the arch starting on C6. It is likely that the pneumaticity of the anterior centrum fossae is directly related to cervical rib pneumaticity (see below). Similarly, the dorsal arch fossae of C6–C10 might bear some relation to the presence of a fossa alongside the prezygapophyseal–epipophyseal lamina in C3 and C4.

The anterior half of the cervical series articulates along a gentle curve in its neutral position, but the last half is nearly straight because of the lack of offset between the anterior and posterior centrum faces. The epipophyses

are more pronounced anteriorly as well, and the neural spine is longer, although still small. Pronounced left-right asymmetry is common with respect to both the presence and degree of development of pneumatic structures.

Although the absence of significant centrum length changes obscures some aspects of the cervicodorsal transition in *Masiakasaurus*, this transition is nonetheless evident in other morphological features. For example, the transverse distance between both the pre- and postzygapophyses declines rapidly from C9–D2, and both articulations become more horizontally oriented (Figure 13). A the same time, the prezygapophysis and its peduncle become vertically oriented in lateral view, and then abruptly lower again.

Dorsal vertebrae: Compared with the most posterior cervicals, the only known first dorsal vertebra (D1; Figure 12M–P; FMNH PR 2837) has a more equilateral profile overall. The centrum remains proportionally long (length:height = 2.0), although the ventral margin is more strongly arched (and this arch has a more posteriorly positioned apex) than in the posterior cervicals. The parapophysis is D-shaped and situated just ventral to the neurocentral suture, which remains visible but not patent (Figure 12M). A large, elliptical pneumatic foramen lies directly posterior to the parapophysis and opens into a chamber within the centrum. Marked, longitudinally oriented striations are present along the rims of the centrum faces.

The arch laminae are well developed (Figure 12M). An extensive pneumatic fossa occupies most of the large infraprezygapophyseal fossa on the left side, whereas the right is perforated by a large foramen; on both sides a smaller, round foramen is present in the posterodorsal corner of the fossa. The infradiapophyseal fossa is small

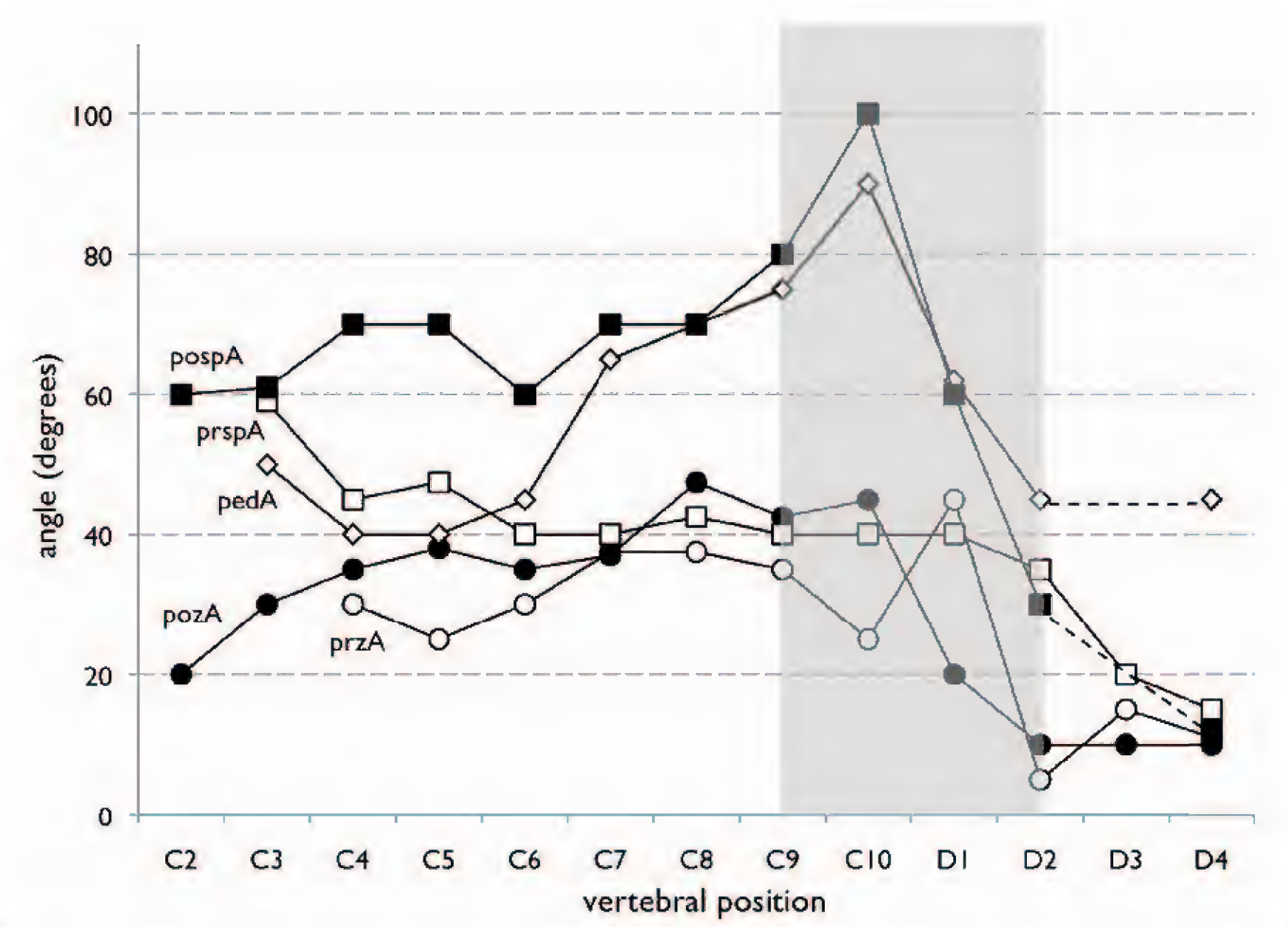

FIGURE 13. Morphological changes in the cervical and anterior dorsal vertebrae of *Masiakasaurus knopfleri*. Dashed lines represent interpolations across missing data; gray area indicates the region of the cervicodorsal transition. Abbreviations: pedA (diamonds) = angle between floor of neural canal and axis of prezygapophyseal peduncle in lateral view; pospA (solid squares) = angle between left and right edges of postspinal fossa in dorsal view; pozA (solid circles) = angle of vertical inclination of postzygapophysis in posterior view; prspA (open squares) = angle between left and right edges of prespinal fossa in dorsal view; przA (open circles) = angle of vertical inclination of prezygapophysis in anterior view.

and leads to the arch interior via a rounded foramen. Likewise, another foramen is present at the anterior corner of the intermediate-sized infrapostzygapophyseal fossa. The transverse processes are broken on both sides, although the left is more complete. The neural spine is moderately tall (about the height of the centrum), anteroposteriorly short, and located on the posterior half of the arch.

In anterior view, the centrum appears weakly concave and slightly wider than tall, whereas the neural canal is nearly circular and much smaller (Figure 12N). The pedicles are imperforate, and the base of the transverse process suggests that it was slightly elevated. The prezygapophyses are angled at 45° and connected medially to the more ventrally positioned hypantrum. Between them, a small fossa is visible at the base of the neural arch, positioned ventral to a flat but extensively roughened contact surface for the interspinous ligaments. The centrum is more strongly concave posteriorly. A narrow kink demarcates the postzygapophyses from the adjacent (and slightly dorsolaterally facing) hyposphene (Figure 12O). The posterior face of the neural spine also bears a surface for the interspinous ligaments, but is somewhat concave and terminates ventrally at a more acuminate fossa.

Dorsally, the prezygapophyses are trapezoidal with rounded edges, and are separated from one another along the midline by a space approximately equal to the transverse width of the neural spine (Figure 12P). The neural spine has a complex dorsal outline that has a "waisted" appearance. In ventral view, the centrum is hourglass-shaped, and bears neither a keel nor a groove.

The second dorsal vertebra (D2) is represented only by the neural arch. This is proportionally taller than the arch of D1, and it has a larger, shallower infradiapophyseal fossa and a more expansive infraprezygapophyseal fossa. The infrapostzygapophyseal fossa is smaller and faces more posteriorly. Here and in successive vertebrae, the hypantrum and hyposphene are more vertically oriented.

Dorsal vertebra three (D3) is identified based on the position of the parapophysis, the dorsalmost portion of which overlaps the neurocentral suture. The parapophysis is dorsoventrally elongate, and lies anterior to a large, elliptical pneumatic foramen. The neurocentral suture is marked and rugose. Proportionally, the infraprezygapophyseal fossa is the largest arch fossa, and is subdivided into at least two chambers. The neural spine is taller than in D2, and the prezygapophyses extend nearly horizontally, with a vertically deep hypantrum visible in lateral view. Dorsally, the neural spine apex is Y-shaped, and located over the posterior half of the centrum. The prezygapophyses are rectangular and separated by a narrow incisure.

In the fourth dorsal vertebra (D4), the parapophysis sits directly on the neurocentral suture. Its dorsal migration intersects the anterior centrodiapophyseal lamina, thereby forming the paradiapophyseal lamina. This lamina is more anteriorly placed, enlarging the infradiapophyseal fossa at the expense of the infraprezygapophyseal fossa. The infrapostzygapophyseal fossa is very small and forms a narrow triangle. The centrum is weakly concave on its lateral surface but bears neither fossae nor foramina. The neural spine is slightly more anteroposteriorly expanded at its tip than in D2, and bears projecting rugosities for the attachment of interspinous ligaments. The centrum faces are more D-shaped than in the preceding dorsals, and the parapophysis projects significantly laterally in anterior view. Posteriorly, the posterior centrodiapophyseal lamina is visible along the entire edge of the transverse process. This process is rectangular but deflected posteriorly about 30° in dorsal view.

It is difficult to determine whether the immediately subsequent vertebrae are represented in our sample, or one or more positions are missing instead. We interpret two dorsal vertebrae associated with a partial skeleton (FMNH PR 2481) to represent the fifth (D5) and sixth (D6) dorsal vertebrae (Figure 14); they are certainly more posteriorly positioned than D4. Both are distinguished from preceding vertebrae in the position of the parapophysis, which is located entirely on the neural arch (Figure 14D). It is hung beneath the transverse process at two-thirds of its length from the centrum, and connected to it via distinct anterior and posterior centroparapophyseal laminae. The transverse process is projected far laterally, and terminates with a stout diapophyseal facet at its posterolateral corner (Figure 14B,C). It is much broader anteroposteriorly than in D4. The neural spine is considerably longer anteroposteriorly than in D4. In anterior view, the prezygodiapophyseal lamina forms a strong ledge along the anterodorsal margin of the diapophysis. The centrum face is slightly taller than wide and much larger than the neural canal. The neural spine shows a slight trasverse widening at its apex.

A third dorsal vertebra associated with partial skeleton FMNH PR 2481 is identified as the seventh dorsal vertebra (D7) based on the preceding interpretation, but could also be placed more posteriorly (although anterior to the vertebrae described below). Here the parapophysis is located farther laterally along the transverse process, closer to the position of the diapophysis. The neural spine is anteroposteriorly longer than in D5. In posterior view, a triangular, deeply inset infrapostzygapophyseal fossa is visible on the transverse process between a marked postzygodiapophyseal lamina and a rounded posterior centrodiapophyseal lamina.

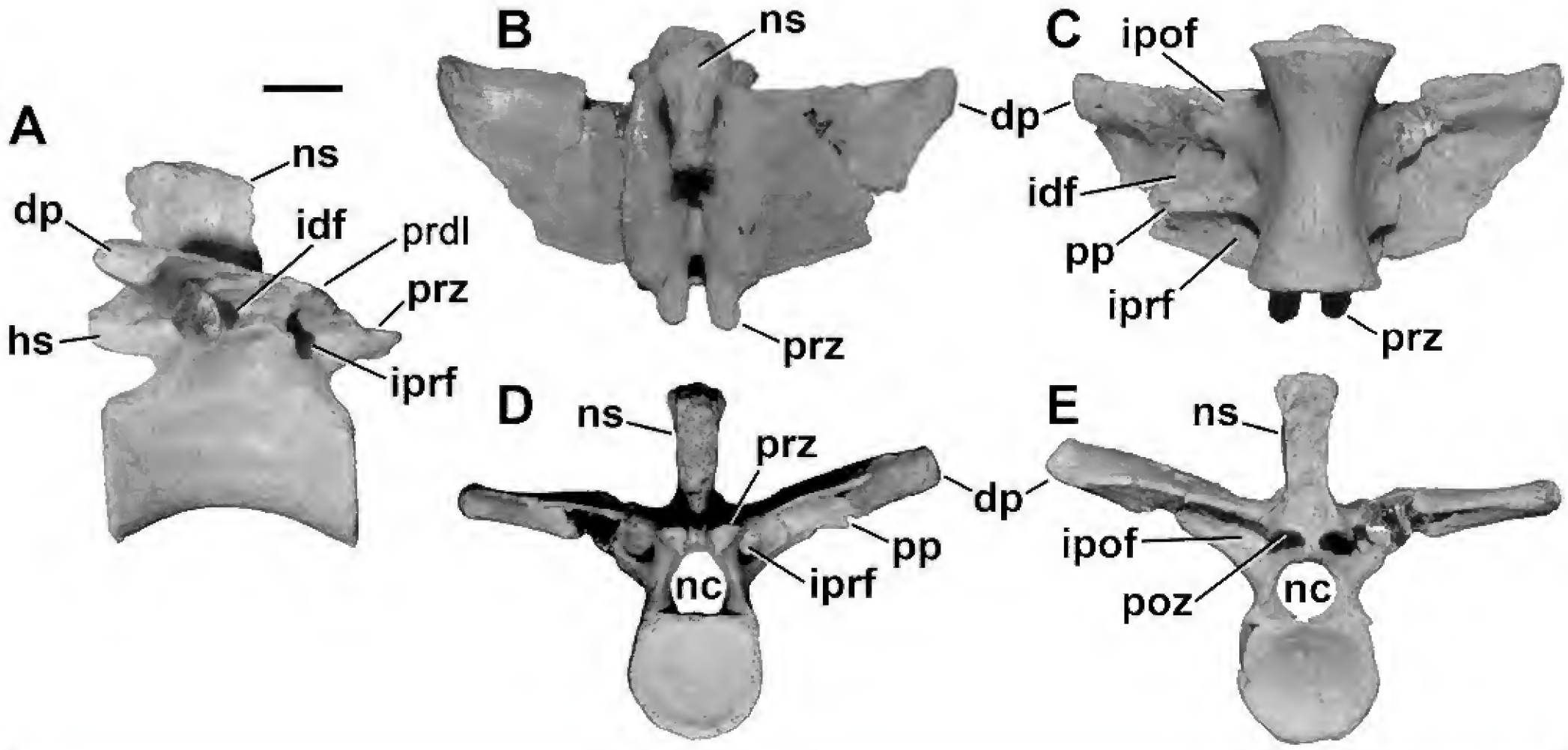

FIGURE 14. Sixth dorsal vertebra (FMNH PR 2481) of *Masiakasaurus knopfleri* in right lateral (A), dorsal (B), ventral (C), anterior (D), and posterior views. Abbreviations: dp = diapophysis; hs = hyposphene; idf = infradiapophyseal fossa; ipof = infrapostzygapophyseal fossa; iprf = infraprezygapophyseal fossa; nc = neural canal; ns = neural spine; poz = postzygapophysis; pp = parapophysis; prdl = prezygodiapophyseal lamina; prz = prezygapophysis. Scale bar = 1 cm.

Several posterior dorsal vertebrae are preserved nearly articulated in this associated specimen (FMNH PR 2481). These dorsals, probably equivalent to D11–D14, show no reduction in centrum length or significant proportional changes from the anterior dorsals. The centra remain apneumatic, but the arches are highly pneumatized. Vertebrae D12 and D13 preserve the parapophysis, which is located on a pedestal that is slung below the anterior edge of the transverse process. The transverse processes are tilted dorsally about 30°. The neural spines are embedded in matrix and cannot be observed.

A similar morphology is also evident in isolated posterior dorsals (UA 9103, 9176), in which the neural spine is located over the posterior two-thirds of the centrum, although the transverse processes are angled upward at about 25°. The anterior centrum face is concave, whereas the posterior face is flattened. The neural canal is nearly round, although the centrum face has a horizontal edge at the entry and exit of the canal. The three lateral arch fossae are subequal in size, although the infrapostzygapophyseal fossa is the deepest and largest. On UA 9176, the infraprezygapophyseal and infradiapophyseal fossae each have a foramen on the right side only; a foramen is present in the infrapostzygapophyseal fossa on both sides. The pre- and postzygapophyses are close together near the midline and approximately horizontal (the prezygapophyses face slightly laterally). The adjacent hyposphene–hypantrum is longer dorsoventrally than the respective zygapophysis is wide transversely. The small prespinal fossa is deep, and it gives way dorsally to a concave interspinous ligament attachment. The incomplete postspinal fossa appears to contain additional foramina. The neural spine is vertical and placed over the posterior half of the centrum.

Trends within the dorsal series: Unlike many other theropods, the dorsal centra of *Masiakasaurus* show little change in proportion from anterior to posterior. The posterior dorsals are unusually long, like the posterior cervicals, and there is no pronounced shortening through the cervicodorsal transition. Neural arch pneumaticity is pronounced throughout, continuing into the sacral series. As in other abelisauroids, the parapophysis migrates onto the neural arch in the first few dorsals and eventually out along the transverse process by the midtrunk. Laminae remain distinct throughout, although they become less pronounced close to the sacrum. Finally, the hyposphene-hypantrum articulation is present in all dorsals.

Sacral vertebrae: Several new specimens nearly complete our knowledge of the sacrum in *Masiakasaurus*, previously known only from three articulated elements (FMNH PR 2142; Carrano et al., 2002). Specimen UA 9098 includes a large sacral 6 that retains an attachment to the partial preceding vertebra. The centrum has a flattened ventral surface but lacks a distinct groove or keel, and its flat, finished posterior face marks it as the last sacral. The posteroventral edge is lower than the anteroventral edge, indicating that the ventral margin of the sacrum was arched. The lateral centrum surface is devoid of fossae or foramina.

The neural arch bears a distinct hyposphene that borders a more anteriorly placed fossa. This fossa is separated from the true infraprezygapophyseal fossa by a vertical ridge (also present on sacral UA 9115). The transverse process and sacral rib are fused, forming a large, curved, dorsally concave structure that sweeps anteroventrally from the centrum. Its attachment spans the upper half of the centrum. A deep, distinct, and subdivided (pneumatic?) fossa is present on the anterior part of the dorsal surface of the transverse process, while another fossa excavates more posteriorly into the postzygodiapophyseal lamina. These fossae are connected internally within the transverse process and sacral rib, as shown by the chambers exposed on the damaged left side.

Another sacrum (FMNH PR 2460) is composed of four fused centra, overlapping the three preserved in FMNH PR 2142 (Carrano et al., 2002) and including one additional vertebra posteriorly (the last sacral). This latter vertebra resembles UA 9098 and shows even more clearly that the sacrum is ventrally arched in *Masiakasaurus* as in abelisaurids, although it lacks the strong mediolateral constriction seen in some other abelisauroids. The first sacral in this series bears a sutural anterior centrum face, indicating the presence of at least one additional sacral.

The ventral surface of the neural canal is exposed in the last two sacrals of this specimen, and is transversely wide and relatively flat. The transverse process and sacral rib are missing at the junction of these two vertebrae; this, along with the sutural face of sacral 3, suggests that this was an immature individual. The ventral surfaces of all preserved sacrals are flat, and none of the centra show evidence of pneumatic foramina.

Finally, an associated specimen (FMNH PR 2481; Figure 15) includes the full complement of six sacrals in near-articulation with the ilia. Although only the dorsal surfaces of the neural arches and sacral ribs are visible in

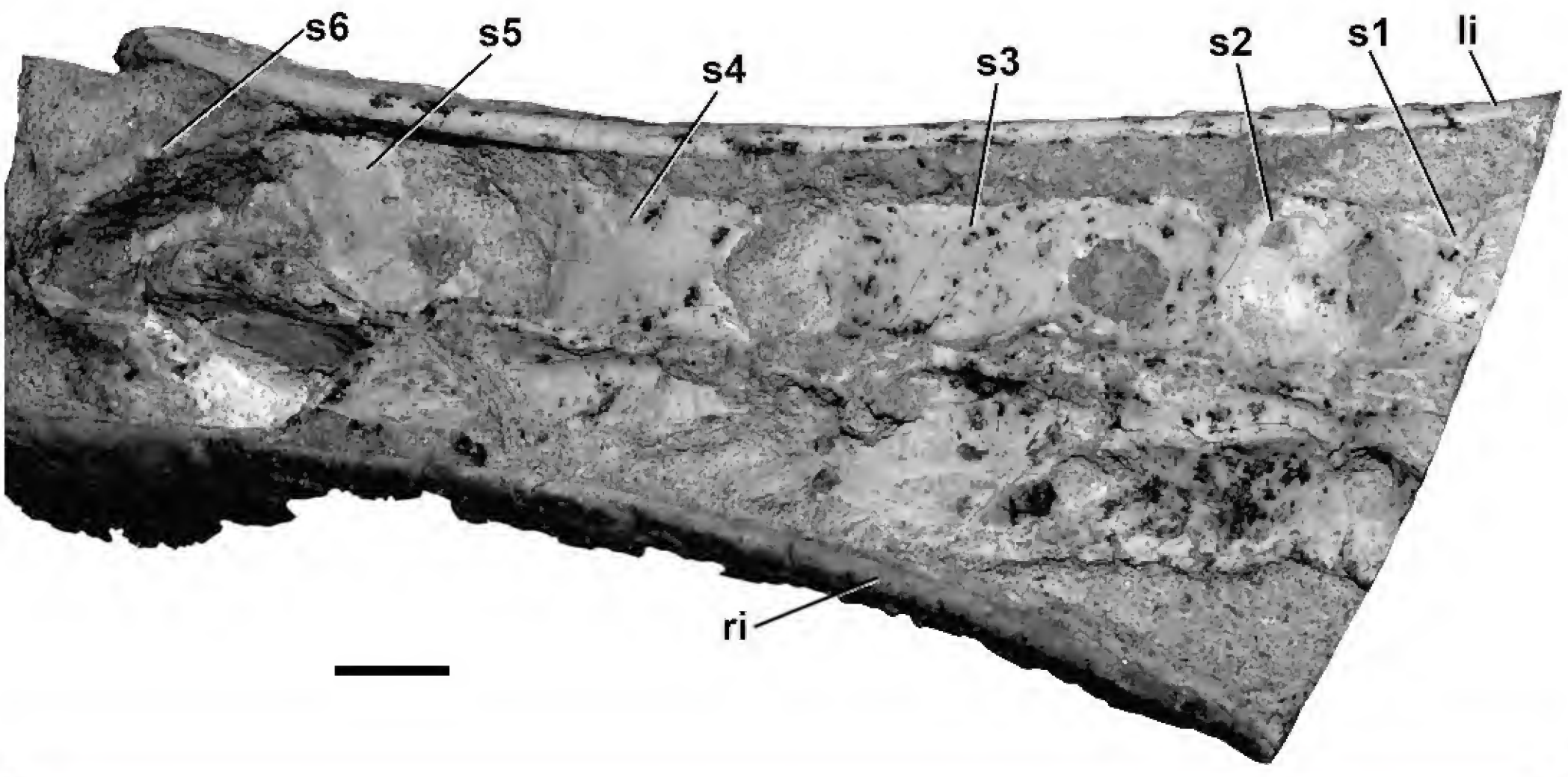

FIGURE 15. Sacrum (FMNH PR 2485) of *Masiakasaurus knopfleri* in dorsal view. Abbreviations: li = left iliac blade; ri = right iliac blade; s1–s6 = sacral vertebrae 1 through 6. Scale bar = 1 cm. (Anterior is to the right.)

this specimen (which is in a block of matrix), it is clear that all six vertebrae contacted the iliac blades. Most of the sacral ribs appear to contact one another at or near their articulation with the ilium. The morphology of the sacral ribs and transverse processes suggests that the full sacrum consisted of two primordial sacrals plus two dorsosacrals and two caudosacrals. In all of the specimens that can be observed in anteroposterior view, the centra are D-shaped as in abelisaurids such as *Majungasaurus* (O'Connor, 2007).

Caudal vertebrae: Additional specimens of anterior caudal vertebrae reveal that, like the presacrals, all the caudals in *Masiakasaurus* are proportionally long, with the centrum length at least twice the height. Unlike the anterior presacrals, the caudal vertebral centra are taller than wide, as in *Carnotaurus* and *Majungasaurus*. These anterior caudals do not show any evidence of centrum pneumaticity, but the neural arch retains three distinct laminae connected to the diapophysis, which delimit three corresponding arch fossae. These are pronounced when compared to those in most other theropods, although weaker than those of sauropods (e.g., Wilson, 1999). The centrum is amphicoelous and often bears a weak ventral groove, as well as chevron facets at the anteroventral and posteroventral corners of the centrum.

The neural arch in these anterior caudals retains a hyposphene and hypantrum, both of which are smaller than their respective zygapophyses, which are large and oriented at about 75° above the horizontal. In most of these vertebrae the neurocentral suture is faint, but the arch and centrum have separated along this suture in one large specimen (UA 9173), indicating immaturity of that individual. The lobate transverse process is swept posteriorly about 45°, and is tilted dorsally approximately 10°. On UA 9112, a shallow longitudinal fossa can be seen alongside the base of the neural spine on the dorsal surface of the transverse process. The prespinal fossa is reduced to a small foramen at the base of a narrow interspinous ligament groove. Here the zygapophyses are angled at only 45°, again contiguous with a smaller, vertical hyposphene–hypantrum.

Vertebrae from toward the middle of the tail show the reduction in centrum height and size of the neural spine that often characterizes theropods (Figure 16). However, a significant transverse process is retained until well into the posterior part of the tail, along with short prezygapophyses. For example, a low, elongate middle caudal associated with FMNH PR 2481 includes a small, acuminate neural spine but also exhibits a large, posteriorly deflected transverse process and a prezygapophysis that extends less than one millimeter beyond the anterior edge of the centrum. The slightly more anteriorly placed FMNH PR 2482 shows the neural spine to be anteroposteriorly short but still tall and rectangular.

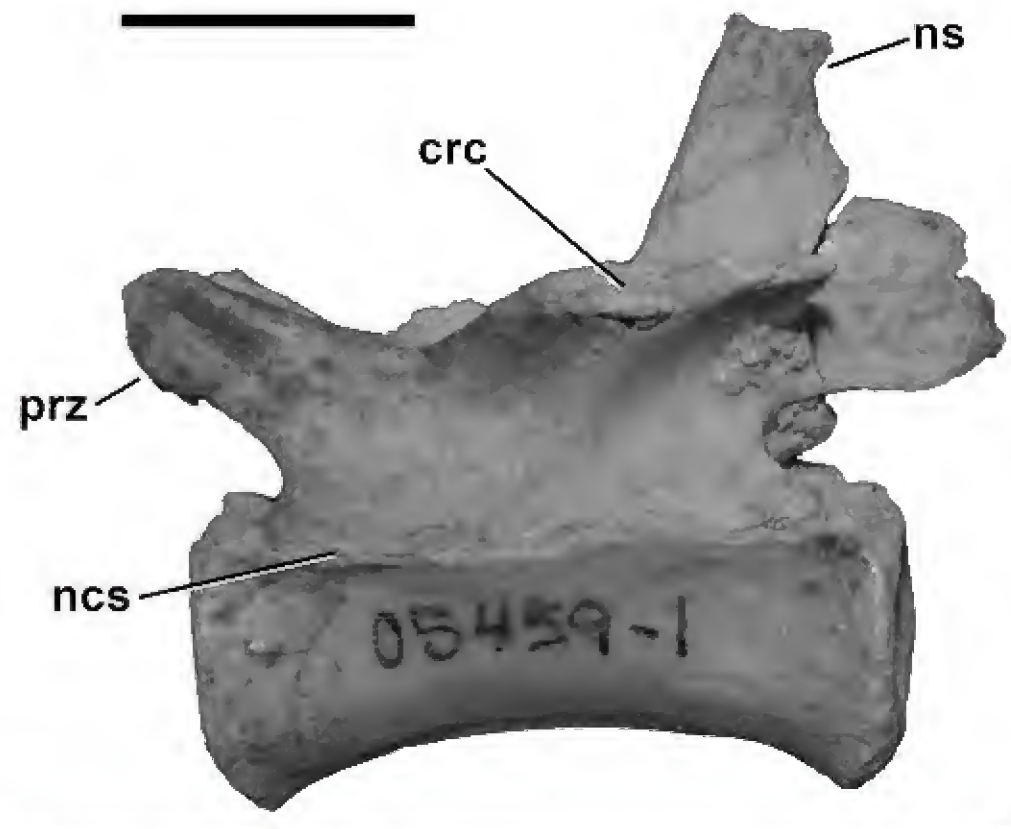

FIGURE 16. Middle caudal vertebra (FMNH PR 2485) of *Masiakasaurus knopfleri* in left lateral view, showing the potential contact surface for a caudal rib at the lateral end of the transverse process. Abbreviations: crc = caudal rib contact; ncs = neurocentral suture; ns = neural spine; prz = prezygapophysis. Scale bar = 1 cm.

The transverse process is reduced to a thin spur in more posteriorly positioned caudals of FMNH PR 2481, which have a more extended prezygapophysis, a lower relative centrum height, and a low, rounded neural spine. In the posterior half of the tail, the prezygapophysis overlaps at least one-third of the preceding centrum, although a rudimentary neural spine and transverse ridge may still be evident (e.g., FMNH PR 2638). The neural spine is absent only in the most posterior caudals, which nonetheless retain both the transverse ridge and a ventral groove.

Trends within the caudal series: The anterior caudals of *Masiakasaurus* are strikingly similar to the posterior dorsals, particularly in their proportions but also in the retention of arch laminae. The transverse processes remain lengthy and pronounced well into the middle caudals, where they become increasingly upturned (although even the transverse processes of the anterior caudals are slightly upturned). As in abelisaurids, anteroposterior expansion of the lateral end of the transverse processes occurs well into the middle caudals (but see "Caudal Ribs?" below). The neural spine becomes increasingly posteriorly

positioned on the arch, then shrinks to a low ridge. The zygapophyses lengthen to overlap the adjacent vertebra in the posterior caudals, subsequent to the disappearance of the transverse process. There does not appear to be any "transition point" in the tail, but rather all features shift gradually and independently along the series.

Cervical and dorsal ribs: Several partial cervical and dorsal ribs have been found. The cervical ribs are highly pneumatized, as in *Carnotaurus*, *Majungasaurus*, *Noasaurus*, and *Spinostropheus*, and bear a web that connects the triangular capitulum to the more rounded tuberculum. On both sides of this capitulotubercular web, pneumatic fossae are variably developed along the cervical series. Although pneumaticity persists into the anterior dorsal ribs, it is much less extensive and does not continue throughout the trunk. Ribs from the most posterior section of the trunk are unknown.

In the fourth cervical rib, the tuberculum and capitulum are closely placed, connected by a thin capitulotubercular web. Both are circular, but the capitulum is concave, whereas the tuberculum is convex. Two foramina pierce the rib between these and the anterior flange. Distal to the capitulotubercular web, a single large fossa, subdivided into two foramina, enters the bone. The shaft flares distally, showing evidence of bifurcation (a small notch) on the broken surface. This morphology is consistent with one of the cervical ribs of *Noasaurus*, which may also pertain to C4 (Bonaparte and Powell, 1980: fig. 8I–J).

The sixth cervical rib (Figure 17) is also bifurcate distally, with a long slender main shaft flanked by a shorter, finger-like accessory process. There is just a shallow concavity between the capitulotubercular web and the short anterior flange, but a true fossa was apparently present on the flange itself (Figure 17D). The circular tuberculum has only a short neck, as does the capitulum. Pneumaticity is variable. In a cervical rib associated with FMNH PR 2485, there is a large pneumatic fossa, which contains three subsidiary foramina, at the shaft base (Figure 17D). Two smaller fossae flank this large one proximally, at the bases of the tuberculum and capitulum, respectively. In contrast, UA 9169 has one foramen both proximal and distal to the capitulotubercular web.

On the seventh cervical rib, the anterior flange is bifurcate, the tubercular neck is quite short, and the fossa between these two and the capitulum is teardrop-shaped and placed closer to the flange. The posterior rib fossae distal to the capitulotubercular web are damaged, but may have interconnected through the interior of the bone.

The ninth cervical rib houses two pneumatic foramina along with a faint, anteriorly directed capitulotubercular

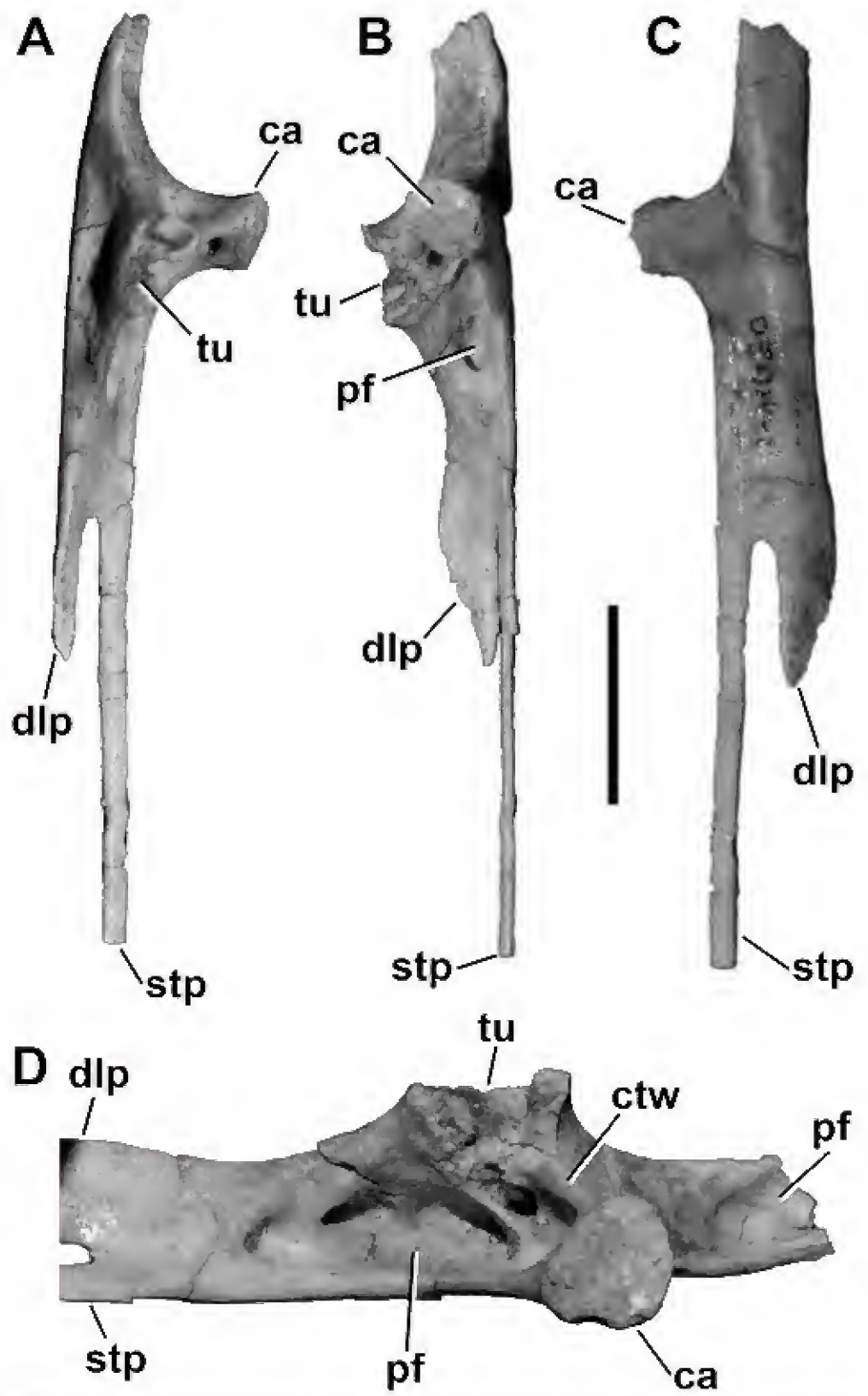

FIGURE 17. Right sixth cervical rib (FMNH PR 2485) of *Masiakasaurus knopfleri* in dorsal (A), medial (B), and lateral (C) views, with a close-up medial view of pneumaticity surrounding the capitulotubercular web (D). Abbreviations: ca = capitulum; ctw = capitulotubercular web; dlp = dorsolateral process; pf = pneumatic fossae and foramina; stp = styliform process; tu = tuberculum. Scale bar = 1 cm for A–C.

web. Four additional pneumatic foramina populate an equally deep fossa distal to this web. The lateral surface of the rib is smooth and convex. The capitulum is not visible in this view, obscured by the prominent, bifurcate anterior flange. In this view the rib can be seen to widen significantly at the base of the shaft, as in abelisaurids (e.g., *Carnotaurus* and *Majungasaurus*).

The tenth cervical rib bears a long, thick anterior flange, and remains wide distal to the capitulum, where it bears both the main shaft and a second, thinner styliform process that terminates in a small knob. Between the capitulum and tuberculum medially, a large fossa bears three distinct foramina, two of which are as large as the tuberculum. The tuberculum sits on a short neck, whereas the capitulum exists as an articular pad that is barely elevated above the connecting web. A single, small, circular foramen penetrates into the rib at the junction of the capitulum, tuberculum, and anterior flange. Another specimen (FMNH PR 2672) may be the tenth cervical or the first dorsal rib. The preserved capitulum sits on a short neck, and is circular. Only a single pneumatic fossa is present, situated anteriorly adjacent to the capitulotubercular web. The second known cervical rib of *Noasaurus* (originally described as a squamosal; Bonaparte and Powell, 1980: fig. 7D–E) corresponds to one of these two positions.

Two fragmentary ribs (FMNH PR 2458, UA 9160) appear to have articulated with approximately the fourth dorsal vertebra. In these, the capitulum is small and square, terminating a long, slender neck. In contrast, the tuberculum is mediolaterally elongate, and sits atop a short but distinct pedicle. The connecting capitulotubercular web is thin. The anterior surface is generally concave, whereas the posterior surface is convex. The proximal part of the shaft exhibits some broadening, created via distinct flanges that extend both anteriorly and posteriorly from the main shaft. The cross-section is T-shaped proximally but becomes oval distally. The shaft bears a posterior neurovascular groove. A small, elliptical fossa is present in the proximal shaft of a dorsal rib associated with FMNH PR 2485 and indicates that, unlike *Majungasaurus* (O'Connor, 2007), at least some of the dorsal ribs of *Masiakasaurus* were pneumatized.

Several ribs are from unknown positions within the trunk but nonetheless are anatomically informative. Specimen FMNH PR 2481 includes the proximal third of a right dorsal rib, preserving only the elongate tuberculum and part of the shaft. The tubercular neck is very short. The lateral part of the shaft is expanded into a T-shaped cross-section just distal to the rib heads. Both the anterior and posterior edges of this expansion are bounded by grooves, the posterior bearing a bisected, oval pneumatic fossa near the proximal end. The rib curves strongly in its proximal part, then acquires a nearly straight shaft for much of its length, suggesting a relatively narrow body shape.

Gastralia: Specimen FMNH PR 2481 includes a fused set of anterior gastralia. This is a partially complete, V-shaped element composed of two very slender rami that meet at a broad angle (approximately 120°). On the anterior surface, a low bump is present along the ventral midline marking the zone of fusion. The distal ends of the rami are lacking.

Chevrons: Several chevrons have been identified, one of which is complete and probably from the middle part of the tail (UA 9152). It is curved posteriorly along its length and terminates in a broad point. The anterior and posterior curvatures are not parallel, however, creating a slight expansion near the distal end. The distal end is neither rounded as in *Allosaurus* and many other basal tetanurans, nor "boat-shaped" as in many coelurosaurs. The saddle-shaped proximal articulation encloses the haemal canal, as is typical of theropod chevrons. In lateral view this articulation bulges dorsally. The anterior and posterior processes are small but distinct; the anterior is moderately sized, blunt, and tall, whereas the posterior is upturned and acuminate. The anterior processes approach one another toward the midline but do not contact.

Caudal ribs? Two caudals of *Masiakasaurus* (FMNH PR 2469, 2481) show an apparent suture directed longitudinally across the lateral part of the transverse process. This suture discriminates the expanded lateral portion of the process from the more conventionally shaped medial part. We interpret this suture as evidence that the expanded lateral end of the transverse process is actually a caudal rib, likely present throughout at least the anterior half of the tail. Two additional caudal vertebrae preserve a roughened, suture-like surface at the ends of both transverse processes (FMNH PR 2126, 2458; Figure 16:crc). In this light, we also reinterpret the similar morphology previously observed in other abelisauroids (*Carnotaurus*, *Aucasaurus*) as evidence of caudal ribs, and suggest that the absence of these structures in *Majungasaurus* (O'Connor, 2007) is due to the subadult nature of many individuals of this taxon.

Appendicular Skeleton

The pectoral girdle and forelimb of *Masiakasaurus* were the most poorly known parts of the animal after the skull, and unfortunately we can shed only some new light on these regions. The radius and ulna remain unknown, but portions of the manus and pectoral girdle can now be described. Fortunately, both the pelvis and hind limb are now almost completely represented.

Pectoral girdle: The scapula and coracoid show an unusual morphology that finds some complement among other members of Ceratosauria. When articulated (Figure 18A), the scapulocoracoid is mediolaterally curved and presents an enormous area for muscle attachment anterior and ventral to the glenoid.

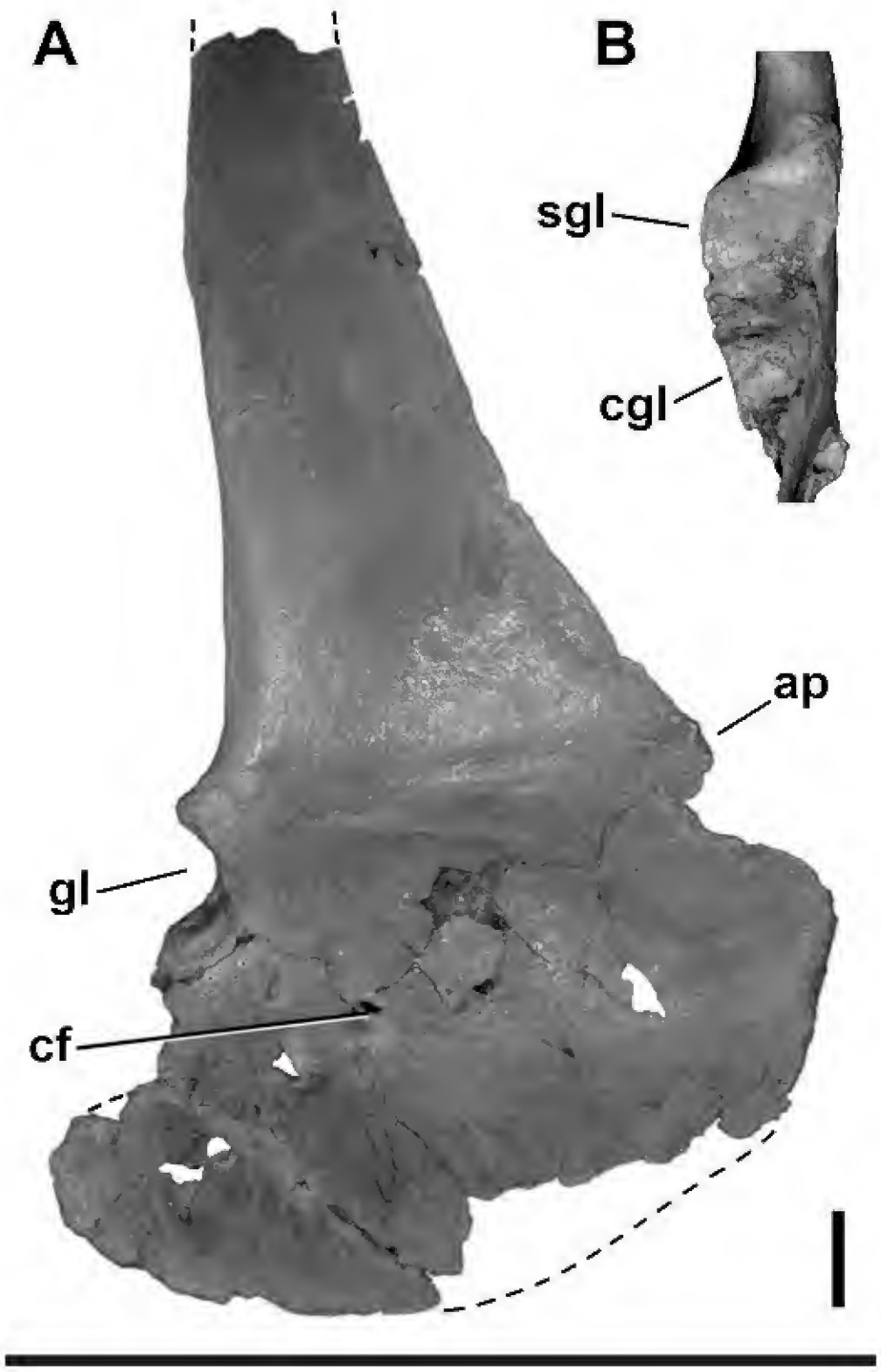

FIGURE 18. Right scapulocoracoid (UA 9160) of *Masiakasaurus knopfleri* in lateral view (A), with a close-up of the glenoid in posterior/articular view (B). Abbreviations: ap = acromial process; cf = coracoid foramen; cgl = coracoid portion of glenoid; gl = glenoid; sgl = scapular portion of glenoid. Scale bar = 1 cm for A.

The scapula has a curved blade that reflects the shape of the underlying rib cage, and is broad relative to its length as in coelophysoids as well as other ceratosaurs. It appears to taper uniformly dorsally, but the dorsal-most end is not known and so we cannot determine whether it was reexpanded as in coelophysoids. As preserved, the blade is almost twice as long as the distance between the glenoid and acromion.

The glenoid has a pronounced anterodorsal rim, as in *Ceratosaurus* and *Majungasaurus*. In posterior view the scapular portion of the glenoid is D-shaped, and substantially taller dorsoventrally than wide mediolaterally (Figure 18B). Its ventral margin along the coracoid suture is oriented obliquely rather than horizontally. This ventral portion is mediolaterally thicker than the blade, especially as it approaches the coracoid suture. In posterior view, nearly the entire scapula is extremely thin, tapering to a sharp edge.

The coracoid is expansive and oval, with the long axis oriented anteroposteriorly (Figure 18A). It is much broader than the same element in basal theropods such as *Dilophosaurus* and *Coelophysis*, more closely resembling the condition in *Elaphrosaurus*, *Limusaurus*, and abelisaurids (although it is more anteroposteriorly elongate than in the latter). The posteroventral process is blunt, projecting only slightly beyond the posteriormost part of the glenoid. It is extremely thin mediolaterally, more so than in almost any other theropod, and lacks the characteristic medial concavity. The coracoid foramen is placed close to the scapular contact, such that most of the coracoid is anterior and ventral to the foramen. The passage between the lateral and medial openings of the foramen runs obliquely ventrolaterally-dorsomedially, as in other theropods. The glenoid region shows that more than two-thirds of the articular surface is formed by the scapula, although a weak rim also bounds the coracoid portion of the glenoid ventrally.

One specimen (UA 9160; Figure 18A) shows a series of openings arranged in a line directed posteroventrally from the coracoid foramen. These could be unhealed puncture marks, created during predation or scavenging. Alternatively, they may have a pathological origin; one of the openings bears a raised rim that may indicate the presence of a suppurating infection.

Humerus: Two complete left humeri associated with partial skeletons (FMNH PR 2481, 2485) provide nearly the entire morphology of this bone. They resemble previously described specimens (e.g., FMNH PR 2143; Carrano et al., 2002) but include the distal end and therefore the correct proportions of the element (Figure 19; Table 1). Overall it is concave curved medially but nearly straight in the anteroposterior plane. The deltopectoral crest is proportionally short, extending down only about one-third of the total shaft length. The distal condyles, although slightly damaged, are clearly flattened proximodistally as in abelisaurids, *Ceratosaurus*, and *Elaphrosaurus*. Both the entepicondyle and ectepicondyle are located along the narrow margins close to the distal end, but are indistinctly developed in this specimen. The FMNH

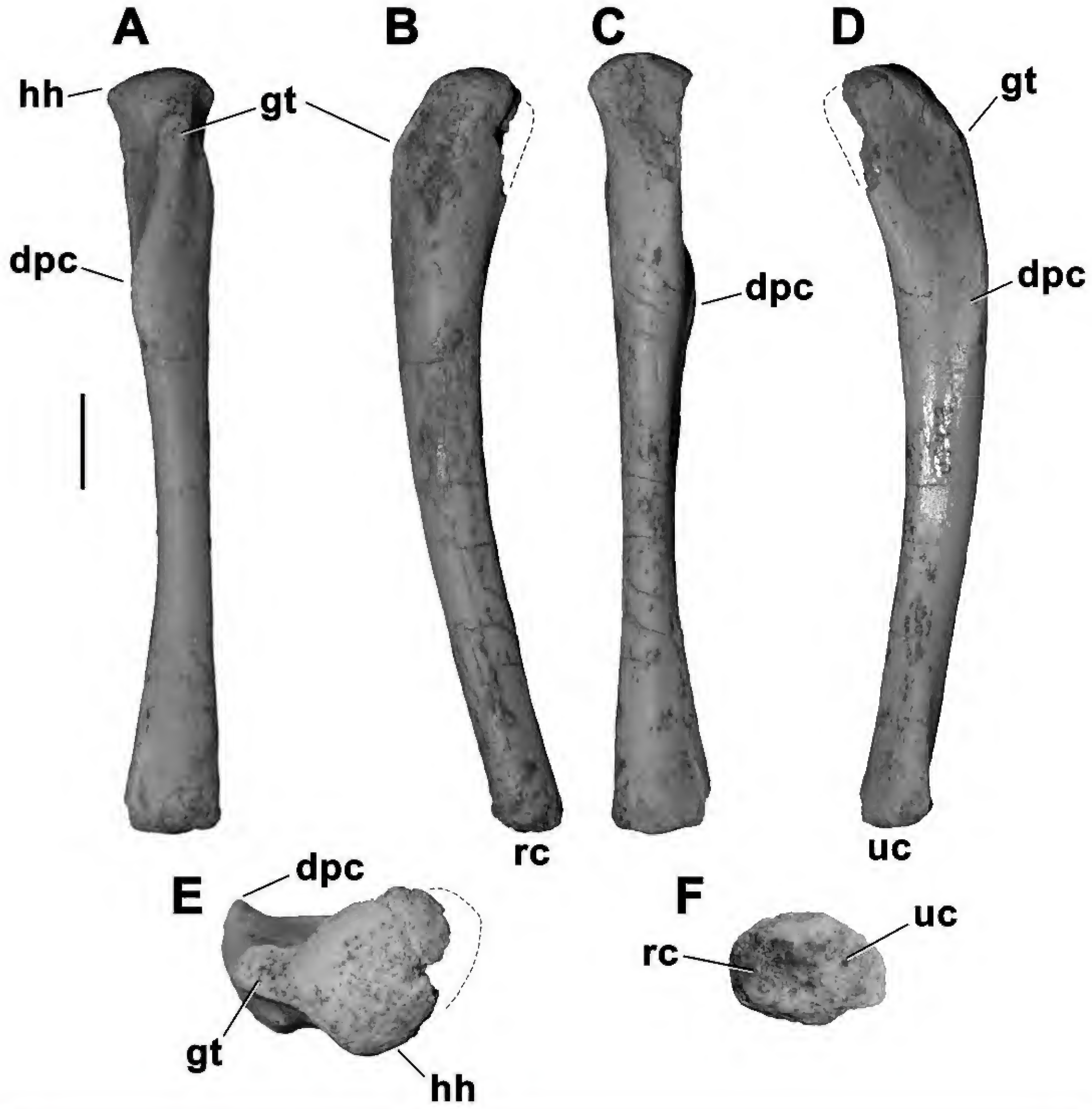

FIGURE 19. Left humerus (FMNH PR 2485) of *Masiakasaurus knopfleri* in lateral (A), posterior (B), medial (C), anterior (D), proximal (E), and distal (F) views. Abbreviations: dpc = deltopectoral crest; gt = greater trochanter; hh = humeral head; rc = radial condyle; uc = ulnar condyle; scale bars = 1 cm.

TABLE 1. Measurements (in mm) of associated individual *Masiakasaurus knopfleri* from locality MAD05-42. At least four different-sized individuals were present at the site. Some specimens are assigned to two of the individuals below; additional elements are preserved but cannot yet be assigned to any individual. Abbreviations: L = anteroposterior length (unless otherwise indicated); AP = anteroposterior diameter; ML = mediolateral diameter; H = dorsoventral height; prz = prezygapophysis; poz = postzygapophysis; s = sacrum; asc proc = ascending process; D = diameter; W = width. An 'x' indicates an inapplicable measurement; a tilde (~) indicates an estimated position; a question mark (?) indicates missing data; an asterisk (*) indicates estimated length; and a dagger (†) indicates an incomplete measurement.)

		Measurement (mm)				
Element	**Field number**	**L**	**AP**	**ML**	**H**	**Other**
		Larger Individual (FMNH PR 2481)				
Atlantal intercentrum	MAD 07508	5.0	x	15.3	9.4	46.9 (prz–poz)
Cervical vertebra ~5	MAD 07494	?	x	?	?	43.5 (prz–poz)
Cervical vertebra 6	MAD 07436	32.7	x	16.2	11.7	36.4 (prz–poz)
Cervical vertebra 7	MAD 07219	29.4	x	17.1	12.2	33.3 (prz–poz)
Cervical vertebra 9	MAD 07212	26.5	x	17.7	12.0	34.5 (prz–poz)
Dorsal vertebra 5	MAD 07215	26.9	x	15.3	14.2	36.4 (prz–poz)
Dorsal vertebra 6	MAD 07445	28.0	x	15.3	14.4	37.7 (prz–poz)
Dorsal vertebra 7	MAD 07213	28.7	x	17.5	15.3	?
Dorsal vertebra 9 (s-4)	MAD 07494-5	29.0	x	?	20.1	?
Dorsal vertebra 10 (s-3)	MAD 07494-4	29.6	x	?	18.6	?
Dorsal vertebra 11 (s-2)	MAD 07494-3	29.3	x	?	19.8	?
Dorsal vertebra 12 (s-1)	MAD 07494-2	28.9	x	?	21.7	?
Sacrum, complete	MAD 07218-3	148.8	x	35.6	?	x
Anterior caudal vertebra	MAD 07494-1	29.3	x	?	?	?
	MAD 07779	29.1	x	13.6	15.7	?
	MAD 07779	29.0	x	14.8	16.8	?
Mid-caudal vertebra	MAD 07690	28.9	x	13.0	15.0	?
	MAD 07507	29.8	x	12.1	11.1	?
Posterior caudal vertebra	MAD 07503	30.0	x	12.0	10.3	?
	MAD 07211	31.2	x	12.7	10.2	?
	MAD 07213	31.1	x	12.9	10.2	?
	MAD 07208-1	?	x	12.5	10.3	?
	MAD 07838	31.0	x	11.0	8.5	?
	MAD 07443	29.2	x	8.9	7.10	?
Right scapula	MAD 07442	128.4	20.6	2.0*	x	Glenoid L: 14.9, glenoid D: 10.8
Left scapula	MAD 07746	128.2	21.0	3.9	x	Glenoid L: 14.7, glenoid D: 11.2
Left coracoid	MAD 07213	38.0	66.1	3.1*	x	x
Right humerus	MAD 07213	94.3	6.9	9.6	x	x
Left ilium	MAD 07218-1	187.2	x	x	43.2 [a]	x
Left pubis	MAD 07218	206.0	14.1	6.8	x	Boot L: 48.5†
Right pubis	MAD 07218	179.3†	8.9†	?	x	?
Right femur	MAD 07493	193.6*	20.5	15.6*	x	x
Right tibia	MAD 07476	195.8	10.9	17.0	x	x
Left tibia	MAD 07687	196.9	12.5	18.0	x	x
Right fibula	MAD 07487	189.6	8.3	4.7	x	x
Left fibula	MAD 07523	?	8.2	4.7	x	x
Right astragalus	MAD 07216	x	x	24.7 [b]	9.9 [b]	Asc proc W: 12.1, asc proc H: 17.1

TABLE 1. (*continued*)

Element	Field number	L	AP	ML	H	Other
			Larger Individual (FMNH PR 2481)			
Left astragalus	MAD 07440	x	x	25.2 [b]	10.4 [b]	?
Right metatarsal II	MAD 05585	93.2	7.5	3.8	x	x
Left metatarsal II	MAD 07700	?	7.7	3.6	x	x
Right metatarsal III	MAD 07833	112.0	10.3	11.6	x	x
Pedal phalanx III-1	MAD 07537	28.2	9.6	10.0	x	x
Pedal phalanx III-x	MAD 07685	18.2	7.1	10.8	x	x
			Smaller Individual (FMNH PR 2485)			
Cervical vertebra 4	MAD 05443-1	24.7	x	10.7	7.8	36.9 (prz–poz)
Cervical vertebra ~6	MAD 05616-1	25.4	x	10.5	8.3	?
Cervical vertebra ~7	MAD 05467-2	23.4	x	10.5	9.1	?
Dorsal vertebra 4 (arch)	MAD 05459-1	?	x	?	?	21.3 (prz–poz)
Dorsal vertebra (arch)	MAD 05460-27	?	x	?	?	30.5 (prz–poz)
	MAD 07682	?	x	?	?	22.5 (prz–poz)
Sacral 1 (centrum)	MAD 07475	22.2	x	14.4	16.8	?
Anterior caudal vertebra	MAD 05593-3	28.3	x	11.9	13.7	?
Mid-caudal vertebra	MAD 05459-1	23.2	x	9.2	9.7	?
Posterior caudal vertebra	MAD 05386	25.4	x	10.5	8.5	?
Posterior caudal vertebra	MAD 07882-2	27.3	x	9.1	6.9	?
	MAD 07474	25.5	x	6.7	5.2	?
Left humerus	MAD 05418	80.8	5.6	7.6	?	x
Left ilium	MAD 05460-3	146.3	?	?	42.5 [a]	Acetabulum L: 29.0
Left ischium	MAD 05444	?	9.4	9.8	?	Boot L: 23.2
Right ischium	MAD 05444	?	9.0	10.5	?	?
Right femur	MAD 05456	160.7	16.7	14.8	?	x
Left femur	MAD 05467-2	159.8	16.3	14.5	?	x
Right tibia	MAD 05456	173.7	11.3	14.4	?	x
Left tibia	MAD 05419	171.7	11.0	14.4	?	x
Right fibula (proximal)	MAD 05456	?	6.9	3.9	?	x
Left fibula (proximal)	MAD 05419	?	7.2	4.1	?	x
Right metatarsal III	MAD 05460-27	96.4	7.8	9.6	?	x
Right metatarsal IV	MAD 05593-2	?	7.7	7.6	?	x
Pedal phalanx	MAD 05593-1	14.8	7.5	8.1	?	x

[a] Height to apex of acetabulum.
[b] Measurement of body.

PR 2485 humerus is about two-thirds the size of FMNH PR 2143 and is correspondingly less rugose, whereas the FMNH PR 2481 humerus is approximately equivalent in size to FMNH PR 2143.

Manus: UA 9146 appears to be the proximal part of a metacarpal, perhaps the fourth judging by its mediolaterally thin proportions. The slender shaft bears an elliptical, concave proximal articular facet. The shaft is also oval in cross-section, and so thin that the dorsal and ventral edges taper to ridges.

Several manual phalanges have been found (Figure 20). They are uniformly short in proportions, and are characterized by a proximal articular facet that is deeper dorsoventrally than the distal articular surface, weak or absent collateral fossae, and pronounced attachment marks on the lateral and medial surfaces. In addition, the

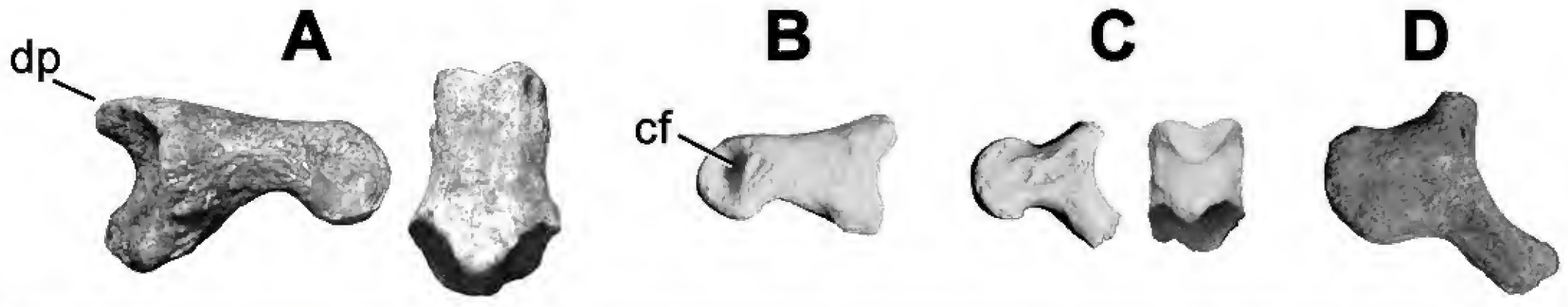

FIGURE 20. Manual phalanges of *Masiakasaurus knopfleri*: (A) FMNH PR 2225 in medial/lateral (left) and dorsal (right) views; (B) FMNH PR 2227 in medial/lateral view; (C) FMNH PR 2132 in medial/lateral (left) and dorsal (right) views; (D) FMNH PR 2224 in medial/lateral view. Abbreviations: cf = collateral fossa; dp = dorsal process. Not to scale.

vertical ridge separating the two halves of the proximal articular facet tends to be well developed and quite visible in mediolateral view, particularly near the dorsal process (Figure 20D).

Different morphologies are evident among the specimens, but with few comparative materials among other ceratosaurs, precise identifications remain tenuous. They vary in overall proportions, shape of the proximal articular surface, and development of collateral fossae. Nonetheless, they bear distinct similarities to the manual phalanges of *Aucasaurus* and *Majungasaurus*.

Specimens FMNH PR 2225 (Figure 20A) and 2227 (Figure 20B) are proportionally the longest phalanges, with lengths 50%–70% greater than their dorsoventral depth; UA 9194 has proportions similar to these although a much larger ventral extension of the proximal articular surface.

Specimens FMNH PR 2132 (Figure 20C) and 2224 (Figure 20D) are extremely short, about as long as they are dorsoventrally deep. They have faint or absent collateral fossae, a very pronounced ventral extension proximally, and oblique, asymmetrical distal condyles.

Specimens FMNH PR 2136 and 2217 (originally referred to the pes; Carrano et al., 2002) share similarly oblique distal condyles with the preceding elements, but the vertical axes of these condyles are not parallel and converge dorsally. The short proportions of these elements suggest that they may be penultimate phalanges, and they resemble the penultimate "pedal" phalanx of *Noasaurus*. Thus we interpret this phalanx in *Noasaurus* as a manual element, along with the supposedly "raptorial" ungual that articulates with it (Carrano and Sampson, 2004b; Agnolin and Chiarelli, 2010). No similar manual unguals are yet known for *Masiakasaurus*.

Pelvic girdle: The pelvic girdle is now completely known. Three ilium specimens together preserve everything except the anteroventral corner of the preacetabular process.

In lateral view (Figure 21A), the ilium exhibits long, deep pre- and postacetabular processes, both of which extended well beyond their respective peduncles. The lateral surface is concave but lacks a centrally placed vertical ridge. A thin, striated scar for the origination of M. iliotibialis extends along the dorsal border (Carrano and Hutchinson, 2002). The acetabulum is open and is overhung by a prominent supraacetabular crest, best seen in FMNH PR 2481. This crest is contiguous with the lateral brevis shelf via a marked ridge, as in *Majungasaurus* and most other abelisaurids. A smaller left ilium (FMNH PR 2485) has a complete postacetabular blade and confirms the very wide brevis fossa. The notched profile of the posterior edge is similar to the condition in *Ceratosaurus* and abelisaurids.

In dorsal view the supraacetabular crest flares posterolaterally, with the greatest overhang located just anterior to the ischial peduncle. As seen in ventral view (Figure 21B), the broad brevis fossa is not particularly deep and widens posteriorly. Both peduncles are similar in size, as in other theropods, but possess prominent pegs that would have lodged into sockets in the pubis and ischium. Similar pegs are also known in abelisaurids, and an ischial peg-and-socket articulation is present in the carcharodontosaurids *Giganotosaurus* (personal observation) and *Mapusaurus* (Coria and Currie, 2006).

The medial surface of the ilium (Figure 21C) bears distinct rugosities that mark the attachment sites for the sacral ribs and transverse processes. Six sacral rib attachments are visible on the ilium associated with FMNH PR 2485, as confirmed by the articulated sacrum of FMNH

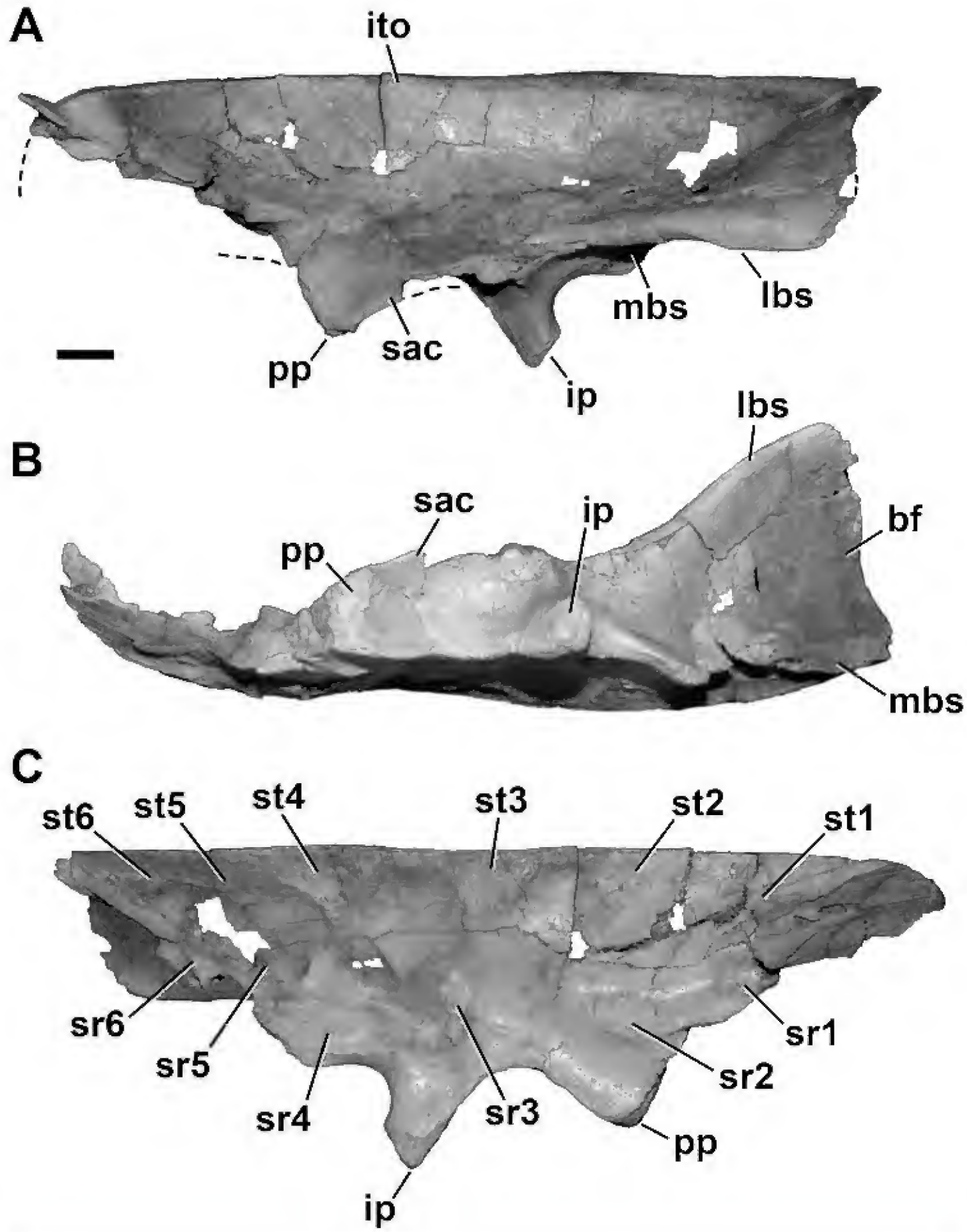

FIGURE 21. Left ilium (FMNH PR 2485) of *Masiakasaurus knopfleri* in lateral (A), ventral (B), and medial (C) views. Abbreviations: bf = brevis fossa; ip = ischial peduncle; ito = origin for *M. iliotibialis*; lbs = lateral brevis shelf; mbs = medial brevis shelf; pp = public peduncle; sac = supraacetabular crest; sr1–6 = attachment sites for sacral ribs 1–6; st1–6 = attachment sites for sacral transverse processes 1–6. Scale bar = 1 cm.

PR 2481. In medial view, the acetabular opening is an ogival arch with a smooth, thin rim. The remainder of the medial surface is smooth and unornamented.

Additional remains of the pubis clarify the morphology of its proximal and distal ends (Figure 22A–C). The right pubis UA 9162 shows evidence of fusion to the articulated ilium and ischium. Much of the exact articulation line has been overprinted by rugose bone growth, although parts of the original path remain discernible, if indistinct. Fusion was also apparently complete along the puboischial contact, although the ventral portion of this area is missing in this specimen. Here again, the suture

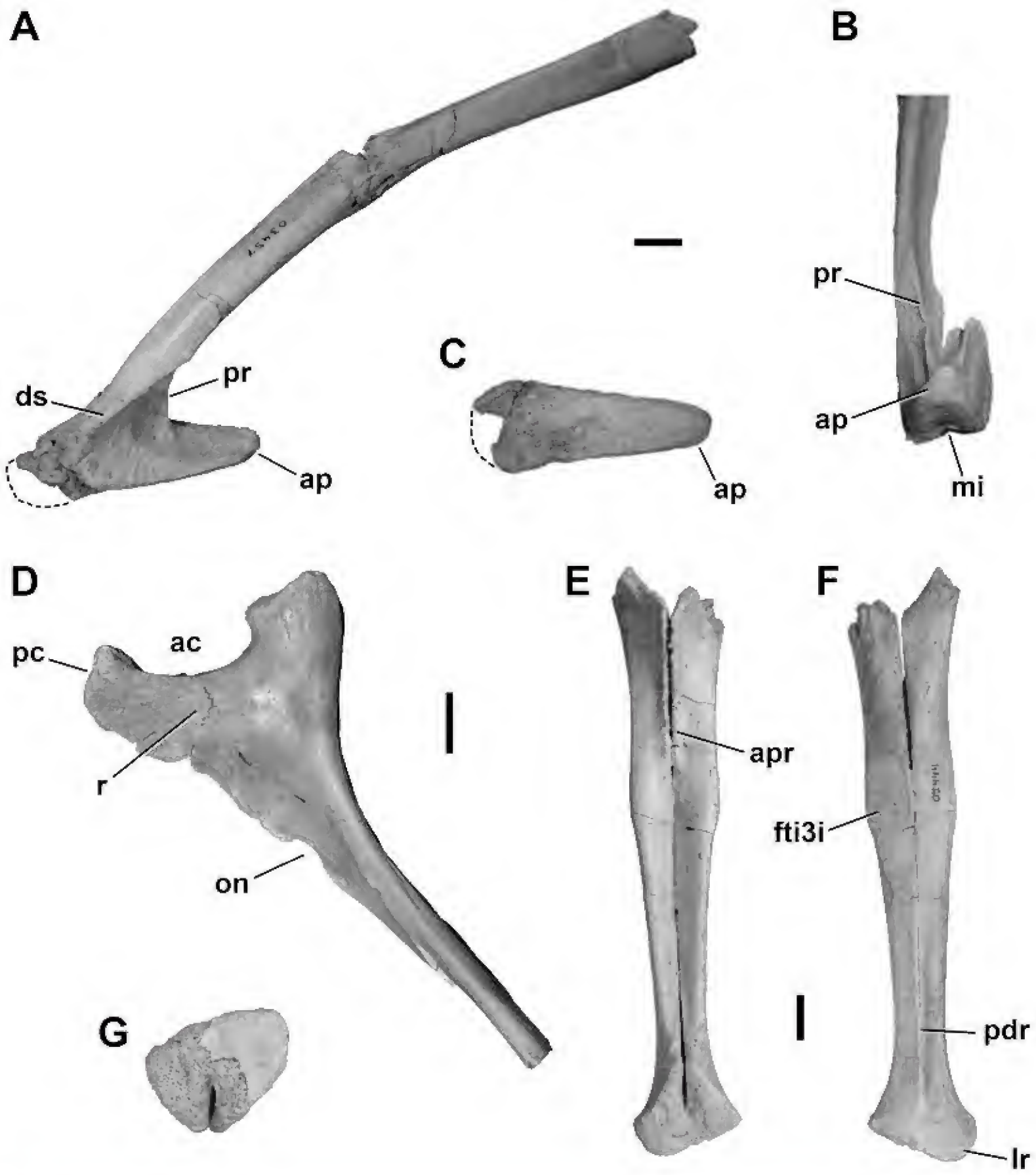

FIGURE 22. Ventral pelvic elements of *Masiakasaurus knopfleri*. Pubes (FMNH PR 2470) in left lateral (A), posterior (B), and distal (C; anterior is to the left) views. Note that a midshaft break has artificially exaggerated the shaft curvature in A. (D) Proximal left ischium (FMNH PR 2468) in lateral view. Distal left and right ischia (FMNH PR 2485) in left anteroventral (E), posterior (F), and distal (G) views. Abbreviations: ac = acetabular opening; ap = apex of pubic boot; apr = anteroproximal ridge; ds = dorsal shelf; fti3i = insertion for M. flexor tibialis internus 3; lr = lateral ridge on ischial boot; mi = midline invaginations; on = obturator notch; pc = contact for pubis; pdr = posterior distal ridge; pr = posterior ridge; r = rugose area. Scale bars = 1 cm.

has been largely obliterated but its original path remains evident. The contact between these bones tapers from a maximum thickness (8 mm in this specimen) at the acetabular border to a minimum thickness (less than 2 mm) at the most ventral preserved part.

The distal end is preserved in two specimens (FMNH PR 2470, 2481), both of which document the fusion of left and right elements into a "boot" (Figure 22A–C). This structure is fully fused along the ventral and dorsal edges, as well as both anteriorly and posteriorly. In ventral view

(Figure 22C), the boot is long and roughly triangular, with the apex directed posteriorly. At the anterior end, the left and right halves are demarcated by a shallow invagination.

The pubic shaft exhibits distinct morphological changes as it approaches the boot (Figure 22A). The lateral surface of the shaft transforms from rounded to shelf-like, extending distally to form a thin rim along the anterodorsal margin of the boot. The flattened dorsal surface of the shaft merges almost imperceptibly into the boot. Posteriorly, a thin ridge arises from the concave surface of the ventral one-quarter of the shaft, eventually meeting its opposite to form a central ridge along the posterodorsal margin of the boot (Figure 22B). A conical cavity leads into the dorsal part of the boot between the two ridges. It exits anteriorly via a thin slit, in contrast to *Carnotaurus* where the anterior opening is large and rounded (Carrano and Sampson, 2008: fig. 12).

The ischium is now represented by several specimens that effectively preserve the entire element (Figure 22D–G). It is fairly straight-shafted, with a striated scar near the (presumed) midshaft marking the origin of M. adductor femoris 2 (Carrano and Hutchinson, 2002). The proximal portion of the ischium is also striated near the pubic contact and bears a discrete, oblong bump, which was probably the origin of M. flexor tibialis internus 3 (Hutchinson, 2001; Carrano and Hutchinson, 2002).

The proximal ischium bears an obturator notch—best seen in FMNH PR 2468—that is located in the ventralmost portion of the puboischial plate (Figures 22D). There does not appear to be a ventral notch setting off an "obturator flange," as in many tetanurans (Rauhut, 2003). Some variation is evident in the morphology of the notch, which was broadly open in FMNH PR 2468 but more nearly closed in UA 9168. The iliac contact is quadrangular and bears a distinct medial socket, as in the proximal pubis, that would have received an iliac "peg." It overhangs the acetabular opening slightly. The pubic contact is an inverted triangle with a laminar ventral segment. The dorsal end of the puboischial contact is rugose and extends into the acetabular opening. The acetabular rim is tightly curved. Medially, the ischial shaft is marked by a low ridge that disappears proximally at the obturator notch. Presumably this ridge either contacted the same ridge on the opposite ischium or anchored an interischial membrane.

The distal ischium is best observed in FMNH PR 2485, which includes fused distal two-thirds of the contralateral elements (Figure 22E–G), thereby illustrating several proximodistal changes in shaft morphology. Near the proximal end, the ischia are triangular in cross-section, meeting along a flat medial contact that is enhanced anteriorly by a ridge formed by rugosities along the contact edge. The posterior shaft is transversely peaked at this point, whereas the anterior shaft is transversely concave. The midshaft becomes slightly convex anteriorly and concave posteriorly, with each ischium exhibiting a more elongate, D-shaped cross-section. The contact surface is no longer rugose at this point, and the posterior shaft is flattened, marking the origination area of M. flexor tibialis internus 3 (Carrano and Hutchinson, 2002). Most distally, the medial contact forms a thin ridge on the posterior surface. Anteriorly the bone remains strongly concave, creating an inverted triangular cross-section.

Distally, the two ischia are fused into an expanded "boot," like the pubes (Figure 22G). This fusion is complete posteriorly but not anteriorly, where a narrow incisure remains between the two elements. Each ischium is teardrop-shaped in distal view, giving the boot a triangular appearance. In lateral view, a thickened rim is visible along the lateral edge, marking where the distal surface curves up onto the lateral side of the bone.

Fibula: The fibula is generally long and slender, slightly shorter than the tibia. In proximal view, the proximal end of the fibula describes a broad, medially concave curve. The anterior and posterior ends are rounded, although the anterior end is broader. The proximal articulation is convexo-concave from anterior to posterior, becoming almost flattened toward its posterior edge (Figure 23A,B). A thickened rim along the proximal end likely marks the original extent of a cartilaginous cap.

Laterally, the fibula shows little discrete surface morphology aside from a large flange for the insertion of M. iliofibularis along the anterior edge of the shaft (Figure 23A,C). As in other ceratosaurs, this flange is well-developed, textured, and sinuous, curving from anterior to lateral as its descends. In addition, a second attachment surface is more proximally placed along the anterior edge; this surface is smaller and more vertically oriented, and was probably associated with the tibial articulation. Otherwise the anterior surface is smoothly rounded. In contrast, the posterior shaft is more acuminate and lacks flanges or tubercles. The anteroposterior breadth of the proximal fibula is approximately three times greater than at midshaft, and continues to narrow distally.

Medially, the fibula shows several ceratosaur characteristics, including the development of a large, posterodistally open fossa (Figure 23A,B). This opening is bordered by a tall anterior wall that turns posteriorly near the proximal end. The medial surface is concave proximal to this wall, forming a second shallow fossa. The long, flat facet for the interosseous membrane appears just distal to the M. iliofibularis tubercle and continues toward the distal

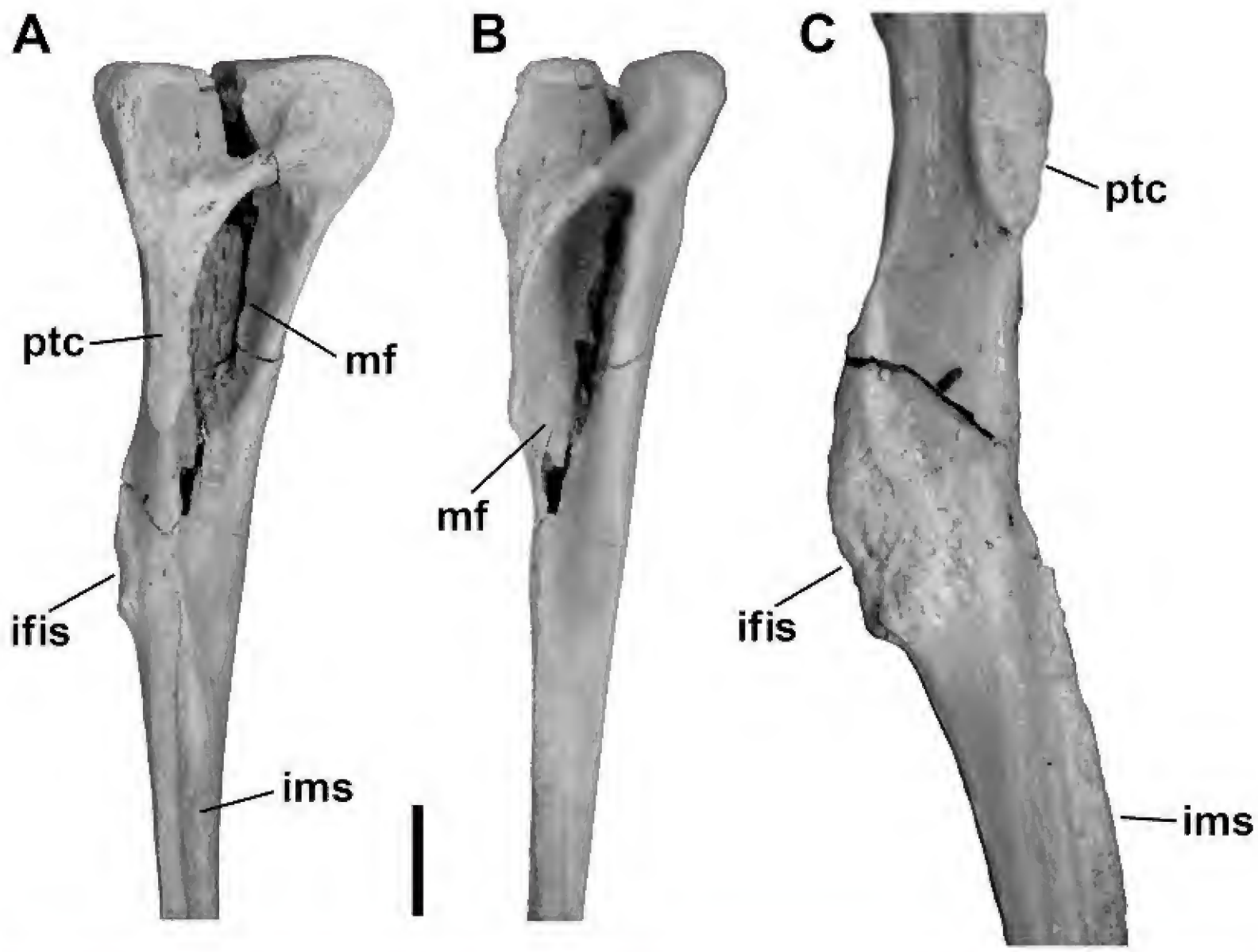

FIGURE 23. Right fibula (UA 9167) of *Masiakasaurus knopfleri* in medial (A) and posteromedial (B) views, with a close-up anteromedial view of the midshaft region (C). Abbreviations: ifis = scar for *M. iliofibularis* insertion; ims = scar for interosseous membrane; mf = medial fossa; ptc = proximal tibial contact surface. Scale bar = 1 cm for A, B.)

end; it occupies more than one-half of the medial shaft surface (Figure 23A,C).

The fibula appears to exhibit dimorphism, as has previously been noted for the femur and tibia (Carrano et al., 2002). For example, UA 9167 exhibits exceptionally pronounced muscle scars and ligament attachment surfaces, yet it is not substantially larger than other specimens lacking these qualities. In particular, the medial surface of the proximal end shows well-developed rugosities along the edges of the medial fossa, and the floor of this fossa is strongly ridged. The M. iliofibularis scar is strongly textured, and the scar for the interosseous membrane is roughened and swollen (Figure 23A,C).

Tarsus: Disarticulated astragali show several aspects of morphology not visible in the fused specimens described previously (Figure 24; Carrano et al., 2002). The ascending process is very tall and has straight lateral and proximal edges; the medial edge is straight along the basal two-thirds but then angles slightly laterally (Figure 24A,C). The process is well inset from the body of the astragalus, and nearly twice as tall as the body is deep. The lateral contact for the calcaneum, though not well preserved, is fairly flat with a distal C-shaped portion that connects to a more proximal triangular part that lies adjacent to a corresponding bulge in the astragalar body (Figure 24B).

The tibial facet bears two concave fossae, one posterior to the ascending process and a second placed medially (Figure 24C). Both have deep portions close to the base of the ascending process that may relate to the hollow (?) interior of the bone, along with the corresponding fossae at the base of the process externally. A thick ridge separates these two tibial facet fossae.

Distal tarsal 3 was found articulated on the proximal surface of its corresponding metatarsal III in two specimens (FMNH PR 2481, UA 9102; Figure 25A–B). The element has the rounded triangular shape that is typical for most basal theropods and is not fused to the metatarsal. The proximal surface is slightly convex, and a small lip from

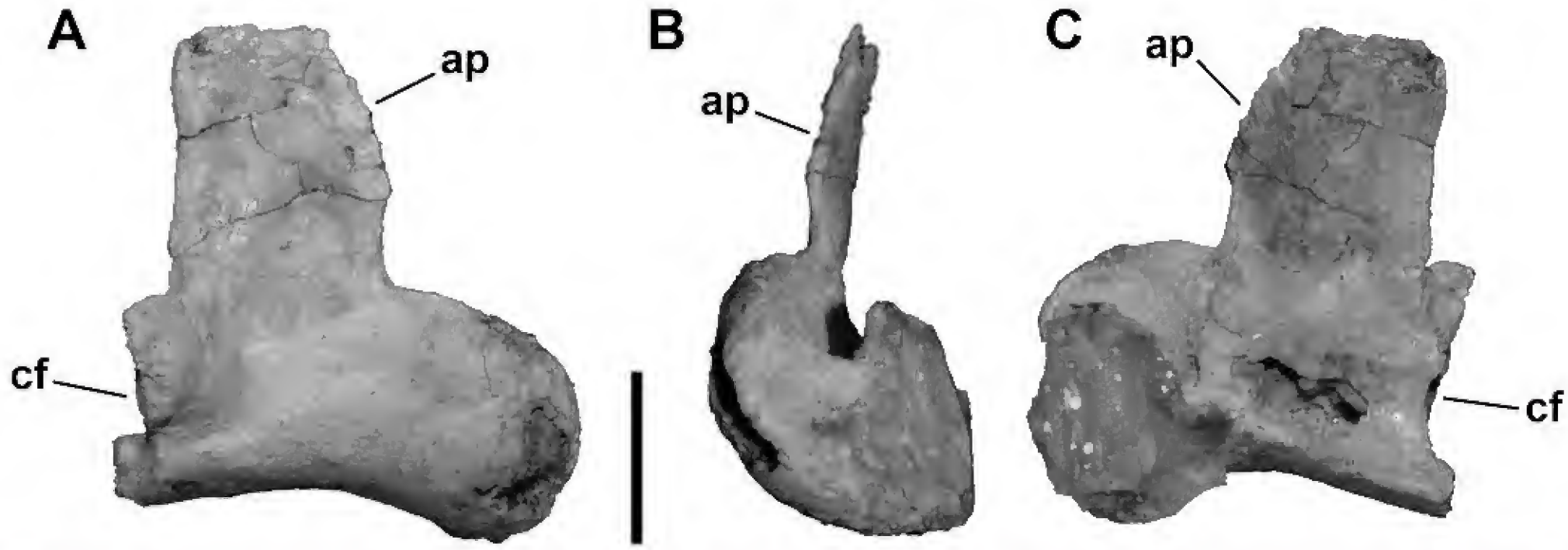

FIGURE 24. Right astragalus (FMNH PR 2481) of *Masiakasaurus knopfleri* in anterior (A), medial (B), and posterior (C) views. (Abbreviations: ap = ascending process; cf = calcaneal facet. Scale bar = 1 cm.

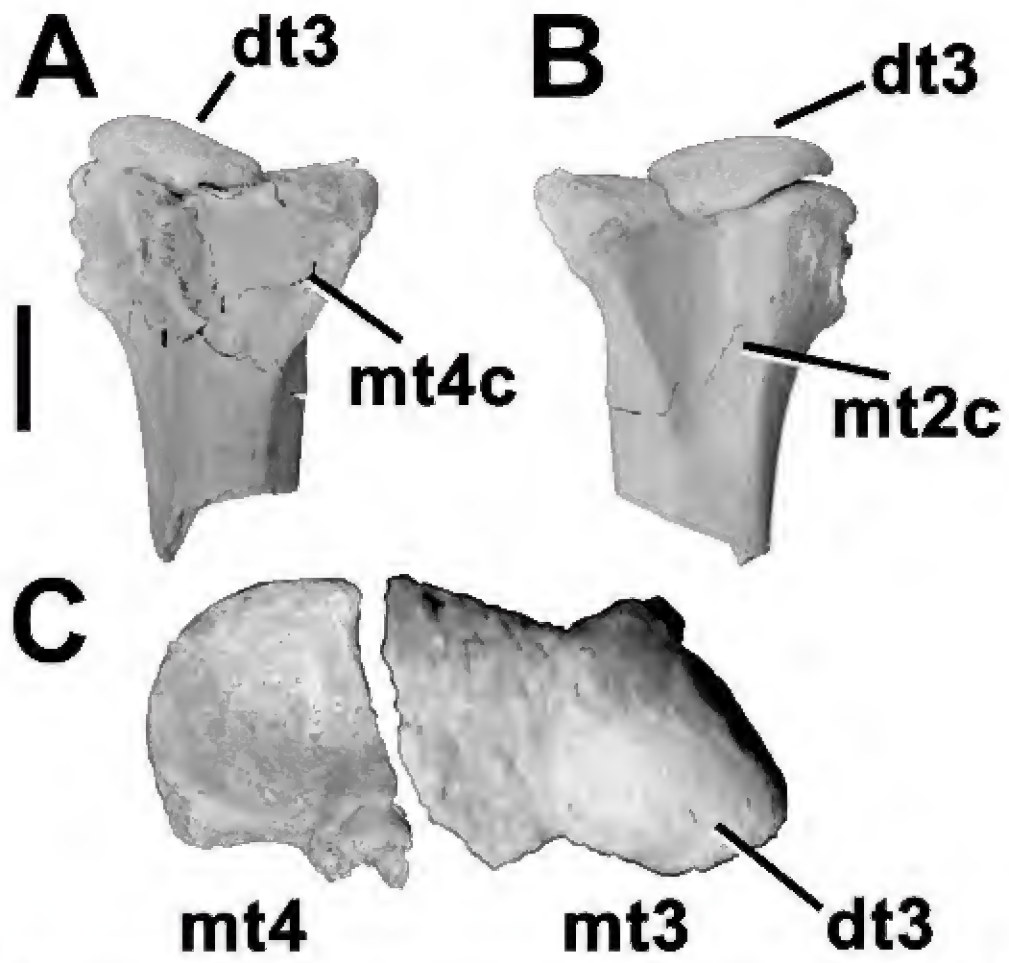

FIGURE 25. Metatarsals of *Masiakasaurus knopfleri*. Proximal end of right metatarsal III with articulated distal tarsal 3 (FMNH PR 2687) in lateral (A) and medial (B) views. Proximal view (C) of left metatarsals III (UA 9102) and IV (UA 9101); anterior is toward the top. Note that the latter two specimens were not associated, and so have been scaled to show the reconstructed articulations between these elements. Abbreviations: dt3 = distal tarsal 3; mt2c = metatarsal II contact surface; mt3 = metatarsal III; mt4 = metatarsal IV; mt4c = metatarsal IV contact surface. Scale bar = 1 cm.

this tarsal overhangs the posterior edge of the metatarsal. In UA 9102 distal tarsal 3 is completely fused to metatarsal III.

Pes: A complete left metatarsal III (UA 9102) reveals this element to be long and slender, with a very straight shaft. The large proximal end is squared but slightly hourglass-shaped to accommodate the articulations for metatarsals II and IV. The medial and lateral invaginations on this end are considerably smaller than those of *Allosaurus* and other tetanurans, but similar to the condition in *Ceratosaurus* and *Majungasaurus*. This is especially true of the expanded proportions of the proximal end of metatarsal III when compared to those of II and IV. The distal end is a squared, dorsoventrally compact roller with two condyles that are approximately symmetrical. The groove between them is weak, as it is on most of the phalanges of digit III. Posteriorly, the shaft of metatarsal III bears prominent muscle scars.

Metatarsal IV is now completely known. It bears the narrow distal condyles that have been highlighted as a noasaurid synapomorphy (Sereno et al., 2004), but this feature is barely evident in some specimens (e.g., UA 9101), which show distal condyles with proportions similar to those of other theropods. The shaft of UA 9101 is also less strongly curved than in other specimens, diverging from its contact with metatarsal III at an angle of about 15° (versus about 30° in FMNH PR 2214). This difference may be attributed to postmortem damage of the latter specimen, or alternatively may represent natural population variation between gracile and robust extremes, as has been

observed in the femora, tibiae (Carrano et al., 2002), and fibulae. The posterior shaft of metatarsal IV bears very pronounced scars for the insertion of M. gastrocnemius, especially along its lateral and medial edges. The proximal end of the bone has a broadly D-shaped outline with a convex anterolateral edge, a concave posterior edge, and a slightly undulating medial edge.

DISCUSSION

Noasaurid Morphology

These new materials greatly clarify several important aspects of noasaurid anatomy, particularly the skull and cervicodorsal vertebral series. Although most of the present fossils probably derive from numerous individuals of *Masiakasaurus*, the presence of at least two associated skeletons at locality MAD 05-42 (FMNH PR 2481, 2485) permits a more accurate assessment of skeletal proportions (Table 1; Figure 26). In addition, there is now a greater overlap with the associated materials of *Noasaurus* and other noasaurids, allowing clarification of the anatomy of related forms. In *Noasaurus*, for example, all preserved elements (maxilla, quadrate, cervical 4, dorsal centrum, cervical ribs, manual phalanx, and metatarsal IV) except the manual ungual can be compared directly.

It is now apparent that the noasaurid skull was not especially modified relative to those of other ceratosaurs except with regard to the anterior portions of the jaws.

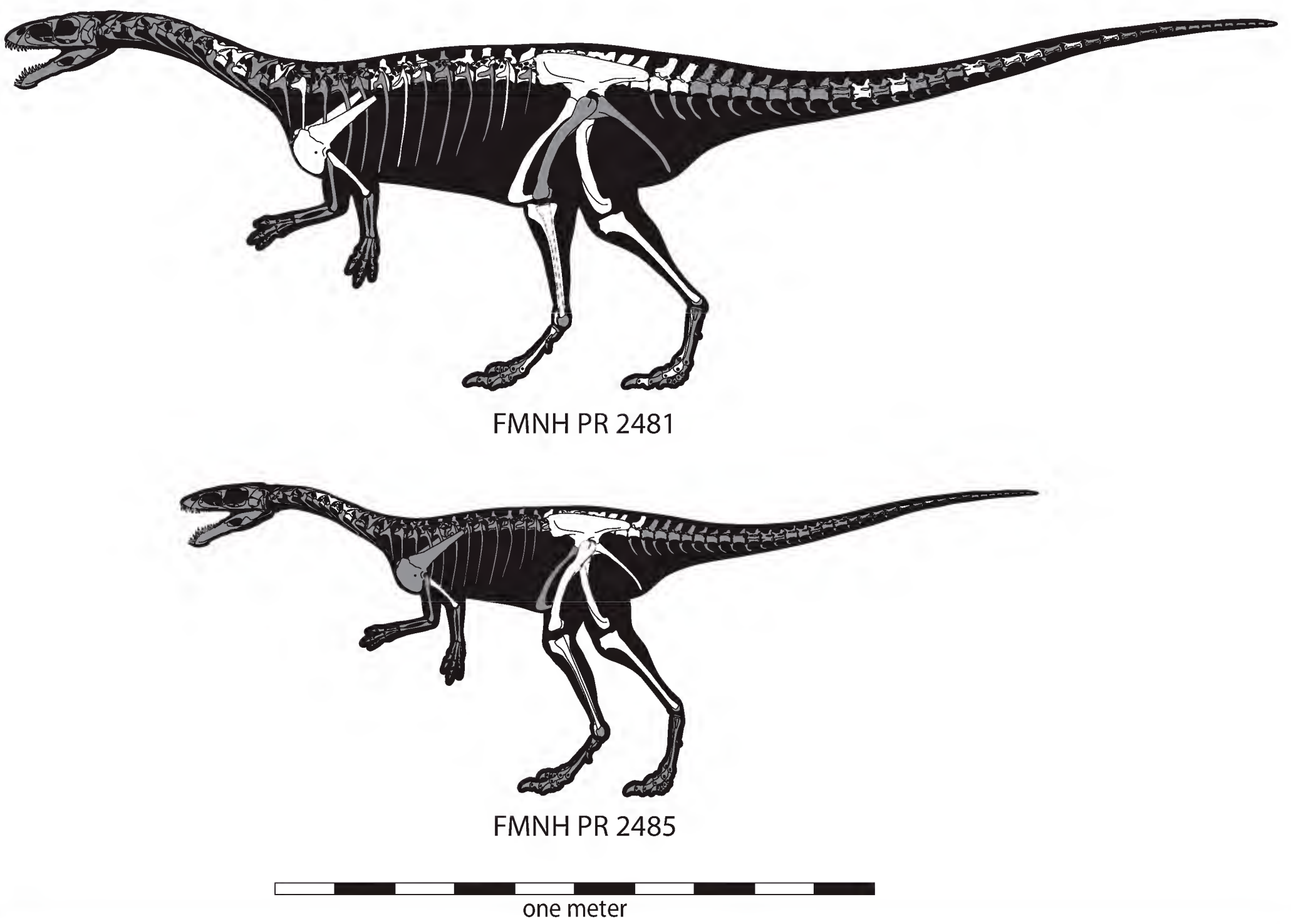

FIGURE 26. Associated individuals of *Masiakasaurus knopfleri* from locality MAD 05-42, illustrating size and proportional differences and showing recovered (white) and missing (gray) elements. (Top) Larger individual (FMNH PR 2481); (bottom) smaller individual (FMNH PR 2485). See Table 1 for measurements.

The remainder of the facial skeleton, the posterior mandible, and the braincase do not show highly derived morphologies with respect to other ceratosaurs and more primitive theropods. In some cases (e.g., external element sculpturing, lacrimal morphology) noasaurids exhibit an intermediate condition between more basal ceratosaurs and abelisaurids.

The neck of noasaurids was relatively longer than in abelisaurids, which exhibit anteroposterior vertebral shortening similar to that seen in other large theropods such as allosauroids and tyrannosaurids. However, the noasaurid neck was not especially lengthened relative to that of other small theropods, and was composed of vertebrae that were proportionally shorter than those of coelophysoids, *Elaphrosaurus*, *Limusaurus*, and *Spinostropheus*. More unusually, there is virtually no change in centrum proportions across the pectoral region, unlike the condition in other ceratosaurs and nearly all other theropods. This implies that the neck would have curved downward from the head, then straightened from the middle cervicals through the anterior trunk before arching slightly upward through the posterior trunk and sacrum.

The pectoral girdle shares with other ceratosaurs the development of an expanded coracoid and ventral scapula and the lack of any constriction posterior to the acromion. Whereas in Abelisauridae (and to a more restricted extent in *Ceratosaurus* and *Limusaurus*) this morphology is paired with a reduction in the length of the forelimb, in noasaurids the forelimb is not appreciably reduced in length. The humerus is long and slender, as may be some of the manual elements. Several features of the humerus are shared with *Elaphrosaurus* and abelisaurids, including the globular head, reduced deltopectoral crest height, and flattened distal condyles (some of these features may also be present in *Limusaurus*). No reduction in functionality is evident from the preserved remains. In contrast, the morphology of the humeral head and the expanded muscle origination areas on the ventral pectoral girdle suggest that mobility was significant and perhaps enhanced over the primitive theropod condition.

The manus remains poorly known, but seems to have been less transformed in noasaurids than in *Limusaurus* or abelisaurids. Although it is possible that some of the manual phalanges were short in noasaurids, the metacarpals apparently retained more primitive proportions. The phylogenetic placement of Noasauridae suggests a four-fingered manus, but we cannot yet confirm this with fossil evidence. Regardless, the manus would likely have had a prehensile function similar to those of other basal theropods.

The hind limb resembles that of abelisaurids, except in its more gracile proportions. No major differences in structure or articulation can be observed between these two groups, especially now that the supposed "raptorial" pedal ungual of *Noasaurus* has been reidentified as a manual ungual (Carrano and Sampson, 2004b; Agnolin and Chiarelli, 2010). Likewise, the overall pelvic structure is shared between most abelisauroids (Carrano, 2007), suggesting similarity of the placement and relative sizes of attached muscles.

It is not clear why abelisauroids might have retained (or reevolved) caudal ribs, a condition that contrasts with all other theropods. However, the overall organization of the axial column in abelisauroids suggests an emphasis of hypaxial relative to epaxial musculature, opposite of what is seen in most theropods. If this trait was also evident in the tail, then the presence of caudal ribs could be interpreted as a means to enhance transverse tail flexibility, the ribs providing increased moment arms for the attached muscles.

Comparative Anatomy

Masiakasaurus remains the best-known noasaurid, but the incompleteness of other taxa greatly reduces the opportunities for substantive comparisons. However, the new materials described here do allow for increased anatomical resolution of some existing specimens, particularly those from the Lameta Formation of India (Huene and Matley, 1933; Novas et al., 2004).

Four vertebrae were originally assigned to *Laevisuchus indicus* (Huene and Matley, 1933), and identified as cervicals and dorsals without further specification. We can now identify GSI K27/696 as C6 (see "Cervical Vertebrae" above), but the remaining vertebrae can only be imperfectly placed because they have not been located in the GSI collections. Specimen GSI K20/613 is a more posterior cervical, approximately C7–C8 based on comparison with *Masiakasaurus*. Specimen GSI K20/614 is shown only in ventral view (Huene and Matley, 1933: pl. XX, fig. 4), but its proportions are very close to those of C5 in *Masiakasaurus*. Specimen GSI K27/588 has a lateral centrum fossa but no foramen. The centrum faces are not offset, and the neural arch is long at its base but tapers toward the apex. Based on these features, we assign this vertebra to the mid-dorsal region.

Jubbulpuria tenuis also appears to comprise noasaurid materials. Both specimens (GSI K20/612, K27/614) were described as dorsal vertebrae, but "almost without any indications of buttresses" (Huene and Matley, 1933:61).

They have long, low centra with transverse processes, as well as posteriorly placed neural spines. Together these features suggest that the specimens are midcaudal vertebrae.

Although it is approximately twice the size of the largest specimen of *Masiakasaurus*, the holotype axis of *Compsosuchus solus* (GSI K27/578) is otherwise very similar in morphology. Like *Masiakasaurus*, it bears a large, rounded pneumatic foramen adjacent to the parapophysis. It differs in exhibiting a slightly more upturned atlantal intercentrum and a proportionally less projected odontoid.

The dorsal (GSI K27/541, K27/531) and midcaudal? (GSI K27/604) vertebrae assigned to *Ornithomimoides*? *barasimlensis* also resemble those of *Masiakasaurus* in size, general proportions, and disposition of laminae, but are too incomplete to be placed more specifically in the axial column.

A number of other Lameta specimens, not assigned to particular taxa, can also be more specifically identified, including a number of "coelurosaurs" (Table 2; see also Novas et al., 2004). For taxonomic purposes, these can be assigned to Noasauridae indet., but it is very possible that all the materials mentioned above pertain to a single noasaurid taxon. Overall, the Lameta specimens are approximately twice as large as those from the Maevarano Formation, and are proportionally more robust. However, even the largest *Masiakasaurus* specimens may derive from individuals that were not fully grown, so this size difference may reflect ontogenetic effects.

Noasaurus leali (Bonaparte and Powell, 1980) is the namesake taxon for the family Noasauridae, but is only represented by a few disassociated elements. As noted above, we have reidentified the putative squamosal as a cervical rib, and the "pedal" phalanx and ungual as belonging to the manus. Although there are strong similarities between *Noasaurus* and *Masiakasaurus*, the two taxa exhibit significant differences as well. For example, the maxilla of *Noasaurus* has a narrower antorbital fossa, and the anterior margin of the antorbital fenestra reaches to the fifth alveolus (versus the fourth in *Masiakasaurus*). The quadrate shaft is much more strongly curved in *Noasaurus* than in *Masiakasaurus*. Finally, the medial collateral ligament pit on metatarsal IV is internally subdivided in *Noasaurus* and connects to a more distinct distal intercondylar sulcus.

A second form from Argentina, *Velocisaurus unicus* (Bonaparte, 1991) is known only from limb elements. These are more poorly preserved than the corresponding elements in either *Noasaurus* or *Masiakasaurus*, but exhibit enough morphology to confirm the taxon's status as a noasaurid. Although the astragalus is damaged, it is similar to the same element in *Masiakasaurus* and likely had a laminar ascending process (as evidenced from the broken base on the astragalar body and flat contact area on the anterior surface of the distal tibia). The pedal elements of *Velocisaurus* are generally similar to those of *Masiakasaurus* but are more slender; this is particularly evident in the proportions of the phalanges of digits III and IV.

Finally, *Genusaurus sisteronis* (Accarie et al., 1995) from the Early Cretaceous of France also shows many similarities to *Masiakasaurus*, and has been recently recovered as a noasaurid (Carrano and Sampson, 2008). The ilium, in particular, bears a peg-shaped articulation for the ischium and shows a similar pattern of sacral rib attachments to *Masiakasaurus*, although it is proportionally

TABLE 2. Isolated noasaurid specimens from the Lameta Formation, Bara Simla, Jabalpur, India. Identifications are based on comparison with materials of *Masiakasaurus knopfleri*. Many of these were identified as Abelisauroidea indet. (and tentatively as Noasauridae and/or *Laevisuchus*) by Novas et al. (2004).

Original taxonomic assignment, and Specimen no. reference	Element	Original
Coelurid		
GSI K27/587	Distal mid-caudal vertebra	pl. XXIII, fig. 5
Coelurosaur		
GSI K27/589	Distal mid-caudal vertebra	pl. XXIII, fig. 3
GSI K27/599	Mid-caudal vertebra	pl. XXIII, fig. 4
GSI K27/526	Right tibia	pl. XXIII, fig. 7
GSI K27/665	Right metatarsal III	pl. XXIV, fig. 2
GSI K27/697, K27/681	Metatarsal III	pl. XXIV, fig. 3
GSI K27/666	Right metatarsal IV	pl. XXIV, fig. 4
GSI K27/667	Right metatarsal II	pl. XXIV, fig. 5
GSI K20/337	Right metatarsal IV	pl. XXIV, fig. 6
GSI K20/626B	Left pedal phalanx IV-1	pl. XXIV, fig. 7
GSI K27/637	Left pedal phalanx IV-4	pl. XXIV, fig. 9
GSI K27/638	Pedal phalanx IV-3	pl. XXIV, fig. 10
GSI K27/648	Right pedal phalanx IV-1	pl. XXIV, fig. 13
GSI K27/646	Pedal phalanx III-2/3	pl. XXIV, fig. 14
GSI K27/647	Right? pedal phalanx IV-4	pl. XXIV, fig. 15
GSI K20/337	Pedal phalanx IV-2	pl. XXIV, fig. 16
GSI K27/524	Left pedal phalanx II-1	pl. XXIV, fig. 17
GSI K27/644	Right pedal phalanx III-1	pl. XXIV, fig. 18
GSI K27/632	Pedal phalanx II-3/IV-5	pl. XXIV, fig. 19
GSI K27/629	Pedal phalanx III-4	pl. XXIV, fig. 20

shallower dorsoventrally. The proximal pubis is fused to the ilium in a manner similar to that in UA 9162, and bears the broken remnants of an obturator foramen. It is approximately 1.5 times the size of the largest specimen of *Masiakasaurus*.

Relationships within Noasauridae

One of the most frustrating aspects of interrelationships within Ceratosauria involves the high degree of uncertainty that surrounds the placement of individual species in the group, and particularly within the clades Abelisauridae and Noasauridae (Carrano and Sampson, 2008). This is partly because many ceratosaur taxa are known from incomplete specimens, thus when large numbers of taxa are analyzed, many most parsimonious trees are produced.

One problem has been the labile placement of several incompletely known abelisauroids (e.g., *Genusaurus*, *Ligabueino*, *Velocisaurus*). *Ligabueino* is extremely fragmentary, represented by a handful of elements. These include a cervical neural arch, a mid to posterior dorsal neural arch, a posterior dorsal centrum, the left femur, left ilium (visible only in medial view), articulated pubic shafts, and two pedal phalanges. The shorter of the latter two elements appears to represent a manual phalanx, and resembles the corresponding bones in *Masiakasaurus* and *Noasaurus*. The specimen is from a tiny individual, and the separation of the cervical and dorsal vertebral centra from their neural arches indicates that it represents a juvenile (*contra* Bonaparte, 1996). There do not appear to be any definitive noasaurid synapomorphies preserved, but there are enough features (e.g., anteroposteriorly short cervical neural spine, cervical prezygapophyseal–epipophyseal lamina, and marked but not hypertrophied flange on mediodistal femoral shaft) to confidently place *Ligabueino* within Abelisauroidea (Carrano and Sampson, 2008).

On the other hand, it now seems clear that *Velocisaurus* represents a true noasaurid. Although in many respects less complete than *Ligabueino*, the holotype of *Velocisaurus* (comprising most of the hind limb distal to the knee) does preserve several noasaurid and abelisauroid features. In particular, the cnemial crest is incomplete but shows the distinctive ceratosaur morphology at its base, curving far anterior to the tibial shaft. Metatarsal III is much larger than the flanking elements (i.e., an "antarctometatarsus"), and metatarsal II is extremely slender, as in *Noasaurus* and *Masiakasaurus*. However, there does not appear to be any compelling morphological reason to ally *Velocisaurus* with *Masiakasaurus* to the exclusion of *Noasaurus* into the clade Velocisauridae (Bonaparte, 1991), as has been suggested (Agnolin et al., 2003). The purported similarities and distinctions rest entirely on the differential preservation of elements, and we can offer no positive support for Velocisauridae, which we therefore consider a junior synonym of Noasauridae.

Similarly, the fragmentary *Genusaurus* also appears to be a noasaurid based on the presence of a hypertrophied flange along the anteromedial edge of the femoral shaft and a bulbous fibular condyle on the femur (Carrano and Sampson, 2008). *Genusaurus* is slightly larger than *Masiakasaurus* and *Noasaurus*, perhaps approaching three meters in length. Its early geological appearance (Albian) provides the oldest definitive evidence of noasaurids, antedating the final Laurasia–Gondwana split (Hay et al., 1999), and the undescribed form from the Elrhaz Formation of Niger may be even older (Sereno et al., 2004.)

It is not yet possible to shed much light on *Laevisuchus* or the other very fragmentary small-bodied theropods from the Upper Cretaceous Lameta Formation of India. Carrano et al. (2002) noted that the holotypic vertebrae of *Laevisuchus* share some synapomorphies with those of *Masiakasaurus* and *Noasaurus*, and grouped these three taxa into Noasauridae. Numerous additional small theropod specimens are known from the Lameta Formation, but unfortunately it is not possible to determine how many discrete taxa are represented (see discussion in Novas et al., 2004). Huene and Matley (1933) almost certainly overstated the taxonomic diversity of their sample in naming four small theropods: *Compsosuchus solus*, *Laevisuchus indicus*, *Jubbulpuria tenuis*, and *Ornithomimoides? barasimlensis*. If the Lameta fauna is very similar to the Maevarano fauna in composition, then all four taxa may represent a single noasaurid species, to which most of the currently unassigned small theropod specimens might also be allocated. Even if this were so, such a taxon would still be too incomplete for its relationships within Noasauridae to be highly resolved without the addition of new specimens. We note, however, that the proportions of the individual pedal phalanges are much closer to those of *Masiakasaurus* than to those of *Velocisaurus*.

In summary, we can now more confidently assign several small theropod taxa (*Genusaurus*, *Velocisaurus*, Lameta forms) to Noasauridae, but we cannot determine their interrelationships with any greater certainty. *Ligabueino* should be excluded from Noasauridae and considered an indeterminate abelisauroid. Until more complete specimens of existing taxa are found, noasaurid phylogeny will remain in flux, but there is some evidence for

a close relationship between the Lameta noasaurid and *Masiakasaurus*.

Evolutionary Implications for Ceratosauria

Noasaurids

Genusaurus appears to be the earliest definitive noasaurid (Albian), although an additional form from the late Early Cretaceous of Niger (Sereno et al., 2004) may be coeval with or slightly older than it. Abelisauridae, the sister taxon to Noasauridae within Abelisauroidea, has its earliest known appearance in the late Early Cretaceous of Niger (Sereno and Brusatte, 2008). Neither group is yet known from pre-Cretaceous rocks, nor from rocks earlier than Aptian–Albian. This represents the minimum divergence time for these two main abelisauroid clades (Carrano and Sampson, 2008).

Subsequent diversification of noasaurids took place at least in South America (*Velocisaurus*, *Noasaurus*), Africa (one unnamed form; Sereno et al., 2004), India (*Laevisuchus*, *Compsosuchus*, *O? barasimlensis*, *Jubbulpuria*), Madagascar (*Masiakasaurus*), and Europe (*Genusaurus*). Sereno et al. (2004) proposed that an additional taxon, *Deltadromeus*, represented a gigantic noasaurid. We have not found independent support for this hypothesis and consider *Deltadromeus* to be a more primitive member of Ceratosauria, close to *Spinostropheus* and *Elaphrosaurus* (Carrano and Sampson, 2004a, 2004b, 2008). Thus there is currently a maximum of 10, and perhaps as few as 6, noasaurid taxa spanning more than 55 million years on at least 5 continental landmasses. Certainly this represents a vast undersampling of the true history of the noasaurid lineage.

It is therefore highly speculative to attempt to decipher biogeographic patterns within Noasauridae. The group appears to be legitimately absent from the Late Cretaceous of eastern Asia and western North America, but may yet prove to have had a wider distribution, particularly in the Early Cretaceous prior to maximum Mesozoic continental separation. Patterns within Noasauridae are impossible to determine without a well-resolved phylogeny, which is lacking and will remain so without additional materials. Furthermore, the fact that more noasaurids are known from South America than elsewhere predisposes many analyses to determine this as the "center of origin" for the group, in spite of their highly incomplete record. (A corresponding problem also exists for taxa in poorly sampled regions, which are predisposed to sister taxon relationships with forms from other areas, leading to an overemphasis on "dispersal" [Carrano and Sampson, 2004a].) We note that there is at least a superficial resemblance between the distributional patterns of Late Cretaceous abelisaurids and noasaurids (Carrano et al., 2002), which may herald some deeper paleobiogeographic significance. However, given the extremely fragmentary record of noasaurids and the lack of fossils from several important regions (Carrano et al., 2002; Carrano and Sampson, 2002, 2004a, 2008), we are skeptical of even these broad conclusions.

Despite this incomplete record, a few features of noasaurid evolution are apparent. First, all definitive noasaurids are medium- or small-bodied forms, less than four meters in length and weighing perhaps hundreds but certainly not thousands of kilograms. All seem to share proportionally slender hind limbs, with elongate distal segments and reduced lateral digits that suggest some degree of cursoriality (e.g., Carrano, 1999). Most specializations were confined to the skull (although this is only partly known, and only in *Masiakasaurus* and *Noasaurus*); primitive ceratosaurian features dominated the appendicular skeleton. Vertebral morphologies are similar to those of abelisaurids, and do not imply any major axial changes in Noasauridae aside from development (or retention) of a relative elongation neck. Noasaurids thus appear to primarily represent a divergence in feeding habits from the primitive ceratosaur, and theropod, condition. The overall distribution of body sizes within Ceratosauria further suggests that small-bodied noasaurids underwent a size reduction during their evolution (Carrano et al., 2002).

Character Distributions

The addition of many new anatomical observations for *Masiakasaurus* has resolved much of the uncertainty surrounding character distributions within Ceratosauria. Specifically, it has been unclear whether numerous features were abelisauroid or abelisaurid synapomorphies, because they had not yet been preserved in any noasaurid specimens. New character codings are detailed elsewhere (Carrano and Sampson, 2008), but certain features are emphasized below.

In the skull, it is now clear that sculpturing on the dermal skull elements is limited to the postorbital and lacrimal in abelisauroids; this trend is elaborated in abelisaurids to include the premaxilla and maxilla (the distributions for the jugal and quadratojugal remain unknown). Similarly, pnematization and elaboration of the frontals and nasals is an abelisaurid, not abelisauroid, characteristic. It is interesting to note that the sculpturing of the skull roof and facial skeleton are considered to indicate distinct

anatomical structures in the overlying dermis (Hieronymus and Witmer, 2008).

In contrast, most vertebral characters of abelisaurids (including the presence of hyposphene-hypantrum articulations in at least the anterior caudals) are also found in noasaurids, and thus characterize Abelisauroidea. This is also the case for the unusual proportions of the cervical vertebrae, in which the epaxial musculature occupied a broad, deep space adjacent to the neural spine and was separated from the hypaxial musculature by a distinct prezygapophyseal–epipophyseal lamina. This division is marked in the tail by the presence of caudal ribs, which significantly expanded the attachment areas for lateral tail musculature well into the distal half of the tail. Highly shortened manual phalanges are also shared between noasaurids and abelisaurids. Aspects of some of these features are also found in more basal ceratosaurs.

CONCLUSIONS

The small-bodied noasaurid ceratosaur *Masiakasaurus knopfleri* is described in detail, focusing on many newly discovered specimens that now document approximately 65% of the cranial and postcranial skeleton. These new elements demonstrate that the skull of *Masiakasaurus* was similar in proportions to those of other small, primitive theropods. The most significant modifications occurred in the anterior dentition and jaws, while aspects of skull texturing, braincase morphology, and the lower jaw are shared with other abelisauroids and ceratosaurs. In the axial column, the most unusual characteristic is the relatively horizontally articulated posterior cervical series, which does not undergo proportional changes into the trunk. The rib cage seems to have been fairly narrow, and the tail may have retained caudal ribs. The pectoral girdle and forelimb include a very broad scapulocoracoid and a long, slender humerus but at least some shortened phalanges. In the pelvic girdle, the ilia articulate against six sacral vertebrae, while both the pubes and ischia terminate distally in fused "boots."

Comparisons with other noasaurids are limited by incomplete materials, but some forms were substantially larger than *Masiakasaurus*. Many of the small theropod specimens from Bara Simla in the Lameta Formation appear to pertain to at least one species of noasaurid. The group primarily differs from other abelisauroids in feeding specializations, as well as body-size reduction, but the many derived characters shared between noasaurids and abelisaurids indicate a great deal of functional similarity in the lower jaw, axial column, shoulder girdle, and hind limb between these groups.

Appendix

The following list of *Masiakasaurus knopfleri* specimens (Table A.1) supplements that given in Carrano et al. (2002) and emends the following information therein: (1) UA 8682 was listed as a dentary, but is actually a pedal phalanx; (2) FMNH PR 2198, 2226, and 2228 have been re-identified as juvenile *Majungasaurus* teeth; (3) FMNH PR 2204 has been re-identified as pertaining to a crocodyliform; (4) FMNH PR 2183 and 2124 were inadvertently switched in the captions for figs. 3 and 4; and (5) FMNH PR 2147 was substituted for 2146 in the caption for fig. 19 (Carrano et al., 2002).

TABLE A.1. Complete list of *Masiakasaurus knopfleri* specimens from the Upper Cretaceous Maevarano Formation of Madagascar collected through 2007. All specimens are from the Anembalemba Member of the Maevarano Formation except those marked with an asterisk (*), which are derived from the underlying Masorobe Member. Other symbols and abbreviations (in order of appearance): NA = not applicable; ND = position not determined; ? = data uncertain; tilde (~) = approximately; ?? = element identification uncertain; NFN = no field number; NR = exact locality not recorded. A dash (-) serves as visual placeholder only; no data were intended.

Element(s)	Notes and comments	Position	Specimen number [a]	Field number [b]	Locality
			Skull		
Premaxilla	-	Left	FMNH PR 2453	03056	MAD 93-18
Maxilla	-	Right	FMNH PR 2183	98199	MAD 93-18
Lacrimal	-	Right	FMNH PR 2473	03584	MAD 93-18
Postorbital	-	Right	UA 9090	01026	MAD 93-18
		Right	FMNH PR 2456	03120	MAD 93-18
Frontal	-	Left	FMNH PR 2475	03586-8	MAD 93-18
	-	Left	UA 9095	01032-1	MAD 93-18
Quadrate	-	Right	FMNH PR 2496	05322	MAD 05-42
Braincase	-	NA	FMNH PR 2457	03174	MAD 03-03*
Basioccipital	-	NA	UA 9178	03592	MAD 93-18
Laterosphenoid?	-	ND	FMNH PR 2495	03280	MAD 93-18
Dentary	-	Left	FMNH PR 2471	03471+03472 [c]	MAD 93-18
	-	Left	UA 9177	03587	MAD 93-18
	-	Left	FMNH PR 2222	95246	MAD 93-18
	-	Left	FMNH PR 2178	98103	MAD 93-18
	-	Left	FMNH PR 2177	98315	MAD 93-18
	-	Right	UA 9145	03204	"East of Mammal"
	Anterior 2/3	Right	UA 8680 (holotype)	95248	MAD 93-18
	-	Right	FMNH PR 2179	98093	MAD 93-18
Splenial	-	Left	FMNH PR 2124	98070	MAD 93-18
Angular	-	Left	UA 9147	03232	MAD 93-18
	-	Left	FMNH PR 2455	03119	MAD 93-18
Prearticular	-	Left	FMNH PR 2454	03118	MAD 93-18
	-	Left	UA 9149	03257	MAD 93-18
Prearticular, articular	-	Right	UA 9166	03420	MAD 93-18
Tooth	-	Anterior	FMNH PR 2180	99181	MAD 93-18
	-	Anterior	FMNH PR 2165	95358	MAD 95-05
	-	Anterior	FMNH PR 2200	95244-1	MAD 93-18
	-	Anterior	FMNH PR 2220	96068-4	MAD 93-35
	-	Anterior	FMNH PR 2818	07126	MAD 05-42
	-	Posterior	FMNH PR 2170	99279	MAD 99-06
	-	Posterior	FMNH PR 2221	98446	MAD 98-26
	-	Posterior	UA 9159	03356	MAD 93-18
	-	Posterior	FMNH PR 2476	03593	MAD 93-18
	2 elements	Posterior	FMNH PR 2181	93008-2, 93008-4	MAD 93-09
	-	Posterior	FMNH PR 2199	93086-4	MAD 93-35
	-	Posterior	FMNH PR 2182	98073	MAD 93-18
	-	Posterior	FMNH PR 2164	98203	MAD 93-18
	-	Posterior	FMNH PR 2201	99016	MAD 93-01
	-	Posterior	UA 9091	01027	MAD 93-18
	-	Posterior	UA 9123	03055	MAD 93-18
	-	Posterior	UA 9126	03068	MAD 93-18
	-	Posterior	UA 9128	03101	MAD 93-18
	-	Posterior	UA 9183	07028	MAD 93-35
	-	Posterior	FMNH PR 2696	07882-1	MAD 05-42
	-	Posterior	UA 9734	07909-1	MAD 93-35
Ceratobranchial	-	-	FMNH PR 2481	07449	MAD 05-42

Element(s)	Notes and comments	Position	Specimen number [a]	Field number [b]	Locality
		Axial Column			
Atlantal intercentrum	-	C1	FMNH PR 2477	03594	MAD 93-18
	-	C1?	FMNH PR 2481	07508	MAD 05-42
Axis	-	C2	FMNH PR 2462	03409	MAD 93-18
	-	C2	FMNH PR 2466	03420-1	MAD 03-40
	Arch	C2	UA 9130	03579+03580 [c]	MAD 93-18
Cervical vertebra	-	C3	UA 9121	03031	MAD 93-18
	-	C4	UA 9189	07225	MAD 07-16
	-	C4	UA 9106	01099	MAD 93-18
	-	C4	FMNH PR 2485	05443-1	MAD 05-42
	-	C5	FMNH PR 2465	03417	MAD 93-18
	-	C6	FMNH PR 2481	07436	MAD 05-42
	-	C7	FMNH PR 2481	07219	MAD 05-42
	-	C7	FMNH PR 2139	95322	MAD 93-18
	-	C7	UA 9111	01120	MAD 93-18
	-	C8	UA 9171	03454	MAD 93-18
	-	C8	UA 9181	03605	MAD 93-18
	-	C8	FMNH PR 2141	98180	MAD 93-18
	-	C9	FMNH PR 2481	07212	MAD 05-42
	-	C9–10	UA 9150	03273	MAD 93-18
	-	C10	FMNH PR 2491	98154-1	MAD 93-18
	-	C10	FMNH PR 2140	98172	MAD 93-18
	-	ND	FMNH PR 2485	05467-2	MAD 05-42
	-	ND	FMNH PR 2485	05616-1	MAD 05-42
	-	ND	FMNH PR 2464	03414	MAD 93-18
	-	ND	FMNH PR 2481	07494	MAD 05-42
	-	ND	FMNH PR 2630	07439	MAD 05-42
	Centrum	ND	UA 9859	98218-3	MAD 93-18
Dorsal vertebra	-	D1	FMNH PR 2837	07214	MAD 05-42
	Arch	D2	UA 9107	01100	MAD 93-18
	-	D2	FMNH PR 2485	07682	MAD 05-42
	-	D3	FMNH PR 2684	07789	MAD 05-42
	Arch	D4	FMNH PR 2144	95283	MAD 93-18
	Arch	D4	FMNH PR 2485	05459-1	MAD 05-42
	-	D4	FMNH PR 2636	07446	MAD 05-42
	-	D5	FMNH PR 2481	07215	MAD 05-42
	-	D6	FMNH PR 2481	07445	MAD 05-42
	-	D7	FMNH PR 2481	07213	MAD 05-42
	-	D11?	FMNH PR 2481	07494-2	MAD 05-42
	-	D12?	FMNH PR 2481	07494-3	MAD 05-42
	-	D13?	FMNH PR 2481	07494-4	MAD 05-42
	-	D14?	FMNH PR 2481	07494-5	MAD 05-42
	-	Posterior	UA 9175	03582	MAD 93-18
	-	Posterior	UA 9103	01087	MAD 93-18
	-	Posterior	UA 9176	03604	MAD 93-18
	-	Posterior	UA 9092	01028	MAD 93-18
	-	Posterior	UA 9097	01036	MAD 93-18
	Arch	ND	FMNH PR 2458	05460-28	MAD 05-42
	Arch	ND	UA 9164	03413	MAD 93-18
	Centrum	ND	FMNH PR 2114	95339	MAD 93-18
	Transverse process	ND	UA 9108	01102	MAD 93-18
	-	ND	FMNH PR 2207	96023	MAD 93-18
	-	ND	FMNH PR 2113	98235	MAD 93-18
	-	ND	FMNH PR 2229	98313-1	MAD 93-18
	-	ND	UA 8701	99162	MAD 93-18
	-	ND	FMNH PR 2171	99262	MAD 99-38

Element(s)	Notes and comments	Position	Specimen number [a]	Field number [b]	Locality
		Axial Column			
	-	ND	FMNH PR 2458	05593-3	MAD 05-42
	-	ND	FMNH PR 2137	95334	MAD 93-18
	-	ND	FMNH PR 2138	95334-1	MAD 93-18
	-	ND	FMNH PR 2145	95283-1	MAD 93-18
	-	ND	FMNH PR 2610	07085	MAD 05-42
Sacral vertebra	-	1	UA 9115	01135	MAD 93-18
	-	5–6	UA 9098	01043	MAD 93-18
	-	3–6	FMNH PR 2460	03407	MAD 03-66
	-	3–5	FMNH PR 2142	98243	MAD 93-18
	Centrum	1	FMNH PR 2485	07475	MAD 05-42
	-	1–6	FMNH PR 2481	07218-3	MAD 05-42
Caudal vertebra	-	Anterior	FMNH PR 2469	03453	MAD 93-18
	Arch	Anterior	FMNH PR 2481	07218-4	MAD 05-42
	2 elements	Anterior	FMNH PR 2481	07494-1	MAD 05-42
	-	Anterior	FMNH PR 2481	07779	MAD 05-42
	-	Anterior	UA 9112	01129	MAD 93-18
	-	Anterior	FMNH PR 2133	93061-2	MAD 93-30
	-	Anterior	FMNH PR 2481	07690	MAD 05-42
	Centrum	Anterior	UA 9173	03474	MAD 93-18
	-	Anterior/middle	FMNH PR 2481	07507	MAD 05-42
	-	Anterior/middle	FMNH PR 2482	05389	MAD 05-42
	-	Middle	UA 9190	07073	MAD 05-04
	-	Middle	UA 8692	95331	MAD 93-18
	-	Middle	FMNH PR 2125	95332	MAD 93-18
	-	Middle	FMNH PR 2110	95195-4	MAD 93-18
	-	Middle	UA 9179	03597	MAD 93-18
	-	Middle	UA 8688	98075	MAD 93-18
	-	Middle	UA 9197	98191	MAD 93-18
	-	Middle	FMNH PR 2126	98394	MAD 93-18
	-	Middle	FMNH PR 2485	05459-1	MAD 05-42
	-	Middle	FMNH PR 2481	07503	MAD 05-42
	+ Rib	Middle/posterior	FMNH PR 2481	07211	MAD 05-42
	-	Middle/posterior	UA 9195	98041	MAD 96-01
	-	Middle/posterior	UA 9858	98218-2	MAD 93-18
	-	Middle/posterior	UA 9120	03017	MAD 93-18
	-	Middle/posterior	UA 9158	03350	MAD 93-18
	-	Posterior	UA 8689	98206	MAD 93-18
	3 elements	Posterior	FMNH PR 2492	98188	MAD 93-18
	-	Posterior	FMNH PR 2485	05386	MAD 05-42
	-	Posterior	FMNH PR 2467	03431-1	MAD 93-18
	-	Posterior	UA 9139	03176	MAD 93-18
	-	Posterior	UA 9119	03015	MAD 93-18
	-	Posterior	FMNH PR 2203	95222-130-1	MAD 93-18
	-	Posterior	FMNH PR 2202	95222-097-1	MAD 93-18
	-	Posterior	UA 8695	95244-6	MAD 93-18
	-	Posterior	UA 8696	95244-7	MAD 93-18
	-	Posterior	UA 8691	95272	MAD 93-18
	-	Posterior	FMNH PR 2162	95275	MAD 93-18
	-	Posterior	UA 8690	96015	MAD 93-18
	-	Posterior	FMNH PR 2156	98165-1	MAD 93-18
	-	Posterior	FMNH PR 2157	98165-2	MAD 93-18
	-	Posterior	FMNH PR 2642	07480	MAD 05-42
	-	Posterior	FMNH PR 2638	07464	MAD 05-42
	-	Posterior	FMNH PR 2163	98169-1	MAD 93-18
	-	Posterior	FMNH PR 2485	07474	MAD 05-42
	-	Posterior	FMNH PR 2481	07213	MAD 05-42

Element(s)	Notes and comments	Position	Specimen number [a]	Field number [b]	Locality
		Axial Column			
	-	Posterior	FMNH PR 2127	98179	MAD 93-18
	-	Posterior	FMNH PR 2128	98179-1	MAD 93-18
	-	Posterior	UA 8703	98415	MAD 93-18
	-	Posterior	FMNH PR 2168	99265	MAD 99-26
	-	Posterior	FMNH PR 2481	07443	MAD 05-42
	-	Posterior	UA 9857	03178	MAD 93-18
	-	Posterior	FMNH PR 2458	05460-26	MAD 05-42
	Arch	ND	UA 9174	03575-2	MAD 93-18
	Centrum	ND	FMNH PR 2230	98236	MAD 93-18
	Centrum	ND	UA 9113	01131	MAD 93-18
	Centrum	ND	UA 9151	03274	MAD 93-18
	Centrum	ND	FMNH PR 2490	98018	MAD 93-18
	Centrum	ND	UA 9110	01119	MAD 93-18
	Centrum	ND	UA 9184	07098	MAD 07-13*
	-	ND	FMNH PR 2481	07838	MAD 05-42
	-	ND	UA 8702	96018	MAD 93-18
	-	ND	FMNH PR 2481	07208-1	MAD 05-42
	-	ND	FMNH PR 2481	07218-4	MAD 05-42
	-	ND	FMNH PR 2485	07882-2	MAD 05-42
	-	ND	FMNH PR 2485	07882-3	MAD 05-42
	-	ND	FMNH PR 2699	07882-4	MAD 05-42
	-	ND	FMNH PR 2700	07882-5	MAD 05-42
	-	ND	UA 9127	03100	MAD 93-18
	-	ND	UA 9140	03179	MAD 93-18
	-	ND	UA 9148	03256	MAD 93-18
	-	ND	FMNH PR 2125	95229	MAD 93-18
	-	ND	UA 9187	95198-4	MAD 93-18
Unidentified vertebra	-	ND	FMNH PR 2485	07465	MAD 05-42
	Arch	ND	UA 9109	01104-2	MAD 93-18
	Arch	ND	FMNH PR 2618	07207	MAD 05-42
	Centrum	ND	UA 9093	01029	MAD 93-18
	Centrum	ND	FMNH PR 2111	95195-5	MAD 93-18
	Centrum	ND	FMNH PR 2677	07775	MAD 05-42
	2 elements	ND	UA 8687	98083	MAD 93-18
Cervical rib	-	C4 (right)	FMNH PR 2485	05384	MAD 05-42
	Proximal portion	C4 (right)	FMNH PR 2481	07787	MAD 05-42
	Proximal portion	C6 (right)	UA 9169	03443	MAD 93-18
	-	C6	FMNH PR 2485	05414-1	MAD 05-42
	Proximal portion	C7 (right)	FMNH PR 2485	07491	MAD 05-42
	Proximal portion	C9 (left)	UA 9104	01088-1	MAD 93-18
	Proximal portion	C10	FMNH PR 2481	07435	MAD 05-42
	Proximal portion	ND	FMNH PR 2481	07776	MAD 05-42
	-	ND	FMNH PR 2481	07213	MAD 05-42
Cervicodorsal rib	-	C10/D1 (right)	FMNH PR 2672	07691	MAD 05-42
Dorsal rib	-	~D4	FMNH PR 2485	05416	MAD 05-42
	Proximal portion	~D4 (right)	UA 9160	03394	MAD 93-18
	Proximal portion	~D4	UA 9862	03574-2	MAD 93-18
	-	(Left)	FMNH PR 2485	05415	MAD 05-42
	-	(Right)	FMNH PR 2481	07788	MAD 05-42
	-	ND	FMNH PR 2481	07784	MAD 05-42
	Proximal portion	ND	UA 9155	03332-1	MAD 93-18
	-	ND	FMNH PR 2481	07500	MAD 05-42
Unidentified rib	-	ND	FMNH PR 2478	03595	MAD 93-18
	Proximal portion	ND	FMNH PR 2634	07444	MAD 05-42
	Proximal portion	ND	UA 9861	03497	MAD 93-18
	Proximal portion	ND	UA 9863	03590	MAD 93-18

Element(s)	Notes and comments	Position	Specimen number [a]	Field number [b]	Locality
		Axial Column			
	Fragments	ND	FMNH PR 2603	05392	MAD 05-42
	Fragment	ND	FMNH PR 2481	07437	MAD 05-42
	Fragment	ND	FMNH PR 2632	07441	MAD 05-42
	Fragment	ND	FMNH PR 2481	07744	MAD 05-42
	Fragment	ND	FMNH PR 2685	07791	MAD 05-42
	-	ND	FMNH PR 2481	07890	MAD 05-42
	5 fragments	ND	FMNH PR 2485	07222	MAD 05-42
Gastrale	-	Anterior	FMNH PR 2481	07213	MAD 05-42
Chevron	-	ND	UA 9196	98175	MAD 93-18
	-	Middle	UA 9152	03285	MAD 93-18
	-	ND	UA 9180	03602	MAD 93-18
	-	ND	UA 9182	03147	MAD 93-18
	-	ND	FMNH PR 2481	05385	MAD 05-42
	-	ND	FMNH PR 2485	07221	MAD 05-42
	-	ND	FMNH PR 2673	07698	MAD 05-42
		Appendicular Skeleton			
Scapula	-	Left	UA 9116	01136	MAD 93-18
	-	Left	FMNH PR 2458	03400	MAD 93-18
	-	Left	FMNH PR 2481	07746	MAD 05-42
	-	Right	FMNH PR 2481	07442	MAD 05-42
	-	Right	FMNH PR 2606	05404	MAD 05-42
Scapulocoracoid	-	Right	UA 9160	03394	MAD 93-18
Coracoid	-	Right	UA 9159	03356	MAD 93-18
	-	Left?	FMNH PR 2481	07213	MAD 05-42
	Fragment?	ND	FMNH PR 2481	07522	MAD 05-42
Humerus	-	Left	FMNH PR 2485	05418	MAD 05-42
	Proximal 2/3	Right	FMNH PR 2143	98007	MAD 93-18
	-	Right	FMNH PR 2481	07213	MAD 05-42
	Proximal portion	Right	UA 9165	03415	MAD 93-18
	Shaft	Right	UA 8693	95244-4	MAD 93-18
	Shaft?	ND	UA 8694	98090	MAD 93-18
Metacarpal IV?	Proximal portion	ND	UA 9146	03213	MAD 93-18
Manual phalanx	-	ND	FMNH PR 2227	98312-6	MAD 93-18
	-	ND	FMNH PR 2224	96353	MAD 93-101
	-	ND	FMNH PR 2132	95244-5	MAD 93-18
	2+ elements	ND	FMNH PR 2225	96392	MAD 96-41
	-	ND	UA 9194	95377	MAD 95-14
Manual ungual	-	ND	FMNH PR 2169	99277	MAD 99-05
	-	ND	FMNH PR 2136	95335	MAD 93-18
Ilium	-	Left	FMNH PR 2485	05460-03	MAD 05-42
	-	Left	FMNH PR 2481	07218-1	MAD 05-42
	??	Left?	FMNH PR 2472	03496	MAD 93-18
	-	Right	FMNH PR 2481	07218-2	MAD 05-42
	Central and posterior portions	Right	UA 9170	03450	MAD 93-18
Pubis	Proximal 2/3	Left	FMNH PR 2463	03411	MAD 93-18
	Distal 2/3	Left, right	FMNH PR 2470	03457	MAD 93-18
	-	Left	FMNH PR 2108	98089	MAD 93-18
	Proximal portion	Left	FMNH PR 2461	03408	MAD 93-18
	Proximal portion	Left	UA 9153	03323	MAD 93-18
	-	Right	FMNH PR 2109	95250-1	MAD 93-18
	Proximal 2/3	Right	UA 9100	01045	MAD 93-18
	Proximal portion	Right	UA 9162	03445	MAD 93-18
	-	Left, right	FMNH 2481	07218	MAD 05-42
	Shaft	ND	UA 9136	03143	MAD 93-18
	Shaft?	ND	UA 9117	01137	MAD 93-18

Element(s)	Notes and comments	Position	Specimen number [a]	Field number [b]	Locality
		Appendicular Skeleton			
Ischium	-	Left	UA 9168	03435	MAD 93-18
	Proximal 1/2	Left	FMNH PR 2468	03439	MAD 93-18
	Proximal portion	Right	UA 9133	03130	MAD 93-18
	-	Right	UA 9172	03470	MAD 93-18
	Distal 2/3	Left, right	FMNH PR 2485	05444	MAD 05-42
Femur	-	Left	FMNH PR 2123	98317	MAD 93-18
	-	Left	FMNH PR 2117	95194	MAD 93-18
	-	Left	FMNH PR 2120	95256	MAD 93-18
	-	Left	FMNH PR 2115	95234	MAD 93-18
	-	Left	FMNH PR 2485	05467-2	MAD 05-42
	Proximal 1/2	Left	FMNH PR 2481	07217	MAD 05-42
	Proximal portion	Left	UA 9193	95222-049-1	MAD 93-18
	Proximal portion	Left	FMNH PR 2150	98245	MAD 93-18
	Proximal portion	Left	FMNH PR 2149	95248-1	MAD 93-18
	Distal shaft	Left	UA 9135	03139	MAD 93-18
	-	Right	FMNH PR 2153	96020	MAD 93-18
	-	Right	UA 9170	03450	MAD 93-18
	-	Right	UA 8712	98238-1	MAD 93-18
	-	Right	FMNH PR 2148	98229	MAD 93-18
	-	Right	FMNH PR 2215	98021	MAD 93-18
	-	Right	FMNH PR 2208	95238	MAD 93-18
	-	Right	UA 8684	98212	MAD 93-18
	-	Right	UA 8681	98237	MAD 93-18
	-	Right	FMNH PR 2481	07493	MAD 05-42
Tibia	-	Left	UA 8685	98022	MAD 93-18
	-	Left	FMNH PR 2481	07687	MAD 05-42
	-	Left	FMNH PR 2214	98124	MAD 93-18
	Proximal portion	Left	FMNH PR 2119	98216-1	MAD 93-18
	Proximal portion	Left	FMNH PR 2118	98216	MAD 93-18
	Distal portion	Left	UA 9142	03199	MAD 93-18
	Distal portion	Left	UA 9613	NFN 5	NR
	Distal 1/2	Left	FMNH PR 2152	95233	MAD 93-18
	-	Right	UA 8687	98083	MAD 93-18
	-	Right	UA 8711	98241	MAD 93-18
	-	Right	FMNH PR 2121	98323	MAD 93-18
	-	Right	FMNH PR 2112	98155	MAD 93-18
	Proximal portion	Right	UA 8710	98125	MAD 93-18
	Proximal portion	Right	UA 9099	01044	MAD 93-18
	-	Right	FMNH PR 2481	07476	MAD 05-42
	-	Left	FMNH PR 2686	07792	MAD 05-42
	-	Left	FMNH PR 2817	05442	MAD 05-42
Femur, tibia, fibula	-	Right	FMNH PR 2485	05456	MAD 05-42
Tibia, fibula	-	Left	FMNH PR 2485	05419	MAD 05-42
Tibia, fibula, tarsus	-	Left	FMNH PR 2122	95325	MAD 93-18
Tibia, fibula, tarsus	-	Right	FMNH PR 2116	98320	MAD 93-18
Fibula	Proximal 2/3	Left	FMNH PR 2481	07523	MAD 05-42
	-	Right	UA 9167	03421+03269 [c]	MAD 93-18
	Proximal 2/3	Right	UA 9172	03470	MAD 93-18
	Proximal 1/2	Right	UA 9143	03201	MAD 93-18
	Proximal portion	Right	UA 9134	03136	MAD 93-18
	Proximal 2/3	Right	UA 9098	01043	MAD 93-18
	Proximal 1/2	Right	UA 9132	03128	MAD 93-18
Fibula, astragalus	-	Right	FMNH PR 2481	07216+07487 [c]	MAD 05-42
Astragalus	-	Left	FMNH PR 2481	07440	MAD 05-42
Calcaneum	-	Right	FMNH PR 2235	95124-2	MAD 93-18
Metatarsal I?	Distal portion	Left	UA 9118	03004	MAD 93-18

Element(s)	Notes and comments	Position	Specimen number [a]	Field number [b]	Locality
		Appendicular Skeleton			
Metatarsal II	-	Left	UA 9122	03053-1	MAD 93-18
	Distal portion	Left	FMNH PR 2175	99166	MAD 93-18
	Distal 1/3	Left	UA 9138	03175	"East of Mammal"
	Distal 1/2	Left	FMNH PR 2481	07700	MAD 05-42
	Distal 1/4	Left	UA 9774	07148	MAD 93-72
	Distal 1/2	Left	FMNH PR 2679	07778	MAD 05-42
	-	Right	FMNH PR 2147	98086	MAD 93-18
	-	Right	FMNH PR 2151	98220	MAD 93-18
	-	Right	FMNH PR 2206	98201	MAD 93-18
	-	Right	FMNH PR 2481	05585	MAD 05-42
	Distal portion	Right	UA 8683	93061-6	MAD 93-30
	-	Right	FMNH PR 2154	95244-10	MAD 93-18
Metatarsal III	-	Left?	FMNH PR 2146	95225	MAD 93-18
	+ Distal tarsal 3	Left	UA 9102	01086	MAD 93-18
	-	Left	FMNH PR 2155	98165	MAD 93-18
	Proximal portion + distal tarsal 3	Right	FMNH PR 2687	07833	MAD 05-42
	-	Right	FMNH PR 2485	05460-27	MAD 05-42
Metatarsal IV	-	Left	UA 9101	01085-1	MAD 93-18
	-	Right	FMNH PR 2459	03406	MAD 93-18
	-	Right	FMNH PR 2214	98124	MAD 93-18
	Distal portion	Right	UA 9163	03577	MAD 93-18
	Distal portion	Left	FMNH PR 2485	05593-2	MAD 05-42
	Proximal portion	Right	FMNH PR 2234	98119	MAD 93-18
Unidentified metatarsal	Distal portion	ND	UA 9773	07909-2	MAD 93-35
	+ Rib fragments	ND	UA 9105	01089	MAD 99-33
Pedal phalanx II-1	-	Left	FMNH PR 2129	98200	MAD 93-18
	-	Left	UA 9154	03327	MAD 93-18
	-	Left	FMNH PR 2160	95122	MAD 93-18
	-	Left	FMNH PR 2616	07186	MAD 05-42
	-	Right	FMNH PR 2161	98196	MAD 93-18
	-	Right	FMNH PR 2709	05433	MAD 05-42
	-	Right	UA 9188	07421	MAD 93-34
Pedal phalanx II-2	-	Left	FMNH PR 2217	93069	MAD 93-33
	-	Right	FMNH PR 2136	95335	MAD 93-18
	-	Left	FMNH PR 2604	05395	MAD 05-42
Pedal phalanx III-1	-	Right	FMNH PR 2159	95041	MAD 93-18
	-	Right	UA 8700	NFN 7	NR
	-	Left	FMNH PR 2218	98094-2	MAD 93-18
	-	Left	FMNH PR 2481	07537	MAD 05-42
Pedal phalanx III-2	-	Left	FMNH PR 2167	98075-1	MAD 93-18
	-	Left	FMNH PR 2480	03609	MAD 93-18
	-	Left	FMNH PR 2176	98280	MAD 93-18
	-	Right	FMNH PR 2173	99120	MAD 99-30
Pedal phalanx III-2/3	-	Right	FMNH PR 2219	99312	MAD 99-33
	-	Left	UA 9199	99052	MAD 93-35
Pedal phalanx III-4	-	Right	UA 9094	01030	MAD 93-18
Pedal phalanx III-x	-	Left	UA 9192	07889	MAD 93-26
	-	Right	FMNH PR 2481	07685	MAD 05-42
	-	Right	UA 9186	07416	MAD 93-34
	-	Right	FMNH PR 2617	07191	MAD 05-42
	-	Right	FMNH PR 2613	07123	MAD 05-42
Pedal phalanx IV-1	-	Left	FMNH PR 2158	98311	MAD 93-18
	-	Left	UA 9156	03337	MAD 93-18
	-	Right	FMNH PR 2614	07135	MAD 05-42
	-	Right	FMNH PR 2172	99270	MAD 93-18
	-	Right	FMNH PR 2605	05397	MAD 05-42

Element(s)	Notes and comments	Position	Specimen number [a]	Field number [b]	Locality
		Appendicular Skeleton			
	-	Right	UA 9185	07543	MAD 93-35
Pedal phalanx IV-2	-	Left	FMNH PR 2216	96271	MAD 96-01
	-	Right	UA 9096	01035	MAD 93-18
	-	Left	UA 9137	01140	MAD 93-35
Pedal phalanx IV-2/3	-	ND	FMNH PR 2479	03598	MAD 93-18
Pedal phalanx IV-3	-	Left	FMNH PR 2130	98200-1	MAD 93-18
	-	Right	FMNH PR 2131	98200-2	MAD 93-18
	-	Right	FMNH PR 2174	99167	MAD 93-18
Pedal phalanx IV-4	-	Right	UA 8686	95323	MAD 93-18
Pedal ungual III-4	-	Left	UA 9157	03339	MAD 93-18
Pedal ungual II/IV	-	Left	FMNH PR 2135	95333	MAD 93-18
	-	ND	FMNH PR 2486	05435	MAD 05-42
	-	Left	FMNH PR 2667	07587	MAD 05-42
	-	Left	FMNH PR 2485	07202	MAD 05-42
Pedal ungual	-	Right	FMNH PR 2134	95332-1	MAD 93-18
	-	Left	FMNH PR 2236	95307	MAD 95-14
	-	Right	UA 9144	03203	MAD 93-18
	-	Left	UA 9198	98284	MAD 93-18
Unidentified pedal phalanx	-	ND	FMNH PR 2205	95271	MAD 93-18
	2 elements	ND	FMNH PR 2223	93104-4	MAD 93-38
	-	ND	FMNH PR 2611	07116	MAD 05-42
	-	ND	UA 8682	93174	MAD 93-74
	-	ND	UA 8713	95123	MAD 93-18
	-	ND	UA 8714	93201	MAD 93-81
	-	ND	UA 9132	03128	MAD 93-18
	??	ND	FMNH PR 2493	98270	MAD 93-18
	??	ND	FMNH PR 2485	05593-1	MAD 05-42

[a] Elements found in direct association are given the same specimen number.
[b] The field number is composed of two initial digits representing the year followed by three digits identifying the specimen; e.g., 03056 is specimen #56 from the 2003 expedition.
[c] Element is composed of two separately numbered specimens.

References

Accarie, H., B. Beaudoin, J. Dejax, G. Friès, J.-G. Michard, and P. Taquet. 1995. Découverte d'un Dinosaure théropode nouveau (*Genusaurus sisteronis* n. g., n. sp.) dans l'Albien marin de Sisteron (Alpes de Haute-Provence, France) et extension au Crétacé inférieur de la lignée cératosaurienne. [Discovery of a New Theropod Dinosaur (*Genusaurus sisteronis* n. g., n. sp.) in the Marine Albian of Sisteron (Alps of Haute-Provence, France) and Extension of the Ceratosaurian Lineage into the Lower Cretaceous.] *Comptes Rendus de l'Académie des Sciences à Paris, Série IIa*, 320:327–334.

Agnolin, F. L. and P. Chiarelli. 2010. The Position of the Claws in Noasauridae (Dinosauria: Abelisauroidea) and its Implications for Abelisauroid Manus Evolution. *Paläontologische Zeitschrift,* 85:293–300.

Agnolin, F. L., F. E. Novas, and S. Apesteguía. 2003. Velocisaurids in South America and Madagascar. *Ameghiniana*, 40(4, Supplement):77R.

Allain, R., R. Tykoski, N. Aquesbi, N.-E. Jalil, M. Monbaron, D. Russell, and P. Taquet. 2007. An Abelisauroid (Dinosauria: Theropoda) from the Early Jurassic of the High Atlas Mountains, Morocco, and the Radiation of Ceratosaurs. *Journal of Vertebrate Paleontology*, 27:610–624.

Bonaparte, J. F. 1991. Los vertebrados fósiles de la Formación Río Colorado, de la Ciudad de Neuquén y cercanías, Cretácico Superior, Argentina. [The Fossil Vertebrates of the Río Colorado Formation, from Neuquén City and Surrounding Area, Upper Cretaceous, Argentina.] *Revista del Museo Argentino de Ciencias Naturales "Bernardino Rivadavia" e Instituto Nacional de Investigación de las Ciencias Naturales, Paleontología*, 4(3):17–123.

———. 1996. Cretaceous Tetrapods of Argentina. *Münchner Geowissenschaftliche Abhandlungen (A)*, 30:73–130.

Bonaparte, J. F., and F. E. Novas. 1985. *Abelisaurus comahuensis*, n.g., n.sp., Carnosauria del Cretácico Tardio de Patagonia. [*Abelisaurus comahuensis*, n.g., n.sp., Carnosauria from the Late Cretaceous of Patagonia.] *Ameghiniana*, 21(2–4):259–265.

Bonaparte, J. F., F. E. Novas, and R. A. Coria. 1990. *Carnotaurus sastrei* Bonaparte, the Horned, Lightly Built Carnosaur from the Middle Cretaceous of Patagonia. *Contributions in Science, Natural History Museum of Los Angeles County*, 416:1–41.

Bonaparte, J. F., and J. E. Powell. 1980. A Continental Assemblage of Tetrapods from the Upper Cretaceous Beds of El Brete, Northwestern Argentina (Sauropoda-Coelurosauria-Carnosauria-Aves). *Mémoires de la Société Géologique de France, Nouvelle Série*, 139:19–28.

Brissón Egli, F., and S. Apesteguía. 2008. "Noasaurid remains from the Candeleros Formation at 'La Buitrera' (early Upper Cretaceous), Río Negro, Argentina." In *Actas III Congreso Latinoamericano de Paleontología de Vertebrados, Neuquén, Argentina, 22–25 Septiembre, 2008, Libro de Resúmenes*, ed. J. O. Calvo, R. Juarez

Valieri, J. D. Porfiri, and D. dos Santos, p. 180. Neuquén: Universidad Nacional del Comahue.

Canale, J. I., C. A. Scanferla, F. L. Agnolin, and F. E. Novas. 2009. New Carnivorous Dinosaur from the Late Cretaceous of NW Patagonia and the Evolution of Abelisaurid Theropods. *Naturwissenschaften* 96:409–414.

Carrano, M. T. 1999. What, if Anything, is a Cursor? Categories versus Continua for Determining Locomotor Habit in Dinosaurs and Mammals. *Journal of Zoology*, 247:29–42.

———. 2007. "The Appendicular Skeleton of *Majungasaurus crenatissimus* (Theropoda: Abelisauridae) from the Late Cretaceous of Madagascar." In *Majungasaurus crenatissimus (Theropoda: Abelisauridae) from the Late Cretaceous of Madagascar*, ed. S. D. Sampson and D. W. Krause. *Society of Vertebrate Paleontology Memoir* 8:163–179; supplement to *Journal of Vertebrate Paleontology*, 27(2).

Carrano, M. T., and J. R. Hutchinson. 2002. The Pelvic and Hind Limb Musculature of *Tyrannosaurus rex* (Dinosauria: Theropoda). *Journal of Morphology*, 253:207–228.

Carrano, M. T., and S. D. Sampson. 2002. Ceratosaurs: A Global Perspective. *Journal of Vertebrate Paleontology*, 22(3, Supplement):41A.

———. 2004a. Madagascar, Ceratosaurs, and the Cretaceous History of Gondwana. *Geoscience Africa 2004 Abstracts*, 1:108–109.

———. 2004b. New Discoveries of *Masiakasaurus knopfleri* and the Morphology of the Noasauridae (Dinosauria: Theropoda). *Journal of Vertebrate Paleontology*, 24(3, Supplement):44A.

———. 2008. The Phylogeny of Ceratosauria (Dinosauria: Theropoda). *Journal of Systematic Palaeontology*, 6:183–236.

Carrano, M. T., S. D. Sampson, and C. A. Forster. 2002. The Osteology of *Masiakasaurus knopfleri*, a Small Abelisauroid (Dinosauria: Theropoda) from the Late Cretaceous of Madagascar. *Journal of Vertebrate Paleontology*, 22:510–534.

Coria, R. A., and P. J. Currie. 2006. A New Carcharodontosaurid (Dinosauria, Theropoda) from the Upper Cretaceous of Argentina. *Geodiversitas*, 28:71–118.

Currie, P. J., and X.-J. Zhao. 1993 [1994]. A New Carnosaur (Dinosauria, Theropoda) from the Jurassic of Xinjiang, People's Republic of China. *Canadian Journal of Earth Sciences*, 30:2037–2081.

Gauthier, J. A. 1986. "Saurischian Monophyly and the Origin of Birds." In *The Origin of Birds and the Evolution of Flight*, ed. K. Padian. *Memoirs of the California Academy of Sciences*, 8:1–47.

Hay, W. W., R. M. DeConto, C. N. Wold, K. M. Wilson, S. Voigt, M. Schulz, A. R. Wold, W.-C. Dullo, A. B. Ronov, A. N. Balukhovsky, and E. Söding. 1999. "Alternative Global Cretaceous Paleogeography." In *Evolution of the Cretaceous Ocean-Climate System*, ed. E. Barrera and C. C. Johnson. *Geological Society of America Special Paper*, 332:1–47.

Hieromymus, T., and L. M. Witmer. 2008. The Facial Skin of *Majungasaurus crenatissimus* (Abelisauridae: Saurischia): Pronounced Dermal Metaplasia as the Cause of Rugosity in Abelisaurid Skulls. *Journal of Vertebrate Paleontology*, 28(3, Supplement):90A.

Holliday, C. M. 2009. New Insights into Dinosaur Jaw Muscle Anatomy. *The Anatomical Record*, 292:1246–1265.

Huene, F. v., and C. A. Matley. 1933. The Cretaceous Saurischia and Ornithischia of the Central Provinces of India. *Memoirs of the Geological Survey of India: Palaeontologica Indica*, 21:1–72.

Hutchinson, J. R. 2001. The Evolution of Femoral Osteology and Soft Tissues on the Line to Extant Birds (Neornithes). *Zoological Journal of the Linnean Society*, 131:169–197.

Janensch, W. 1925. Die Coelurosaurier und Theropoden der Tendaguru-Schichten Deutsch-Ostafrikas. [The Coelurosaurs and Theropods of the Tendaguru Beds of German East Africa.] *Palaeontographica, Supplement VII*, 1(teil 1, leif 1):1–100.

Marsh, O. C. 1881. Principal Characters of American Jurassic Dinosaurs. Part V. *The American Journal of Science and Arts, Series 3*, 21:417–423.

———. 1884. The Classification and Affinities of Dinosaurian Reptiles. *Nature*, 31:68–69.

Novas, F. E., F. L. Agnolin, and S. Bandyopadhyay. 2004. Cretaceous Theropods from India: A Review of Specimens Described by Huene and Matley (1933). *Revista del Museo Argentino de Ciencias Naturales, Nuevo Serie*, 6:67–103.

O'Connor, P. M. 2007. "The Postcranial Axial Skeleton of *Majungasaurus crenatissimus* (Theropoda: Abelisauridae) from the Late Cretaceous of Madagascar." In *Majungasaurus crenatissimus (Theropoda: Abelisauridae) from the Late Cretaceous of Madagascar*, ed. S. D. Sampson and D. W. Krause. *Society of Vertebrate Paleontology Memoir* 8:127–162; supplement to *Journal of Vertebrate Paleontology*, 27(2).

Owen, R. 1842. Report on British Fossil Reptiles, Part II. *Report of the British Association for the Advancement of Science*, 11:84–110.

Rauhut, O. W. M. 2002. Dinosaur Evolution in the Jurassic: A South American Perspective. *Journal of Vertebrate Paleontology*, 22 (3, Supplement):89A.

———. 2003. The Interrelationships and Evolution of Basal Theropod Dinosaurs. *Special Papers in Palaeontology*, 69:1–213.

———. 2004. Braincase Structure of the Middle Jurassic Theropod Dinosaur *Piatnitzkysaurus*. *Canadian Journal of Earth Sciences*, 41:1109–1122.

———. 2005. Post-cranial Remains of 'Coelurosaurs' (Dinosauria, Theropoda) from the Late Jurassic of Tanzania. *Geological Magazine*, 142:97–107.

Rogers, R. R., and J. H. Hartman. 1998. Revised Age of the Dinosaur-bearing Maevarano Formation (Upper Cretaceous), Mahajanga Basin, Madagascar. *Gondwana 10: Event Stratigraphy of Gondwana, Journal of African Earth Sciences*, 27:160–162.

Rogers, R. R., J. H. Hartman, and D. W. Krause. 2000. Stratigraphic Analysis of Upper Cretaceous Rocks in the Mahajanga Basin, Northwestern Madagascar: Implications for Ancient and Modern Faunas. *Journal of Geology*, 108:275–301.

Rogers, R. R., D. W. Krause, K. A. Curry Rogers, A. H. Rasoamiaramanana,, and L. Rahantarisoa. 2007. "Paleoenvironment and Paleoecology of *Majungasaurus crenatissimus* (Theropoda: Abelisauridae) from the Late Cretaceous of Madagascar." In *Majungasaurus crenatissimus (Theropoda: Abelisauridae) from the Late Cretaceous of Madagascar*,

ed. S. D. Sampson and D. W. Krause. *Society of Vertebrate Paleontology Memoir* 8:21–31; supplement to *Journal of Vertebrate Paleontology*, 27(2).

Sadleir, R., P. M. Barrett, and H. P. Powell. 2008. The Anatomy and Systematics of *Eustreptospondylus oxoniensis*, a Theropod Dinosaur from the Middle Jurassic of Oxfordshire, England. *Monograph of the Palaeontographical Society, London*, 160:1–82.

Sampson, S. D., M. T. Carrano, and C. A. Forster. 2001. A Bizarre Predatory Dinosaur from the Late Cretaceous of Madagascar. *Nature*, 409:504–506.

Sampson, S. D., and L. M. Witmer. 2007. "Craniofacial Anatomy of *Majungasaurus crenatissimus* (Theropoda: Abelisauridae) from the Late Cretaceous of Madagascar." In *Majungasaurus crenatissimus (Theropoda: Abelisauridae) from the Late Cretaceous of Madagascar*, ed. S. D. Sampson and D. W. Krause. *Society of Vertebrate Paleontology Memoir* 8:32–102; supplement to *Journal of Vertebrate Paleontology*, 27(2).

Sampson, S. D., L. M. Witmer, C. A. Forster, D. W. Krause, P. M. O'Connor, P. Dodson, and F. Ravoavy. 1998. Predatory Dinosaur Remains from Madagascar: Implications for the Cretaceous Biogeography of Gondwana. *Science*, 280:1048–1051.

Seeley, H. G. 1888. On the classification of the fossil animals commonly named Dinosauria. *Proceedings of the Royal Society of London*, 43:165–171.

Sereno, P. C., and S. L. Brusatte. 2008. Basal Abelisaurid and Carcharodontosaurid Theropods from the Lower Cretaceous Elrhaz Formation of Niger. *Acta Palaeontologica Polonica*, 53:15–46.

Sereno, P. C., J. A. Wilson, and J. L. Conrad. 2004. New Dinosaurs Link Southern Landmasses in the Mid-Cretaceous. *Proceedings of the Royal Society of London B*, 271:1325–1330.

Sipla, J. 2007. The Semicircular Canals of Birds and Non-avian Dinosaurs. *Journal of Vertebrate Paleontology*, 27(3, Supplement):147A.

Tykoski, R. S., and T. Rowe. 2004. "Ceratosauria." In *The Dinosauria*,2nd ed., ed. D. B. Weishampel, P. Dodson, and H. Osmólska, pp. 47–70. Berkeley: University of California Press.

Wilson, J. A. 1999. A Nomenclature for Vertebral Laminae in Sauropods and other Saurischian Dinosaurs. *Journal of Vertebrate Paleontology*, 19:639–653.

Wilson, J. A., P. C. Sereno, S. Srivastava, D. K. Bhatt, A. Khosla, and A. Sahni. 2003. A New Abelisaurid (Dinosauria, Theropoda) from the Lameta Formation (Cretaceous, Maastrichtian) of India. *Contributions from the Museum of Paleontology, University of Michigan*, 31:1–42.

Xu, X., Clark, J.M., Mo, J., Choiniere, J., Forster, C.A., Erickson, G.M., Hone, D.W.E., Sullivan, C., Eberth, D.A., Nesbitt, S., Zhao, Q., Hernandez, R., Jia, C.-k., Han, F.-l. Guo, Y. 2009. A Jurassic Ceratosaur from China Helps Clarify Avian Digital Homologies. *Nature*, 459:940–944.

REQUIREMENTS FOR SMITHSONIAN SERIES PUBLICATION

ALL MANUSCRIPTS ARE REVIEWED FOR ADHERENCE TO THE SISP MANUSCRIPT PREPARATION AND STYLE GUIDE FOR AUTHORS (available on the "Submissions" page at www.scholarlypress.si.edu). Manuscripts not in compliance will be returned to the author. Manuscripts intended for publication in the Contributions Series are evaluated by a content review board and undergo substantive peer review. Accepted manuscripts are submitted for funding approval and scheduling to the Publications Oversight Board.

MINIMUM MANUSCRIPT LENGTH is thirty manuscript pages. If a manuscript is longer than average, an appropriate length will be determined during peer review and evaluation by the Content Review Board. Authors may be asked to edit manuscripts that are determined to be too long.

TEXT must be prepared in a recent version of Microsoft Word; use a Times font in 12 point for regular text; be double spaced; and have 1" margins. Each chapter/section must be saved in a separate file.

REQUIRED ELEMENTS are title page, abstract page, table of contents, main text, and reference section. See the SISP Manuscript Preparation and Style Guide for Authors for the order of all elements.

HEADINGS should be styled so different levels of headings are distinct from each other and so the organization of the manuscript is clear. Insert one line space above and one line space below all headings.

FRONT MATTER should include title page, abstract page, and table of contents. All other sections are optional. Abstracts must not exceed 300 words. Table of contents should include A-, B-, and C-level headings.

TABLES (numbered, with captions, stubs, rules) should be submitted in separate MS Word files; should include footnotes, if appropriate; should have rules only at top, bottom, and beneath column heads. Print outs of each table should accompany the manuscript to ensure correct layout of data. Tabulations within running text should not be numbered or formatted like formal tables, and should be included in the text of the manuscript.

FIGURE CAPTIONS should be provided in a separate MS Word file.

FIGURES (e.g., photographs, line art, maps) should be numbered sequentially (1, 2, 3, etc.) in the order called out; be placed throughout text, not at end of manuscript; have all components of composites lettered with lowercase letters and described in the caption; include a scale bar or scale description, if appropriate; include any legends in or on the figure rather than in a caption.

ART must not be embedded in the main text.

Figures must be original and submitted as individual TIFF or EPS files. Resolution for art files must be at least 300 dpi for grayscale and color images and at least 1200 dpi for line art. Electronic images should measure no more than 100% and no less than 75% of final size when published. JPG files will not be accepted. Color images significantly increase costs so should be included only if required. Funding for color art is subject to approval by SISP and the Publications Oversight Board.

TAXONOMIC KEYS in natural history papers should use the aligned-couplet form for zoology. If cross referencing is required between key and text, do not include page references within the key but number the keyed-out taxa, using the same numbers with their corresponding heads in the text.

SYNONOMY IN ZOOLOGY must use the short form (taxon, author, year:page), with full reference at the end of the paper under "References."

IN-TEXT REFERENCES should be used rather than bibliographic notes and should follow the author-date system in the following format: "(author last name, year)" or ". . . author (year)"; "(author, year:page used within the text)" or ". . . author (year:page)." A full citation should be included in a "References" section.

ENDNOTES are to be used in lieu of footnotes and should be keyed manually into a separate MS Word file, in a section titled "Notes". Notes should not contain bibliographic information. Manually type superscript numerals in text and use full-sized numerals at the beginning of each note in the "Notes" section. SISP will determine the best placement of the notes section, either at the end of each chapter or at the end of the main text.

REFERENCES should be in alphabetical order, and in chronological order for same-author entries. Each reference should be cited at least once in main text. Complete bibliographic information must be included in all citations (e.g., author/editor, title, subtitle, edition, volume, issue, pages, figures). For books, place of publication and publisher are required. For journals, use the parentheses system for volume(number):pagination [e.g., "10(2):5–9"]. Do not use "et al."; all authors/editors should be included in reference citations. In titles, capitalize first word, last word, first word after colon, and all other words except articles, conjunctions, and prepositions. Examples of the most common types of citations are provided in the SISP Manuscript Preparation and Author Style Guide.

For questions regarding the guidelines, please email SISP at schol.press@si.edu.